Top Med Chem (2015) 9: 283–382
DOI: 10.1007/7355_2013_29

Published online: 28 January 2014

The Influence of Bioisosteres in Drug Design: Tactical Applications to Address Developability Problems

Nicholas A. Meanwell

Abstract The application of bioisosteres in drug discovery is a well-established design concept that has demonstrated utility as an approach to solving a range of problems that affect candidate optimization, progression, and durability. In this chapter, the application of isosteric substitution is explored in a fashion that focuses on the development of practical solutions to problems that are encountered in typical optimization campaigns. The role of bioisosteres to affect intrinsic potency and selectivity, influence conformation, solve problems associated with drug developability, including P-glycoprotein recognition, modulating basicity, solubility, and lipophilicity, and to address issues associated with metabolism and toxicity is used as the underlying theme to capture a spectrum of creative applications of structural emulation in the design of drug candidates.

Keywords Isostere, Bioisostere, Conformation, Carboxylic acid isosteres, Guanidine and Amidine isosteres, Phosphate isosteres, Drug-water isostere, Heterocyle isostere

Contents

N.A. Meanwell (✉)
Department of Discovery Chemistry, Bristol-Myers Squibb Research and Development, 5 Research Parkway, Wallingford, CT 06492, USA
e-mail: Nicholas.Meanwell@bms.com

Abbreviations

BACE	β-site amyloid precursor protein cleaving enzyme
CYP 450	Cytochrome P450
DFT	Density functional theory
FAAH	Fatty acid amide hydrolase
HCV	Hepatitis C virus
hERG	Human *ether a go-go*-related gene
hH-PGDS	Human prostaglandin D2 synthase
HIV-1	Human immunodeficiency virus-1
Hsp	Heat shock protein
KSP	Kinesin spindle protein
LE	Ligand efficiency
LELP	Lipophilicity-corrected ligand efficiency
LLE	Ligand-lipophilicity efficiency
NMR	Nuclear magnetic resonance
PAMPA	Parallel artificial membrane
PARP	Poly(ADP-ribose) polymerase
PGI_2	Prostacyclin
P-gp	P-glycoprotein
PPAR	Peroxisome proliferator-activated receptor
SAR	Structure–activity relationship

1 Introduction

Bioisosterism is a powerful concept that has found widespread application in drug design and continues to be an important tactical element in contemporary medicinal chemistry practices [1–10]. Bioisosterism, which evolved from the concept of shape

isosterism exhibited by simple structural elements, was originally recognized by Langmuir almost a century ago, and the first experiments that demonstrated the potential of bioisosterism in a practical setting were reported in 1932 and 1933 [1, 11–13]. In a series of experiments, Erlenmeyer and his colleagues showed that antibodies recognizing *ortho*-substituted tyrosine moieties in synthetic antigens, derived by reaction with diazonium ions, were not able to distinguish between a phenyl and thiophene ring or O, NH, and CH_2 in a linker element [12, 13]. The description of this phenomenon as bioisosterism is attributed to Harris Friedman who introduced the term in 1951 to define compounds demonstrating similar biological activities [14]. However, Friedman recognized that bioisosterism and isosterism were distinct concepts, an observation that anticipated contemporary drug design principles in which the utility of bioisosteres is frequently dependent on context and relies upon a less than exact structural or physicochemical mimicry for the manifestation of biological effect. The thoughtful deployment of a bioisostere offers potential value in drug design campaigns by providing an opportunity to probe the effect of steric size and shape, the modulation of dipole and electronic properties, lipophilicity and polarity, or pK_a on a biological response, which may be functional mimicry or antagonism of a biological regulator [1, 2, 10]. In addition to affecting potency and function, isosteres have demonstrated utility in addressing problems associated with pharmacokinetic and pharmaceutical properties, specificity, toxicity, and metabolic activation pathways in vivo in addition to being a source of novel intellectual property [1–10]. This chapter will summarize some of the more interesting tactical applications of bioisosteres in drug design where problems of the type commonly encountered by medicinal chemists have inspired innovative solutions that offer useful instruction. The vignettes are organized based on a specific property or problem under examination rather than the perhaps more traditional approach of cataloguing based on functional group mimicry.

2 Bioisosteres Designed to Enhance Drug Potency and Selectivity

2.1 Fluorine as an Isostere of Hydrogen

Fluorine has emerged as a remarkable element in drug design, and its applications continue to provide interesting effects on biological activity that can often be somewhat surprising, leading to its broad deployment by the medicinal chemistry community which, in turn, has promoted a deeper understanding of its properties [15–24]. The strategic introduction of fluorine to replace a hydrogen atom can markedly influence potency [25–30]. For example, the L-nucleoside analogue emtricitabine (**2**, FTC) is the 5-fluoro analogue of lamivudine (**1**, 3TC) and is consistently the more potent HIV-1 inhibitor in cell culture by four- to tenfold, which is reflected in the inhibition of HIV-1 reverse transcriptase by the respective triphosphate derivatives [25–27]. The F atom *ortho* to the piperazine and morpholine in the antibacterial agents, the quinolone-based DNA gyrase inhibitor **3** and the protein synthesis inhibitor linezolid **4**, respectively, is

of importance to both potency and efficacy in vivo while in indole-based HIV-1 attachment inhibitors, the 4-F substituent installed in **6** enhanced the potency of prototype **5** by more than 50-fold [15, 16, 28–30].

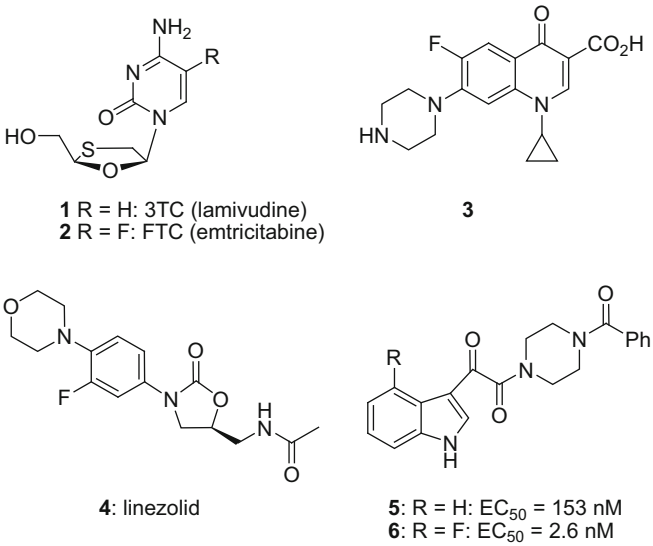

In a series of γ-secretase inhibitors that reduced Aβ protein production in a cell-based assay, the modest potency associated with the parent molecule **7** (evaluated in racemic form) was markedly improved by complete fluorination at C-5 although in this particular example gem-dimethyl substitution at C-5 also improved biological activity [31]. The introduction of a F atom at the *para*-position of the benzylated imide **10** enhanced thrombin inhibitory activity by over fivefold along with selectivity over the related serine protease trypsin by fourfold with **11** exhibiting a 67-fold preference for the coagulation cascade enzyme [17, 32]. An X-ray crystallographic structure of **11** bound to thrombin provided an understanding of the structure–activity relationship (SAR) observation with the F substituent proximal (2.4 Å) to the backbone C_{α}-H atom of Asn_{98} and aligned to establish an interaction with the C atom of the backbone amide C=O of Asn_{98} at a distance of 3.5 Å and an angle of 96° to the plane of the C=O (Fig. 1) [17, 18, 32]. The F to C=O carbon interaction is the one with broader occurrence, and although this interaction is considered to be energetically modest, it appears to be sufficient to differentiate the potency between **10** and **11** by playing a supporting role to the primary interactions between the enzyme and the inhibitor [33]. In an analogous matched pair study, the thrombin inhibitory activity of the amidine **12** is embellished sixfold by F substitution to afford **13**, with an X-ray crystallographic co-crystal structure suggestive of a H-bonding or electrostatic interaction between the F atom and backbone NH of Gly_{216} which are 3.47 Å apart, close to the upper distance limit for a H-bond [16]. The importance of this interaction was underscored from a comparison with the co-crystal of **12** and thrombin in which the aromatic ring adopted a significantly different conformation to that of **13** [16].

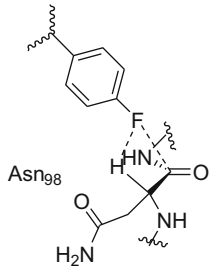

Fig. 1 Key interactions of the 4-F substituent of **11** with Asn_{98} of thrombin

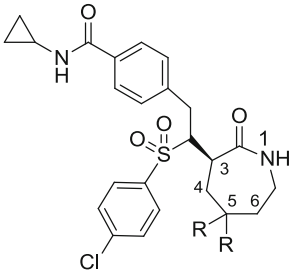

7: R = H (racemic): EC_{50} = 170 nM
8: R = F: EC_{50} = 4 nM
9: R = CH_3: EC_{50} = 15 nM

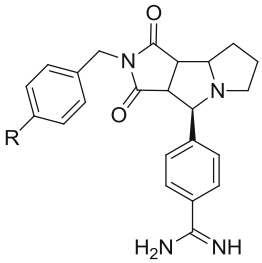

10: R = H: K_i = 310 nM
11: R = F: K_i = 57 nM

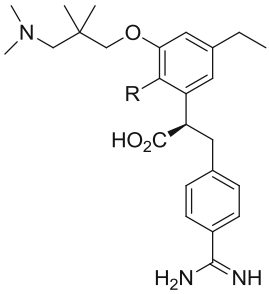

12: R = H: K_i = 1.6 μM
13: R = F: K_i = 0.26 μM

2.2 *Carboxylic Acid Isosteres to Improve Potency*

Carboxylic acid isosteres are a familiar part of the medicinal chemistry landscape and have been deployed to address a number of challenges in drug design, including positively influencing potency. A particularly compelling example that illustrates the importance of carefully selecting the optimal isostere is provided by the SARs that subtended the discovery of the potent angiotensin II receptor antagonist

losartan (**15**) and its analogues **14** and **16–20** [34–38]. A key insight was that the tetrazole moiety in **15** enhances potency over the carboxylic acid analogue EXP-7711 (**14**) by tenfold, attributed to the topological geometry in which the *2H* isomer depicted projects the acidic NH or negative charge 1.5 Å further from the aryl ring than does the carboxylic acid moiety [34, 39, 40]. Interestingly, as summarized by the comparison presented in Table 1, the position of the carboxylic acid moiety on the phenyl ring exerts minimal effect on potency, with **14** and **18** similarly active, while the *ortho*-tetrazole isomer **19** is over 50-fold more potent than the *meta*-substituted analogue **20** [38]. The carboxylic acid and tetrazole moieties are considered to bind in the same pocket in the angiotensin II receptor and interact with Lys_{199} [41]. However, this interaction does not appear to depend on the formation of a classic salt bridge since mutation of Lys_{199} to Gln exerted only a modest twofold effect on the binding of losartan (**15**) and a fivefold effect on the binding of EXP-7711 (**14**), data that are more consistent with a H-bonding interaction between drug and protein [41]. The poor activity of **20** may be a consequence of increased steric bulk compared to the carboxylic acid analogue **18**.

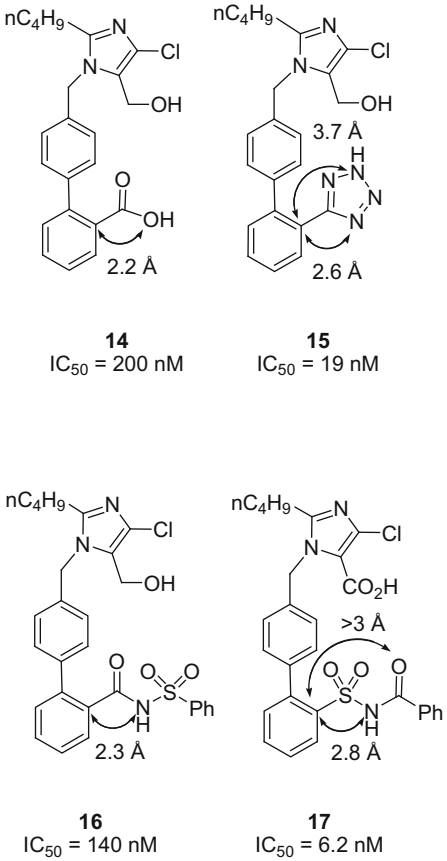

Table 1 Structure–activity relationships associated with the topology of the acidic moiety in angiotensin II receptor antagonists

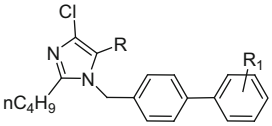

Compound no.	R	R_1	Inhibition of specific binding of [^{3}H]-angiotensin II (2 nM) to rat adrenal cortical microsomes IC_{50} (μM)
14	CH_2OH	2-CO_2H	0.20
18	CH_2OH	3-CO_2H	0.49
19	CHO	2-CN_4H	0.02
20	CHO	3-CN_4H	>1

The importance of topology and the associated geometric implications are also apparent in acylsulfonamide-based angiotensin II antagonists where this functionality functions suitably as an acid surrogate. The $CONHSO_2Ph$ moiety of **16** is a 20-fold less potent ligand than the topologically reversed $SO_2NHCOPh$ isomer **17**, an observation that is consistent with the longer C–S bond in **17** more effectively mimicking the topology of the tetrazole **15** by projecting the charge further from the biphenyl core than **16**, which more closely resembles the carboxylic acid **14** [34, 38, 42].

The discovery of the macrocyclic hepatitis C virus (HCV) NS3 protease inhibitor BILN-2061 (**21**) represented a milestone in HCV drug design by providing proof-of-concept for this mechanistic approach to the control of viremia in infected subjects. The disclosure of this series of tripeptide-based inhibitor stimulated considerable interest in further structural optimization, an endeavor that became of particular importance in the context of overcoming the cardiotoxicity that resulted in termination of this pioneering molecule [43–45]. The conversion of the carboxyl terminus to an acylsulfonamide, particularly the cyclopropyl acylsulfonamide moiety, afforded compounds with increased potency as a consequence of the cyclopropyl ring complementing the P1′ pocket and the sulfone oxygen atoms engaging the protein via H-bonding interactions with the catalytic elements of the enzyme. The significant advantage conferred by this structural modification can be readily assessed by comparing the potency of the matched pairs of acyclic inhibitors **22** and **23** and the P4-P2* macrocycles **24** and **25** [46–49].

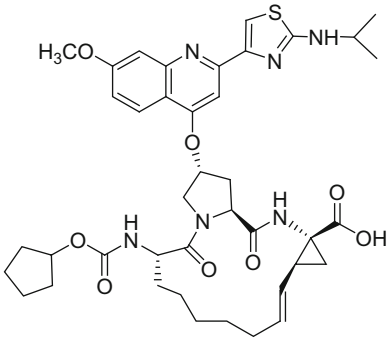

21

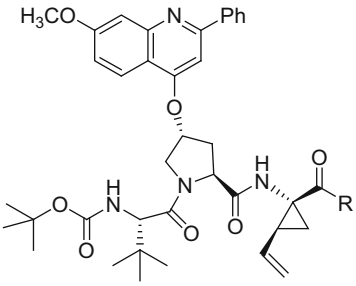

22: R = OH: IC_{50} = 54 nM

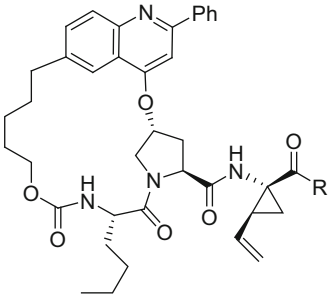

24: R = OH: K_i = 8.5 nM

23: R = 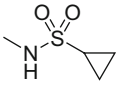 IC_{50} = 1 nM

25: R = 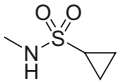 K_i = <0.016 nM

The optimization of inhibitors of the anti-apoptotic B-cell lymphoma 2 proteins Bcl-2, Bcl-x_L, and Bcl-w, for which the fragment leads biphenyl carboxylic acid **26** and phenol **27** were identified using a nuclear magnetic resonance (NMR) screen, involved tethering of the two molecules which bound weakly to proximal pockets in the Bcl-x_L protein [50–52]. Initial attempts to link acid **26** to phenol **27** focused on substituting at the C atom *ortho* to the carboxylic acid moiety of **26**, a topology that was probed based on an analysis of NMR data [50, 51]. However, this approach was not initially successful in identifying hybrid molecules with increased affinity, attributed to poor geometric vectors that gave suboptimal binding. An acylsulfonamide was conceived to offer an improved vector while preserving the acidic moiety, of importance as a complement to Arg_{139} of the Bcl protein, and a library of 120 molecules were prepared after establishing that the simple methyl acylsulfonamide exhibited comparable affinity for Bcl as **26** [51]. The acylsulfonamide **28** emerged from that exercise with further optimization to navitoclax (ABT-263, **30**) proceeding via the intermediacy of compound **29** [50–52].

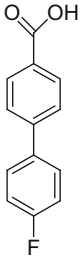

26
IC_{50} FPA = 0.3 mM

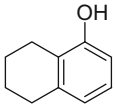

27
IC_{50} FPA = 4.3 mM

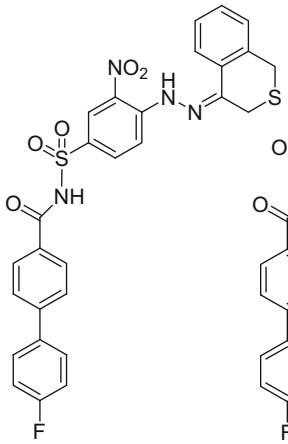

28
K_i FPA = 245 nM

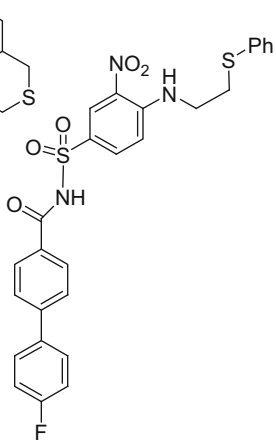

29
IC_{50} FPA = 93 nM

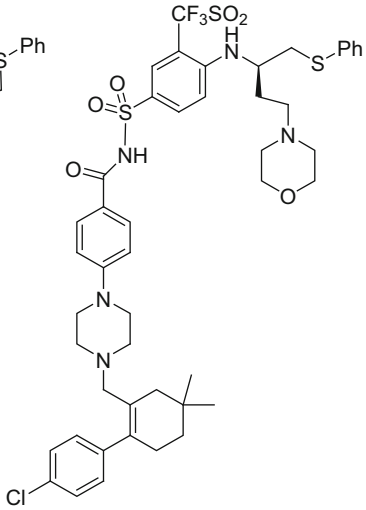

30: ABT-263
EC_{50} = 5.9 nM

2.3 *Applications of Heterocycles as Isosteres and Isosterism Between Heterocycles*

Heterocycles find widespread application in drug design as important scaffolds for deploying functionality or as critical pharmacophoric elements that interact intimately with target proteins, a cue taken from Mother Nature who takes significant advantage of heterocycles. The immense utility of heterocycles resides in their typically facile synthetic accessibility combined with the versatility to project a range of vectors while the electronic properties of the ring can readily be modulated by the introduction of additional heteroatoms and substituent selection. Aspects of heterocycles that are of importance to the medicinal chemist revolve

around their ability to act as H-bond donors or acceptors, to influence the properties of substituents by withdrawing or donating charge and to engage in π–π and dipole–dipole interactions. Thus, the careful selection of a heterocycle for a specific application is frequently of considerable importance and there are many examples where the effects of substitution by rings offering a similar silhouette can be quite subtle in nature and not always well understood.

The H-bonding potential of a wide range of functionality, designated pK_{BHX}, has been determined based on the association of 4-fluorophenol with an acceptor in CCl_4 monitored at room temperature by the shift in the infrared stretching frequency of the OH bond [53–55]. On this scale, a stronger H-bond acceptor is associated with a higher pK_{BHX} value that shows dependence on several physical properties, including the position of the acceptor atom in the periodic table, polarizability, field and inductive/resonance effects, electronic resonance, and steric effects associated with substituents and their interaction with the acceptor atom. A particularly important aspect of H-bonding potential is that across a range of functionality it is not quantitatively related to basicity (pK_{BH}^{+} or pKa) and there are several examples where a H-bonding interaction occurs preferentially at an atom of low basicity in the presence of a more basic acceptor [56–62]. For example, nicotine (**31**) protonates initially on the pyrrolidine nitrogen atom in H_2O, but H-bonding with 4-fluorophenol in CCl_4 occurs primarily at the pyridine nitrogen atom. For cotinine (**32**), the amide carbonyl is the primary site for H-bonding, which contrasts with basicity since the amide exhibits a pK_{BH}^{+} value of −0.71 compared to 5.20 for the pyridine nitrogen atom where protonation occurs [56–62].

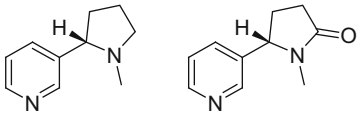

31 **32**

Table 2 presents a comparison of pK_{HBX} and pK_{BH}^{+} (pKa) values for some common 5- and 6-membered ring heterocycles where within a homologous series there is some correlation between H-bonding potential (pK_{BH}^{+}) and pK_a values although isoxazole and pyridazine are notable exceptions. In the case of pyridazine, a heterocycle that has been proposed to be a privileged scaffold in medicinal chemistry, the high H-bonding potential for this poorly basic molecule is attributed to the α-effect in which unfavorable lone pair-lone pair interactions are relieved by one of the N atoms engaging in a H-bonding interaction, as depicted in Fig. 2 [63, 64].

The topological deployment of an oxazole heterocycle influenced the potency of blood platelet aggregation inhibition associated with the non-prostanoid prostacyclin (PGI_2) mimetics **33** and **34** [65–68]. The oxazole **33** is fivefold more potent than the isomer **34** which, in turn, is comparable to the *cis*-olefin **35** [65–68]. These data were interpreted in the context of the nitrogen atom of the central oxazole

Table 2 Comparison of pK_{HBX} and pK_{BH}^{+} (pK_a) values for common 5- and 6-membered ring heterocycles

Heterocycle	pK_{BHX}	pK_{BH}^{+}(pK_a)
5-Membered heterocycles		
1-Methyl-imidazole	2.72	7.12
Imidazole	2.42	6.95
1-Methyl-pyrazole	1.84	2.06
Thiazole	1.37	2.52
Oxazole	1.30	0.8
Isoxazole	0.81	1.3
Furan	−0.40	–
6-Membered heterocycles		
Pyridine	1.86	5.20
Pyridazine	1.65	2.00
Pyrimidine	1.07	0.93
Pyrazine	0.92	0.37
Triazine	0.88	–

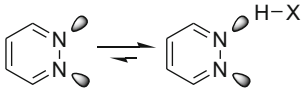

Fig. 2 H-bonding associated with the pyridazine heterocycle

of **33** being ideally positioned to accept a H-bond from a donor within the PGI_2 receptor protein, consistent with earlier SAR observations. This interaction is not available to the isomer **34** since the O atom of an oxazole ring is a poorer H-bond acceptor or the olefin **35**, suggesting that the central oxazole ring of **34** is acting merely as a scaffold that is structurally analogous to **35** [65–68]. In the solid-state structures of **33** and **34**, although the molecules adopt an almost identical shape, the central oxazole rings accept H-bonds from the CO_2H moiety of an adjacent molecule in the unit cell, leading to a markedly different pattern of crystal packing between the two isomers [68]. Ab initio calculations indicate that a H-bond to the N atom of an oxazole is 10.4 kJ/mol or 2.48 kcal/mol more stable than that to the O atom (Fig. 3), reflected in the essentially exclusive occurrence of H-bonds only to the N atom of oxazoles observed in the Cambridge Structural Database (CSD) [68–70].

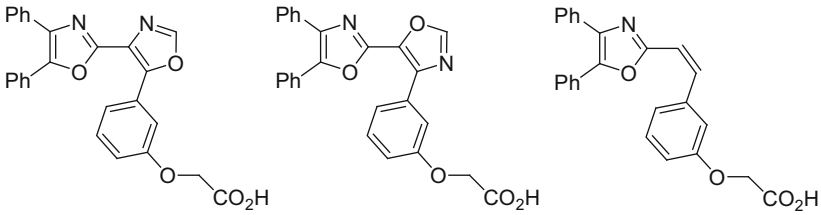

33: EC_{50} = 27 nM **34**: EC_{50} = 160 nM **35**: EC_{50} = 180 nM

In a series of quinolone-based inhibitors of HCV NS5B polymerase, the 1,2.4-oxadiazole **36** exhibited potent enzyme inhibition, IC_{50} = 41 nM, in part by

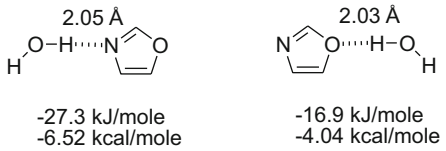

Fig. 3 Energetics of H-bonding in oxazoles based on ab initio calculations

establishing a H-bond with the backbone NH of Ser_{476}, as determined by X-ray crystallographic analysis [71]. The topological isomer **37** is an order of magnitude weaker, consistent with the weaker potential for the O atom to engage in H-bonding despite projecting the benzyl moiety in a similar vector to **36**. In order for **37** to present the sterically somewhat hindered N-4 to the Ser_{476} NH, the benzyl moiety would be required to adopt an alternate and unfavorable vector. Interestingly, the several other azole heterocycles **38–40** examined were relatively poor inhibitors of the enzyme, with **38** and **39** perhaps the most surprising given that they combine a strong H-bond acceptor with the preferred topology of the benzyl moiety that is found in **36** [71, 72].

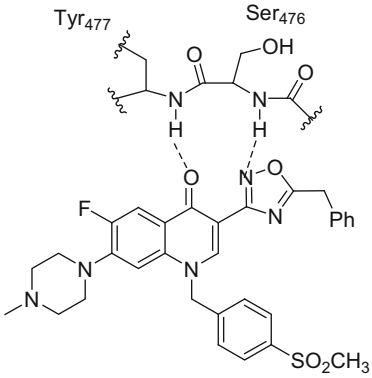

36: IC_{50} HCV NS5B = 0.041 μM

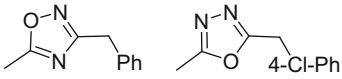

37: IC_{50} = 0.73 μM **38**: IC_{50} =1.6 μM

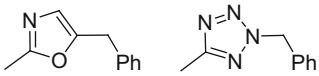

39: IC_{50} =1.8 μM **40**: IC_{50} =>10 μM

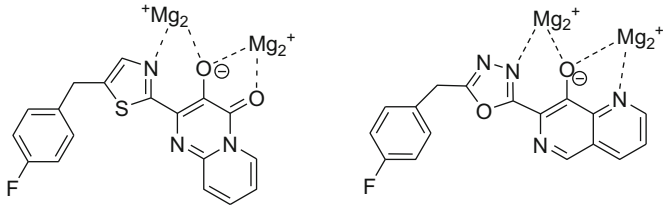

Fig. 4 Interactions between representative azole-substituted pyrido[1,2-*a*]pyrimidines and −1,6-naphthyridines and the catalytic Mg^{2+} atoms of HIV-1 integrase

Table 3 Structure–activity relationships for a series of azole-substituted pyrido[1,2-*a*]pyrimidine-based inhibitors of HIV-1 integrase

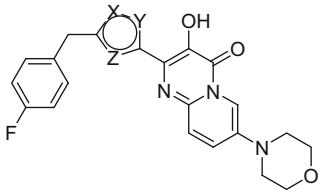

Compound no.	Heterocycle	IC_{50} (nM)	Compound no.	Heterocycle	IC_{50} (nM)
43	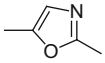	59	**47**	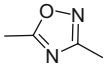	450
44	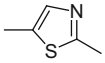	20	**48**	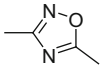	>10,000
45	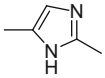	45	**49**	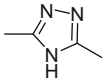	–
46	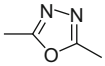	310	**50**	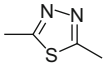	225

The metal binding properties of azole rings were explored in the context of inhibitors of HIV-1 integrase and conducted with a chemotype in which the binding topology of the fluorobenzyl substituent controlled the presentation of the heteroatom to one of the catalytic magnesium atoms [73–77]. As depicted in Fig. 4, the positioning of the fluorobenzyl moieties in **41** and **42** dominates the binding conformation thereby dictating which azole heteroatom is presented to the active site metal atom, providing a sensitive assessment of metal binding potential, with SARs summarized in Table 3 [73–77]. The importance of Mg^{2+} coordination potential and its impact on potency is most evident in the comparison between the two 1,2,4-oxadiazoles **47** and **48** in which the O atom of **48** is an ineffective metal coordinator, an observation that is concordant with heteroatom H-bonding potential and was recapitulated in a series of 1,6-naphthyridine derivatives [73–75].

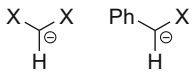

Fig. 5 Charge demand is defined as the fraction of π-charge transferred from a negatively charged trigonal carbon atom to the adjacent X group

Interestingly, in the pyrido[1,2-*a*]pyrimidine series, the thiazole **44** was selected as the basis for further optimization while in the 1,6-naphthyridine chemotype, the 1,3,4-oxadiazole ring that performs only modestly in this series (refer to compound **46**) was the most effective amide surrogate studied, presumably reflecting subtle differences in binding between the two structural classes [75–77].

The electron-withdrawing properties of heterocyclic rings have been exploited as an important element in drug design with two aspects prominent: the acidifying effect of a heterocycle on a NH substituent, which enhances H-bonding donor properties and confers carboxylic acid mimicry in the case of sulfonamide antibacterial agents, and, secondly, the electron-withdrawing properties of a heterocycle ring that has been used to advantage in the design of mechanism-based inhibitors of serine-type proteases and hydrolases [78–81]. The site of attachment of substituents on a heterocyclic ring has been shown to be of importance to potency in all of these settings, interpretable based on the quantification of electron withdrawal. A scale of electron withdrawal has been formulated as the concept of charge demand, defined as the fraction of π-charge transferred from a negatively charged trigonal carbon atom to the adjacent X group, typically measured by ^{13}C-NMR chemical shifts of trigonal benzylic carbanions, as depicted in Fig. 5 [82–85]. The resonance electron-withdrawing capacity of common functional groups and a selection of heterocycles is summarized in Table 4, data that reveals interesting trends and emphasizes the importance of carefully selecting specific heterocycles for a particular application.

An important aspect associated with the design of serine protease inhibitors has focused on substrate mimetics that present the enzyme with an electrophilic carbonyl element. This acts as a decoy for the scissile amide bond that reacts with the catalytic serine hydroxyl to form a stable but unproductive tetrahedral intermediate [79]. The equilibrium in favor of the adduct is a function of the electrophilicity of the C=O moiety, with peptidic aldehydes an early vehicle that established the viability of this concept but which was subsequently refined by deploying trifluoromethyl ketones and α-ketoamides. Trifluoromethyl ketones provide an additional example of the beneficial effect on potency of replacing H with F since the corresponding methyl ketones are typically inactive [86]. α-Ketoamides are particularly interesting in inhibitor optimization because they provide an opportunity for the incorporation of structural elements designed to interact more extensively with the S′ pockets of an enzyme [87]. This design concept was further explored in the context of human neutrophil elastase (HNE) inhibitors that focused on tripeptidic, mechanism-based inhibitors that incorporated heterocycles as the carbonyl-activating element [88–94]. α-Ketoamides were included in this study for purpose of comparison and inhibitory potency was found to correlate nicely with

Table 4 Charge demand associated with functional groups and heterocycles

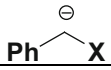

Substituent	Charge demand C^{Ph}_{X}
$P(O)(OEt)_2$	0.26
SO·Ph	0.26
SO_2Ph	0.28
CN	0.28
Ph	0.29
$CONMe_2$	0.42
CO_2Me	0.40
4-Pyridyl	0.408
2-Pyridyl	0.411
3-pyridazinyl	0.417
2-Pyrimidinyl	0.430
Pyrazinyl	0.446
4-Pyrimidinyl	0.501
CO.Me	0.51
CO.Ph	0.56
2-Thiazolyl	0.380–0.413
2-Benzothiazolyl	0.457–0.471
2-Oxazolyl	0.346
2-Benzoxazolyl	0.424–0.436
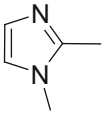	0.283
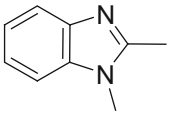	0.382
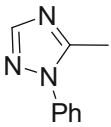	0.411
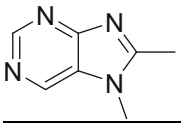	0.536

the electrophilicity of the carbonyl moiety, as captured in the SARs summarized in Table 5 [89]. In addition to providing the potential for unique interactions with enzyme and the ability to probe interactions with S′ sites, the heterocycle moiety was also considered to offer the potential to sterically interfere with reductive metabolism of the carbonyl moiety [88–90, 94].

Table 5 SAR associated with a series of tripeptidic inhibitors of HNE incorporating activated carbonyl moieties to interact with the catalytic serine

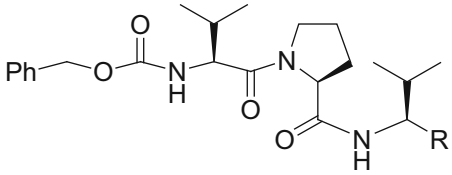

R	HNE K_i (nM)
CO·CH_3	8,000
CHO	41
CO·CF_3	1.6
CO·Ph	16,000
CO-2-thienyl	4,300
CO-2-benzoxazole	3
CH(OH)-2-benzoxazole	21,000
CO-2-oxazole	28
CO-2-oxazolidine	0.6
CO-2-benzothiazole	25
CO-2-thiazole	270
CO-2-(1-Me)-imidazole	80,000
CO-2-(1-Me)-benzimidazole	12,000
CO-2-benzimidazole	5,600
CO-2-pyridine	22,000
CO-2-benzofuran	3,400

Studies with a matched pair of oxadiazole derivatives found that HNE inhibitory activity was sensitive to the topology of the heterocycle, a structure–activity relationship clearly rooted in the electron-withdrawing properties of the heterocycle [91, 92]. The 1,3,4-oxadiazole **51** is a potent inhibitor of HNE with a $K_i = 0.025$ nM, but the isomeric 1,2,4-oxadiazole **52** is 20-fold weaker, with a $K_i = 0.49$ nM [90]. In these inhibitors, the electron-withdrawing effect of the 1,3,4-oxadiazole moiety is similar to an oxazole, whereas the 1,2,4-oxadiazole ring performs more like an imidazole (Table 4). Based on this result, the 1,3,4-oxadiazole moiety was adopted as the carbonyl-activating moiety in more advanced SAR studies that ultimately led to the identification of ONO-6818 (**53**) as an orally bioavailable, non-peptidic inhibitor of HNE that was advanced into clinical trials [92].

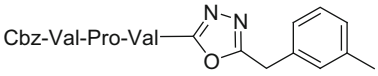

51

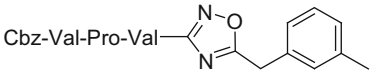

52

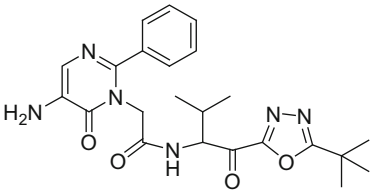

53

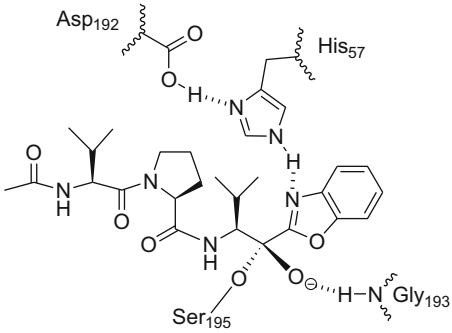

Fig. 6 Key interactions between a tripeptidic ketobenzoxazole derivative and HNE

The basic design principles were confirmed by an X-ray crystallographic analysis of a benzoxazole-based HNE inhibitor bound to the enzyme which revealed that the catalytic serine hydroxyl had reacted with the activated carbonyl moiety as anticipated to afford a tetrahedral intermediate [88]. In addition, the benzoxazole nitrogen atom engaged the NH of the imidazole of His_{57}, the residue that is part of the catalytic triad, in a H-bonding interaction, as summarized in Fig. 6 [88].

2-Keto-oxazole derivatives have featured prominently in the design of inhibitors of fatty acid amide hydrolase (FAAH), a serine hydrolase responsible for degrading endogenous lipid amides, including anandamide and related fatty acid amides that have been identified as neuronal modulators [80, 81, 95–103]. The electronic properties of the oxazole heterocycle were influenced by electron-donating and electron-withdrawing substituents introduced at C-5 of the ring that indirectly influenced the electrophilicity of the carbonyl moiety designed to react with the enzyme serine hydroxyl; a survey that provided the structure–potency relationships is compiled in Table 6. FAAH inhibitory activity was found to correlate with the Hammett σ constant associated with the substituent, with the plot of the data allowing the conclusion that the 5-CO_2H derivative bound as the anion while the 5-CHO and 5-$CO.CF_3$ analogues bound as their hydrated forms [82, 94–96, 104].

A particularly striking example of the importance of correctly deploying a heterocycle based on its electronic and H-bonding properties that relates closely to biological potency is illustrated by the series of 3 non-peptidic heteroaryl nitriles compiled in Table 7 that have been explored as inhibitors of the cysteine proteases cathepsins K and S [105]. These compounds depend on the electron-withdrawing properties of the heterocycle to activate the nitrile moiety toward addition of the catalytic cysteine thiol of the enzyme to form a stable, covalent but reversible imino thioether-based complex. The 2-cyanopyrimidine **54** is a potent and effective inhibitor of both cathepsins, but the high charge demand at this site (0.43, Table 4) is such that the nitrile moiety is indiscriminately reactive and forms adducts with thiols of microsomal proteins. The isomeric 2-cyanopyridines **55** and **56** are of lower intrinsic electrophilicity based on the reduced charge demand (0.41, Table 4) which would be expected to translate into weaker enzyme inhibition. However, **55** and **56** exhibited markedly different protease inhibition profiles that provided

Table 6 Structure–activity relationships associated with a series of ketooxazole-based inhibitors of FAAH

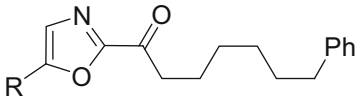

R	σ	FAAH K_i (nM)
H	0.00	48
CO_2H	0.00 (anion) 0.45 (acid)	30
CO_2CH_3	0.45	0.9
$CONH_2$	0.36	5
$CON(CH_3)_2$		2
$CO{\cdot}CH_3$	0.50	2
CHO	0.42 (C=O)	6
$CO{\cdot}CF_3$		3.5
CN	0.66	0.4
CH_3	−0.17	80
CF_3	0.54	0.8
I	0.18	3
Br	0.23	3
Cl	0.23	5
F	0.06	30
SCH_3	0.00	25

Table 7 Inhibitors of cathepsins S and K

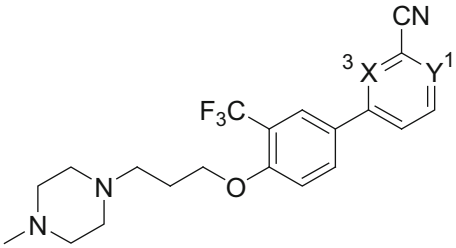

			IC_{50} (nM)	
Compound no.	X	Y	Cathepsin S	Cathepsin K
54	N	N	1.3	13
55	N	CH	58	1,660
56	CH	N	Inactive	Inactive

unique insights into drug–target interactions. Pyridine **55** is 44- and 127-fold less potent toward cathepsins S and K, respectively, while the isomer **56** is inactive toward both cysteine proteases [105]. This observation was attributed to the concept that the pyrimidine N-3 is involved in cysteine thiol activation by acting as a general base to engage the thiol H atom, thereby catalyzing addition to the nitrile moiety, as depicted in Fig. 7. Replacing the pyrimidine N-3 atom with a C–H, as in pyridine **56**, not only removes this function but also introduces a negative steric interaction between the ring CH and the cysteine SH [105].

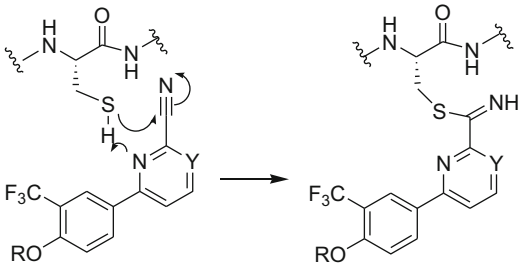

Fig. 7 Role of the pyrimidine N3 or pyridine N1 atom as a general base catalyst to facilitate addition of the catalytic cysteine thiol to the activated nitrile in cathepsin S and K inhibitors

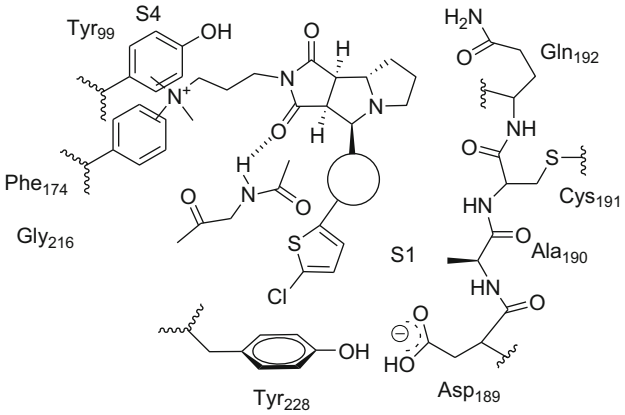

Fig. 8 Binding interactions of factor Xa inhibitors with structural elements in the active site

In a study inspired by observations of the marked potency differences between the two oxazole-based factor Xa inhibitors **57** and **58**, which represent a matched pair differing only by the topology of the oxazole rings, dipole–dipole interactions between the heterocycle ring and an amide moiety of the protein were analyzed [106, 107]. The oxazoles **57** and **58** differed in potency by over tenfold while the isoxazole **59** was the most potent with a $K_i = 9$ nM. X-ray co-crystal data indicated that these inhibitors were not engaging the enzyme via a H-bond donor–acceptor interaction, but the heterocycle rings were noted to be close to the amide bond between Cys_{191} and Gln_{192} with the planes of each almost parallel, leading to the suggestion of a dipole–dipole interaction, as illustrated in Fig. 8. Indeed, potency was shown to correlate with a favorable dipole–dipole interaction in the more active compound **57** that is mismatched in the less active isomer **58** (Fig. 9). The experimental dipole moment for oxazole is 1.7 D and for isoxazole is 3.0 D and gas phase calculations indicate that under optimal conditions the interaction energies between these heterocycles and *N*-methylacetamide, which has a dipole moment of 3.7 D, are −2.74 kcal/mol for oxazole and −2.95 kcal/mol for isoxazole.

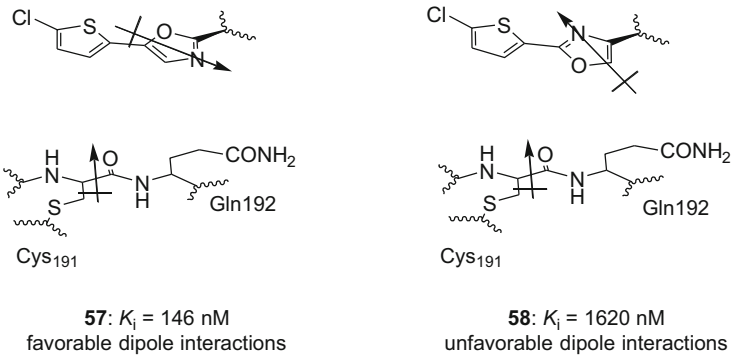

Fig. 9 Dipole–dipole interactions between oxazole-based factor Xa inhibitors and the enzyme that are proposed to subtend the observed potency differences

Although the energies in an aqueous environment are expected to be lower based on solvation issues, these differences are sufficient to explain the differences in potency observed with the azoles **57**–**59**. A plot of the calculated energies versus dipole moment for a series of heterocycles interacting with *N*-methylacetamide exhibited a good correlation, $R^2 = 0.84$, while for benzene, pyrazine, and triazine, heterocyclic rings without a dipole moment, the interacting energies increase as the ring becomes more electron deficient. These studies suggested that potency can be optimized by the careful deployment of heterocycle rings in a fashion that aligns dipole moments in an antiparallel orientation compared to proximal amide moieties in a target protein. This effect can be enhanced by decreasing the π-electron density of the heteroarene in order to improve heteroarene-amide π interactions.

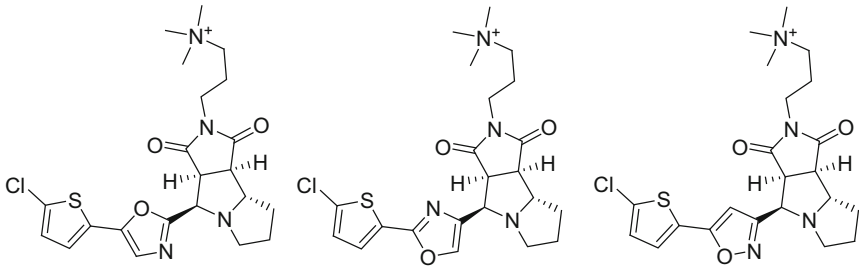

57: FXa K_i = 146 nM **58**: FXa K_i = 1620 nM **59**: FXa K_i = 9 nM

2.4 *Isosteres of Drug and Water Molecules*

Displacing a water molecule that mediates protein–ligand binding by introducing an appropriate structural element into the ligand to produce an isostere of the ligand–water complex can provide significant enhancements in potency by establishing new

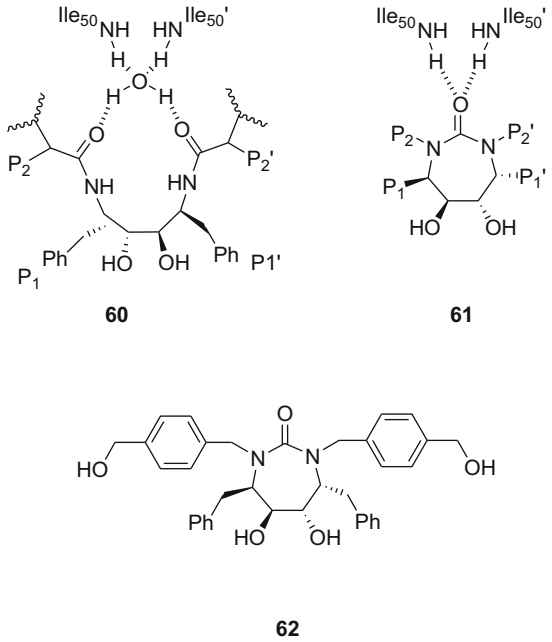

Fig. 10 Cyclic HIV-1 protease inhibitors designed based on the premise of replacing a bound water molecule

H-bonding interactions directly between the protein and ligand [108]. The increased potency arises from both increasing the enthalpic contribution to the thermodynamic signature of the association and taking advantage of the entropic energy gain that arises from releasing the bound water molecule into bulk solvent [108]. Although this can be a challenging enterprise since success depends on several factors, including the specific topology of the ligand-water-protein complex and the ability to effectively mimic the key interactions, several examples have been described where this approach has been used to considerable advantage [109–119]. The design of a series of cyclic urea-based inhibitors of human immunodeficiency virus-1 (HIV-1) protease provides a particularly compelling pioneering example of the concept that in this case is based on displacing the water molecule that mediates the interaction between the NHs of the 2 flap residues $Ile_{50}/Ile_{50'}$ and the P2/P2′ carbonyl O atoms of linear peptidomimetic inhibitors represented by **60**, as depicted in Fig. 10 [109–111]. A series of cyclic ureas exemplified by **61** were conceived based on the premise that the urea carbonyl moiety would displace the water molecule and establish H-bonds directly with the flap residues. As an additional benefit, the conformational constraint provided by the cyclic template would preorganize the inhibitor for recognition by the protease, providing an additional entropic advantage [109–111]. The urea **62** was identified from the initial phase of these studies as a potent HIV-1 protease inhibitor, $K_i = 0.27$ nM, that demonstrated antiviral activity in cell culture, $EC_{90} = 57$ nM [109].

Poly(ADP-ribose) polymerase-1 (PARP-1) is a DNA repair enzyme and inhibitors are potentially useful when combined with specific anticancer therapeutic

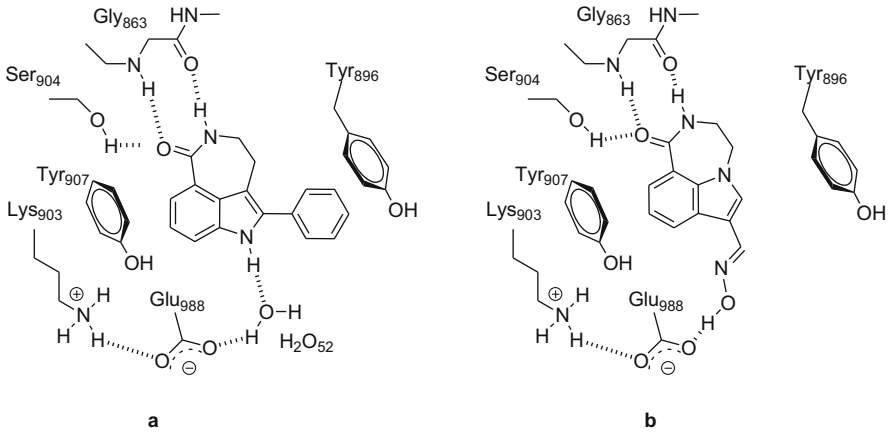

Fig. 11 Depiction of the key intermolecular interactions between chicken poly(ADP-ribose) polymerase-1 and indole-based inhibitors

Table 8 Inhibitor of human poly(ADP-ribose) polymerase-1 by 3,4-dihydro-[1,4]diazepino [6,7,1-*hi*]indol-1(2*H*)-ones

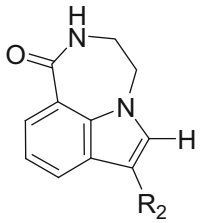

Compound no.	R_2	K_i vs human PARP (nM)
63	H	105
64	CH_2OH	79
65	(E)-CH=NOH	9.4
66	(*E*)-C=$NOCH_3$	809
67	(*Z*)-C=$NOCH_3$	121

agents by prolonging their antitumor activity [113–115]. Co-crystallization of the potent human PARP-1 inhibitor 5-phenyl-2,3,4,6-tetrahydro-1*H*-azepino[5,4,3-*cd*] indol-1-one, $K_i = 6$ nM, with chicken PARP revealed the presence of a water molecule, designated H_2O_{52}, that interfaced between the indole NH and Glu_{988}, as depicted in Fig. 11a [113]. A family of 3,4-dihydro-[1,4]diazepino[6,7,1-*hi*] indol-1(2*H*)-ones **63–67** (Table 8) was designed that relied upon the concept of topological inversion of the indole heterocycle to an isostere that allowed functionalization at C-3 with substituents capable of displacing H_2O_{52} and directly engaging Glu_{988} [114]. The (*E*)-carboxaldehyde oxime **65** depicted in Fig. 11b

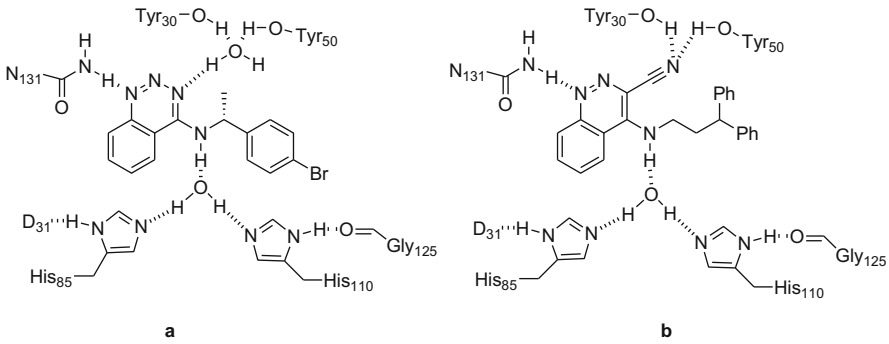

Fig. 12 Binding interactions between scytalone dehydratase and inhibitors

satisfied the design criteria and is characterized as a potent human PARP-1 inhibitor, $K_i = 9.4$ nM, that is over tenfold more potent than the prototype **63**. Indole **65** is severalfold more potent than the hydroxymethyl derivative **64** and the key structure-activity observations with the O-methylated derivatives **66** and **67** are consistent with the fundamental design hypothesis that the oxime moiety displaced H_2O_{52}. This was definitively confirmed by solving the co-crystal structure of oxime **65** with the enzyme which revealed the oxime OH engaging Glu_{988} as proposed, as captured in Fig. 11b. Interestingly, the potency-enhancing effect of introducing the oxime moiety was muted in a series of compounds that incorporated a C-6 aryl substituent [113–115].

The enzyme scytalone dehydratase catalyzes two steps in melanin biosynthesis in *Magnaporthe grisea*, a plant fungal pathogen [116]. The benzotriazine **68** is a potent scytalone dehydratase inhibitor and modeling of the analogue **72** in the active site of the enzyme (Fig. 12a) recognized its isosteric relationship with the salicylamide **71** which had been co-crystallized with the enzyme. A water molecule that played a critical role in mediating the interaction between the inhibitor and two enzyme residues, Tyr_{30} and Tyr_{50}, by H-bonding to the benzotriazine moiety of **68** and the amide carbonyl of **72** was viewed as an opportunity for optimization of the scaffold. The removal of the key benzotriazine nitrogen atom that accepted a H-bond from the water molecule afforded the much weaker inhibitor cinnoline **69**, but the introduction of a nitrile moiety at the 3-position of the heterocycle provided a molecule, **70**, that is over 18,000-fold more potent than the progenitor [116]. The remarkable increase in potency for the addition of just two atoms represents a highly ligand-efficient modification that was also observed with an analogous quinazoline/quinoline matched pair [116, 121]. An X-ray co-crystal structure of **70** bound to the enzyme confirmed the modeling hypothesis and validated the design principle, as summarized in Fig. 12b [116].

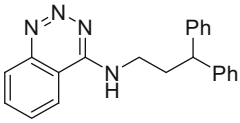

68, K_i = 0.22 nM

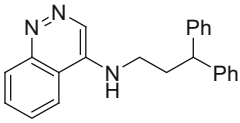

69, K_i = 140 nM

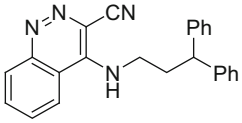

70, K_i = 0.0077 nM

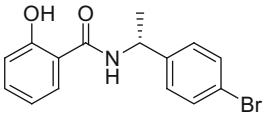

71

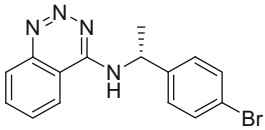

72

A similar strategy was adopted to enhance the potency of the triazine-based p38α MAP kinase inhibitor **73**, $K_i = 3.7$ nM, in which the key N atom of the triazine heterocycle was replaced by C-CN in order to displace a bound water molecule observed in an X-ray co-crystal structure [117]. This rationalization led to the design of the cyanopyrimidine **74** which, with a $K_i = 0.057$ nM, conferred a 60-fold enhancement of potency. X-ray crystallographic data obtained with a closely analogous compound demonstrated that the cyano moiety engaged the NH of Met_{109} in a H-bonding interaction, displacing the water molecule interfacing Met_{109} with the triazine N of **73**, as hypothesized during the design exercise.

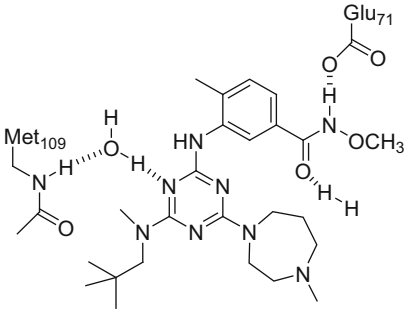

73

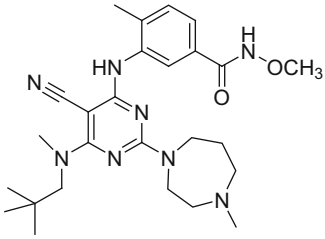

74

The displacement of a water molecule mediating the interaction between a series of heat shock protein 90 (Hsp90) inhibitors and the protein by the introduction of a strategically deployed cyano substituent contributed significantly to potency [119]. The pyrrolopyrimidine **75** was designed from the fragment screening lead **77** but was devoid of significant potency based on the results of a fluorescence polarization assay. This was attributed to the loss of a key H-bond between the imidazole

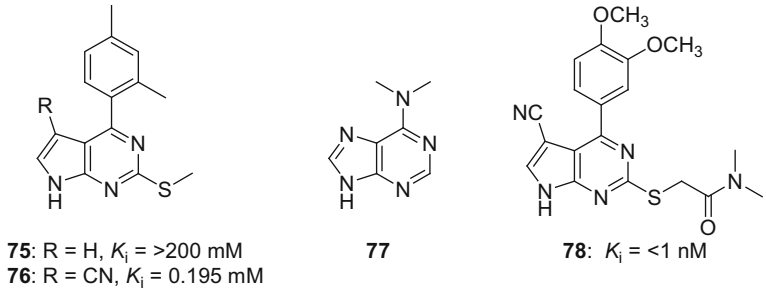

Fig. 13 Principal drug–target interactions between pyrrolopyrimidine **78** and Hsp90

nitrogen atom of **77** and a water molecule that interfaced with Asn_{51} of Hsp90 and another water molecule in the active site. The introduction of the 3-cyano moiety to **75** gave the significantly more potent Hsp90 inhibitor **76** with the nitrile nitrogen atom engaging Asn_{51} directly, displacing the water molecule. Further optimization afforded the more potent **78** that engaged the Hsp90 protein principally via the interactions summarized in Fig. 13 [119].

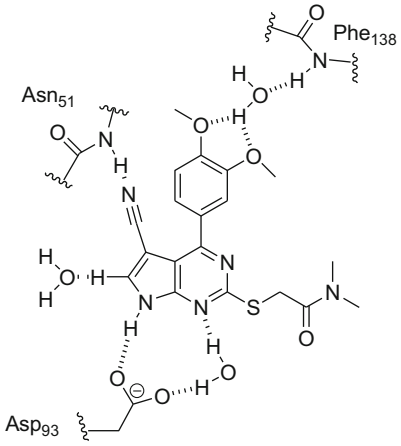

One of the difficulties associated with displacing bound water molecules is illustrated by observations with a series of human prostaglandin D2 synthase (hH-PGDS) inhibitors based on the prototype **79**, $IC_{50} = 2.34$ nM [120]. In the X-ray co-crystallographic structure of **79** with the enzyme, the isoquinoline nitrogen was observed to engage the hydrogen atom of a water molecule that interacted with Thr_{159} and Leu_{199} of hH-PGDS, leading to a study of the effect of incorporation of structural elements designed to displace the bridging water. The hydroxymethylated naphthalene derivative **80** and its amine analogue **81** were synthesized and confirmed by X-ray studies to perform as anticipated, displacing the water molecule and directly engaging Thr_{159} and Leu_{199} with the full complement of interactions. However, the potency of these compounds was significantly diminished compared

to **79** with IC_{50}s of 1,480 nM for **80** and 845 nM for **81**, representing 360- and 630-fold differences, respectively [120]. A potential explanation was suggested based on a closer analysis of the crystal structures which revealed that the topographical disposition of the hydroxyl and amino moieties of **80** and **81** was close to the plane of the naphthalene ring (21° and 27°, respectively), an energetically unfavorable arrangement that incurs allylic 1,3 strain [10, 122]. In addition, the dihedral angle between the phenyl and naphthalene rings was ~20° less than the 117° observed for **79**, data that taken together suggested that the increased energy associated with the imposed conformational constraints outweighed the entropic gains associated with displacing the water molecule [120].

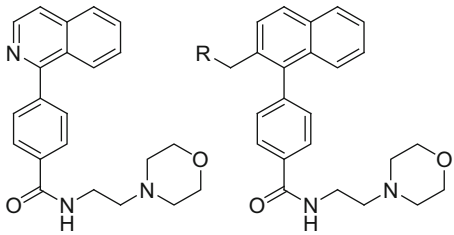

79 **80**: R = OH
81: R = NH_2

3 Bioisosteres to Modulate Conformation

3.1 Fluorine as a Hydrogen Isostere

The properties of fluorine make it an intriguing and useful isostere of a hydrogen atom, particularly in the context of alkanes where its unique properties have only recently begun to be examined in detail and more fully appreciated [16–21, 123–125]. Fluorine is the most electronegative of the atoms that forms covalent bonds with carbon and the polarization associated with the C–F bond affords a strong dipole moment, 1.85 D for CH_3F, that interacts with proximal functionality to influence conformational preferences in a fashion that can be exploited in drug design. These effects, the strength of which are dependent on the identity of the interacting substituent, are based on several underlying principles that include dipole–dipole interactions, attractive electrostatic effects, repulsion between fluorine and electronegative atoms, p orbital repulsion, and a hyperconjugative effect between an adjacent C–H bond and the low-lying C–F σ* orbital [21, 124–126]. Density functional theory (DFT) calculations have provided a relative ranking of the interaction energies between a fluorine atom and several elements and functional groups, with interactions with amine, alcohol, amide, and fluorine substituents of sufficient strength to be of practical utility in drug design exercises, data that are summarized in Table 9 [124–126].

Table 9 Energy differences between the *gauche* and *anti* conformers of α-substituted fluoroethanes based on DFT calculations

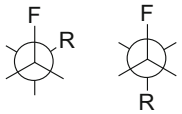

gauche *anti*

R	Δ Energy *gauche-anti* (kcal/mol) B3LYP	Δ Energy *gauche-anti* (kcal/mol) M05-2X	Preferred conformer	Predicted underlying effect
$-NH_3^+$	−6.65	−7.37	Strongly gauche	Electrostatic Fδ⁻ and NH_3^+ δ^+
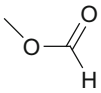	−1.40	−2.18	Strongly gauche	Electrostatic C-F δ^- and C=O C δ^+
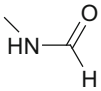	−1.00	−1.12	Strongly gauche	Electrostatic C-F δ^- and N-H δ^+
–F	−0.82	−0.66	Strongly gauche	σC(F)-H to σ*C-F
$-N_3$	−0.76	−1.21	Strongly gauche	Electrostatic C-F δ^- and central N δ^+
–CHNH	−0.25	−0.65	Strongly gauche	
$-CH_3$	−0.18	−0.35	Weakly gauche	
$-CHCH_2$	−0.01	−0.17	Weakly gauche	
–C≡N	0.64	−0.64	Strongly anti	p Orbital repulsion
–CHO	0.84	−1.20	Strongly anti	p Orbital repulsion and anti-parallel dipole: C=Oδ⁻... δ^+HCF δ^-
–C≡CH	0.98	−1.03	Strongly anti	p Orbital repulsion

1,2-Difluoroalkanes prefer a *gauche* conformation between the two fluorine atoms that is favored by 0.8 kcal/mol based upon a hyperconjugative interaction between an adjacent C–H bond donating into the low-lying C–F σ* orbital (Fig. 14a) [126, 127]. For 1,3-difluoroalkanes, the conformational preference depicted in Fig. 14b is favored by dipole–dipole interactions between the C–F bonds that is estimated to amount to a difference of 3.3 kcal/mol [128]. However, while these interactions have been shown to influence the conformational preferences of structurally simple fluoroalkane derivatives, they have yet to be fully exploited in drug design [126–130].

The conformation of an α-fluoro amide is influenced by the preference for the dipoles of the C–F and C=O moieties to align in an antiparallel fashion that in secondary amides can be reinforced by an electrostatic interaction between the electronegative F atom and amide NH [21, 131–136]. An interesting illustration of the utility of this effect is provided by the biological evaluation of the enantiomers of **83**, the α-fluorinated derivative of the vanilloid receptor agonist capsaicin (**82**) [136]. The *trans* conformer in which the C–F and C=O dipoles are aligned

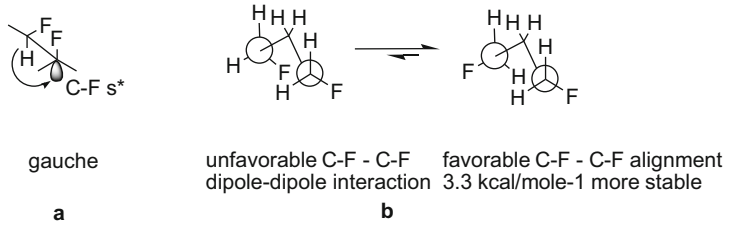

Fig. 14 Conformational preferences of 1,2- and 1,3-difluoroalkanes and the underlying interactions

in the same plane in an antiparallel fashion is calculated to be 6 kcal/mol more stable than the *gauche* conformer and 8 kcal/mol more stable than the *cis* conformer based on ab initio calculations, attributed to a favorable dipole alignment and an electrostatic interaction between the F and NH atoms, as depicted in Fig. 15 [131–136]. This conformational preference provided a potentially useful probe of the shape of the receptor based on the stereo-differentiation of the (*R*)- and (*S*)-enantiomers of **83** should the alkyl side chains project orthogonally to the plane of the amide moiety in the bound state, as depicted by the hashed bonds. However, the TRPVI receptor failed to discriminate between the two enantiomers of **83**, leading to the conclusion that the bound conformation of **82** is that in which the alkyl side chain vector projects in a plane similar to that of the amide moiety which for (*R*)- and (*S*)-**83** would be disposed in the parallel fashion depicted [136].

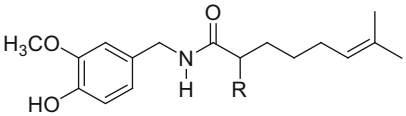

82: R = H, capsaicin
83: R = F, F-capsaicin

A fluorine atom deployed β- to the nitrogen atom of an amide also influences conformational preferences by favoring a *gauche* arrangement between these functionalities, a phenomenon established by X-ray crystallographic and NMR studies in the context of a series of β-peptide derivatives [126, 134, 135, 137–139]. For the difluoro succinamide esters **85** (*threo*) and **87** (*erythreo*) and the corresponding acids **84** (*threo*) and **86** (*erythreo*), solid-state structures revealed that all 4 molecules adopted a conformation that satisfied a vicinal F–F *gauche* interaction, a phenomenon that extended to solution based on an analysis $^3J_{HF}$ and $^3J_{HH}$ coupling constants in the NMR spectra [134, 135]. In the case of the *threo* isomers **84** and **85**, this conformational preference places the amide carbonyl moieties in an anti-periplanar arrangement while for the *erythreo* isomers, the amide carbonyls are disposed *gauche* [134, 135].

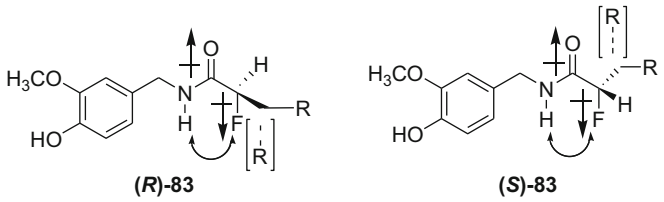

Fig. 15 Conformational analysis of the enantiomers of α-fluoro capsaicin (**83**)

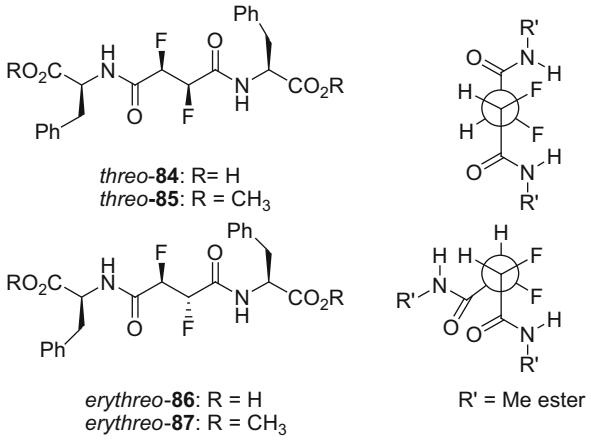

For the GPR119 agonist **88**, $EC_{50} = 868$ nM with intrinsic activity of 111% in a cAMP assay, isosteric replacement of the pro-(*S*) H atom β- to the amine moiety resulted in **89**, a compound with tenfold enhanced potency, $EC_{50} = 80$ nM, and similar intrinsic agonistic properties, measured as 107% [140]. The F atom was introduced based on an appreciation of its potential to influence conformational preferences, a hypothesis confirmed by NMR analysis which revealed a population of the conformation in which the F and NH atoms are *gauche* amounting to 75% in $CDCl_3$ solution [140].

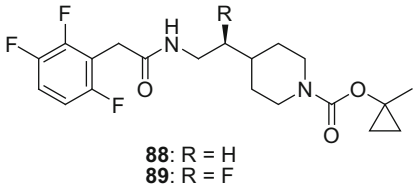

The *gauche* interaction between a fluorine atom and an amide influences the conformational preference of proline with the 4-(*R*)-F and 4-(*S*)-F derivatives **90** and **91**, respectively, favoring complementary conformers [124]. The incorporation of (*R*)- and (*S*)-4-F-Pro into collagen fibrils markedly affects the properties of the polymer in a fashion that has provided insight into the stabilizing effects of the

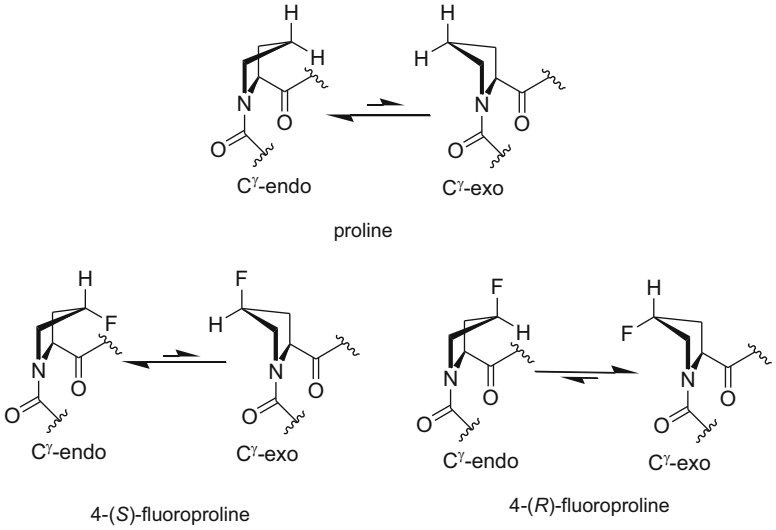

Fig. 16 Conformational preferences for proline, 4-(*S*)-fluoroproline, and 4-(*R*)-fluoroproline

4-(*R*)-hydroxyproline that occurs naturally in collagen [124, 141–146]. These studies have led to the suggestion that the stabilizing effect of 4-(*R*)-hydroxyproline on collagen, which is manifested as favoring a tightly wound helix structure, is the result of an inductive effect rather than a H-bonding interaction of the 4-OH substituent. The C^{γ}-endo conformation of proline is preferred by a modest 0.41 kcal/mol, leading to a 2:1 population of this conformer at room temperature while 4-(*R*)-hydroxyproline favors the C^{γ}-exo conformer by a calculated 0.48 kcal/mol (Fig. 16) [147]. For 4-(*S*)-F proline (**91**), the C^{γ}-endo conformation is favored by 0.61 kcal/mol, attributed to stabilization by the *gauche* effect between fluorine and the amide moiety which leads to the F atom adopting an axial disposition, an arrangement that is observed in the single-crystal X-ray structure (Fig. 16) [147, 148]. In contrast, 4-(*R*)-fluoroproline (**92**) prefers the C^{γ}-exo conformation by 0.85 kcal/mol, with the *gauche* effect between the F and amide moieties favoring an equatorial disposition of the F atom [147]. The C^{γ}-exo conformation mimics that preferred by 4-(*R*)-hydroxyproline and provides an explanation for the structural similarity of collagen fragments that incorporate either 4-(*R*)-hydroxy- or 4-(*R*)-fluoroproline [149].

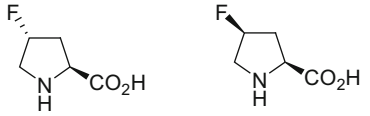

90 4-(*R*)-fluoroproline **91** 4-(*S*)-fluoroproline

3-Fluoroproline also exhibits conformational bias as illustrated by studies with the diastereomeric esters **92** and **93** [150]. Both of these compounds crystallize with a *trans* configuration between the amide and ester moieties, as depicted in the structures of **92** and **93**, but the proline rings adopt quite different conformations. In each case, the F atom is axially disposed, favored by a stabilizing *gauche* interaction with the amide moiety such that the pyrrolidine ring of the (*R*)-isomer **92** adopts the C^{γ}-exo conformation while, in contrast, the (*S*)-isomer **93** favors the C^{γ}-endo arrangement [150]. In solution, the C^{γ}-endo conformation of **93** dominated based on the $\leq$1 Hz coupling constant between the α- and β-protons in the ^{1}H-NMR spectrum, an observation supported by calculations that indicate that this conformation should be preferred by a ratio of 97:3. For the 3-(*R*)-isomer **92**, unfavorable steric and electronic repulsive effects between the F atom and ester moiety led to a preference for the C^{γ}-exo conformation, populated to the extent of 69%. Notably, the conformational preferences of each of these 2 proline derivatives were expressed when they were incorporated into short peptide sequences [145, 150, 151].

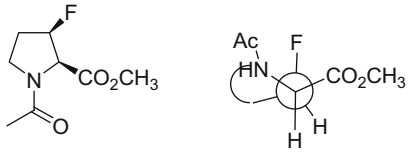

92: 3-(*R*)-fluoroproline

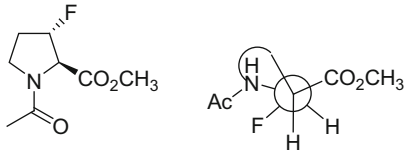

93: 3-(*S*)-fluoroproline

β-Amino fluoroalkanes exhibit conformational bias based on *gauche* interactions between the amine and F moieties, the energetics of which depend on the protonation state [21, 124, 152]. In the unprotonated form, a *gauche* relationship between the NH_2 and F of 2-fluoroethylamine is weakly favored by an energy estimated to be ~1 kcal/mol, an interaction considered to be a bridging H-bond. However, protonation results in a much stronger preference for a *gauche* relationship between the F atom and the charged amine that is estimated to be 5.8 kcal/mol and attributed to a favorable electrostatic (charge–dipole) interaction between the charged amine and the electronegative F atom [21, 124, 152]. These energetic preferences are such that cyclic amines experience considerable conformational bias, exemplified most effectively by the analysis of the protonated form of 3-fluoro-*N*-methyl-piperidine (**94**) as summarized in Fig. 17 [153–155]. Despite experiencing steric compression, the ring F atom of **94** overwhelmingly prefers an axial disposition, with conformer A in Fig. 17 representing the global minimum and favored to the extent of 95–96%,

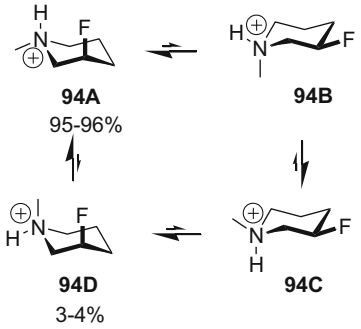

Fig. 17 Conformational preference of *N*-methyl-3-fluoropiperidine (**94**) in its protonated form

stabilized by an electrostatic interaction between the F and NH^+ moieties [155]. Conformer D contributes only 4–5% of the population at equilibrium, with a productive electrostatic effect compensating for unfavorable diaxial interactions between the F and CH_3 moieties.

The synthesis and evaluation of the two fluorinated enantiomers **96** and **97** of γ-aminobutyric acid (GABA, **95**) provided some insight into the conformation of the neurotransmitter when bound to cognate receptors or that recognized by the aminotransferase (Fig. 18) [156, 157]. Fluorination of GABA (**95**) increases the acidity of the carboxylic acid moiety and decreases the basicity of the amine but preserves the zwitterionic nature of the molecule at neutral pH. NMR analysis indicated that all molecules adopted an extended conformation in solution but with **96** and **97** further preferring an arrangement in which a favorable *gauche* interaction occurs between the fluorine and the NH_3^+ moiety [156]. The available conformations for each of the enantiomers **96** and **97** are captured in Fig. 18 with those that are disfavored based on the absence of a *gauche* effect noted [156]. Both **96** and **97** activated the cloned human $GABA_A$ receptor with comparable potency, although both were significantly less potent than the natural neurotransmitter **95**, results that are consistent with the bound form of the neurotransmitter being the extended conformation represented by B in Fig. 18 that is accessible to all three compounds [156, 157]. However, GABA aminotransferase was able to differentiate **96** and **97**, catalyzing elimination of HF from the latter with 20-fold higher efficiency than for **96**, an observation that suggested that the enzyme recognizes a conformation in which the NH_3^+ and CH_2CO_2- moieties are disposed in a *gauche* arrangement, as represented by conformation C in Fig. 18 [156, 157]. Both fluorinated derivatives were agonists at ρ1 and ρ2 $GABA_C$ receptors, with the (*R*)-isomer **97** tenfold weaker and the (*S*)-isomer **96** 20-fold weaker than the natural ligand **95** [158]. This was attributed to weaker electrostatic interactions due to the reduced basicity of the amine, observations that taken together suggested that GABA (**95**) binds to the $GABA_C$ receptor in the folded orientation represented by conformation C in Fig. 18 [158].

In an analogous fashion, the bound conformation of *N*-methyl-D-aspartate (**99**), an agonist mimetic of glutamic acid (Glu, **98**), at recombinant GluN2A and GluN2B receptors expressed in *Xenopus laevis* oocytes was probed through the synthesis

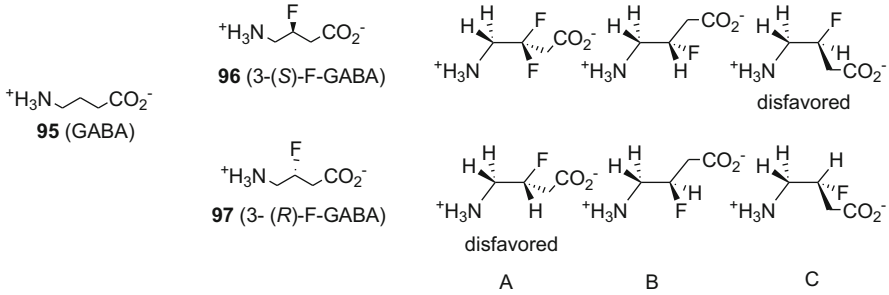

Fig. 18 Structures of GABA (**95**), the enantiomeric fluorinated derivatives **96** and **97**, and their preferred conformations

and evaluation of (2*S*,3*S*)-3F-NMDA (1**00**) and (2*S*,3*R*)-3F-NMDA (**101**), the available conformations of which are depicted in Fig. 19 [159]. ^{1}H- and ^{19}F-NMR spectral data were consistent with **100** adopting conformation A in solution while DFT calculations suggested that **101** would prefer the conformation represented by B in Fig. 19, which was observed in the single-crystal X-ray structure. (2*S*,3*R*)-3F-NMDA (**101**) exhibited no significant effect in the biological assays while (2*S*,3*S*)-3F-NMDA (**98**) induced currents in oocytes expressing either GluN2A or GluN2B receptors, although the maximal responses were less than that observed with NMDA (**99**) [159]. These observations are consistent with only (2*S*,3*S*)-3F-NMDA (**100**) being able to adopt a conformation that mimics the receptor-bound form of NMDA (**99**), designated as A in Fig. 19, results that concur with the X-ray crystallographic structure of NMDA (**99**) bound to the GluN2D receptor that is highly homologous to GluN2A and GluN2B.

β-Fluoroethanol derivatives do not exhibit a strong conformational preference in the absence of an intramolecular interaction between the F and OH moieties which stabilizes a *gauche* arrangement by approximately 2 kcal/mol [152, 160, 161]. However, this effect is significantly reinforced by protonation of the alcohol which stabilizes the *gauche* conformer by an energy estimated at ~7 kcal/mol and which has been attributed to the combination of a stereoelectronic effect and an intramolecular H-bonding-type interaction. The HIV-1 protease inhibitor indinavir (**102**) and its epimer **103** presented an interesting opportunity to probe the consequences of introducing F-OH interactions on conformational disposition, probed with the congeners **104–107**, that could readily be equated with enzyme inhibitory activity, measured as the K_i values that are summarized in Fig. 20 [162]. In addition to influencing conformation, it was anticipated that the introduction of a F atom to indinavir (**102**) would affect the acidity of the OH, potentially introduce steric interactions between drug and target, and also affect solvation. In the indinavir series, the *syn*,*syn* analogue **104** exhibits potency comparable to the prototype **102** while the *anti*,*anti* isomer **106** is tenfold less active. The *syn*,*anti* epi-indinavir derivative **107** is eightfold more potent than progenitor **103**, but the *anti*,*syn* diastereomer **105** with a K_i of 5,900 nM is substantially (36-fold) less active [162]. The 2 most potent fluorinated compounds *syn*,*syn* (**104**) and *syn*,*anti* (**107**) were

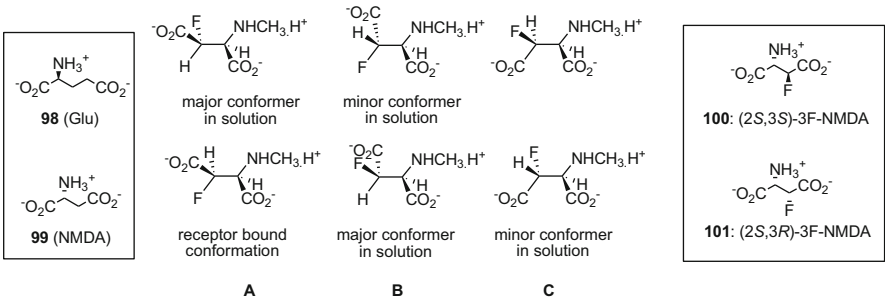

Fig. 19 Structures of glutamate (**98**) NMDA (**99**), the enantiomeric fluorinated derivatives **100** and **101**, and their preferred conformations

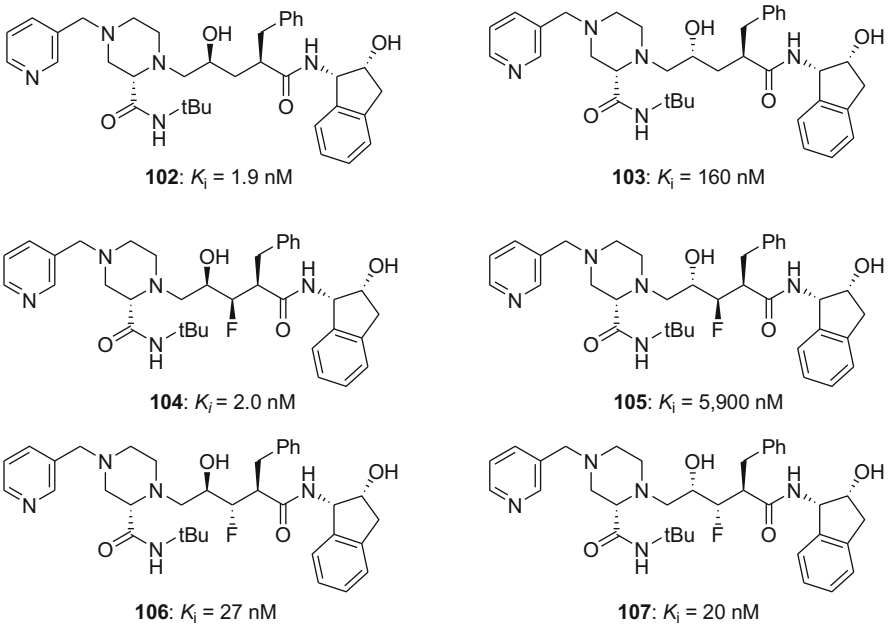

Fig. 20 The structures and HIV-1 protease inhibitory activity associated with indinavir (**102**), epi-indinavir (**103**), and the 4 fluorinated analogues **104–107**

both shown to adopt a fully extended conformation in solution based on ^{1}H-^{1}H and ^{1}H-^{19}F coupling constants, stabilized by a *gauche* relationship between the F and OH moieties, which is similar to that of indinavir (**102**) when bound to HIV-1 protease. However, the solution conformations of the less potent fluorinated diastereomers **105** and **106** were considerably more complex, sampling several additional populations and providing a potential explanation for the weaker protease inhibitory activity.

3.2 The Conformation of Substituted Phenyl and Heteroaryl Derivatives and Isosterism

The topographical preferences of substituted aryl and heteroaryl rings are dependent upon both ring structure and the identity of the substituent atom [10, 163]. An illustration of the effect of substituent identity on biological activity is illustrated by the structure–activity relationships associated with the three non-prostanoid prostacyclin agonists **108–110** compiled in Table 10 which reveal a significant limitation on one of the simplest of the classic isosteric relationships, that between O and CH_2 [10, 65, 66]. The results have been interpreted based on the conformational preferences captured in Fig. 21 with the ether **108** and cinnamate **110** considered to be more potent based on the facility with which they are able to adopt an overall coplanar configuration with the phenyl ring, which contrasts with **109** in which the alkyl side chain projects orthogonally to the plane of the aromatic ring as a consequence of allylic 1,3-strain [10, 65, 66, 122, 163].

For the HIV-1 non-nucleoside reverse transcriptase inhibitor (NNRTI) **111**, replacing the OCH_2 moiety with a CH_2 linker afforded **112** which largely preserved antiviral activity, suggesting that in this context there is an isosteric relationship between the OCH_2 and CH_2 moieties [164]. This thesis was supported by the good alignment of the key elements of **112** when docked over the X-ray crystallographic structure of **111** bound to the enzyme and reflects the specific orientation of **111** in the enzyme in which the plane of the chlorophenyl and azaindazole rings approach orthogonality.

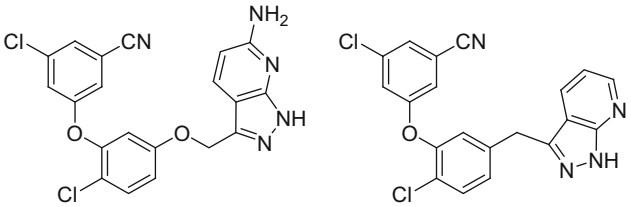

111: EC_{95} WT = 8.4 nM **112**: EC_{95} WT = 22 nM

The conformational preference for arylmethyl ethers that are devoid of *ortho* substitution is one in which the MeO moiety is close to coplanarity with the phenyl ring and is rationalized on the basis of a rehybridization of the substituent to maximize electronic overlap between the oxygen lone pair and the π system [163]. However, in trifluoromethoxy- and difluoromethoxy-substituted benzenes, the substituent behaves more like an alkyl moiety, projecting orthogonally to the plane of the aromatic ring [165–169]. This conformation is calculated to be energetically favored by ~0.5 kcal/mol over the coplanar topography, which contrasts with the 3 kcal/mol preference for planarity calculated for anisole. An example where this effect appears to be manifested, at least in part, is provided by the cholesteryl ester transfer protein inhibitor **113**, $IC_{50} = 1.6$ μM, which

Table 10 Platelet aggregation inhibition associated with a series of non-prostanoid prostacyclin agonists

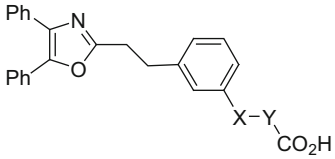

Compound no.	X	Y	Inhibition of platelet aggregation EC_{50} (μM)
108	O	CH_2	1.2
109	CH_2	CH_2	16
110	*t*CH=CH		0.66

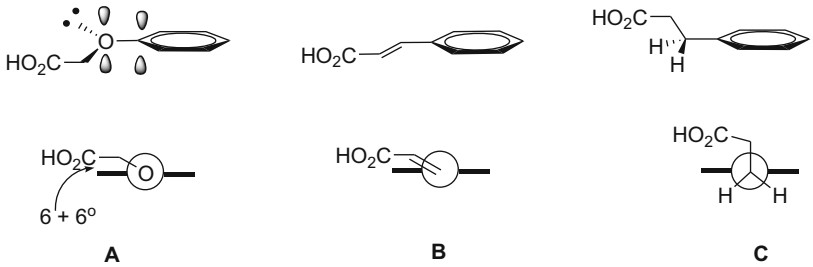

Fig. 21 Preferred conformations of phenoxyacetic acid, cinnamic acid, and phenylpropanoic acid

is eightfold less potent than the fluorinated analogue **114**, $IC_{50} = 0.2$ μM, a structure–activity relationship attributed to both the effect of steric presentation of the substituent and a favorable drug–protein interaction [16, 166]. In this example, ab initio calculations indicate that while the ethoxy moiety in **113** is more stable when coplanar with the phenyl ring, the substituent in **114** prefers a vector that is closer to perpendicular.

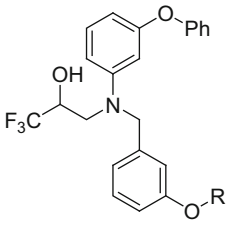

113: R = CH_2CH_3
114: R = CF_2CHF_2

Heteroaryl ethers, in which the substituent is attached to a carbon atom adjacent to a heteroatom, exhibit a topological preference based on lone pair-lone pair repulsive interactions, the energetics of which can be considerable and of both significance and utility in drug design [170–174]. The conformational preferences for a series of methoxy-substituted 5- and 6-membered heterocycles based on DFT calculations are summarized in Fig. 22 and reveal that, with the exception of furan and thiophene, the equilibrium is significantly biased for all cases examined [170]. This preference was used as a design principle to good effect in the identification of the factor Xa inhibitor ZK-807834 (**117**), a compound that has its origin in the 2,7-dibenzylidenecycloheptanone **115** [171–173]. The progenitor **115** gave a cause for concern based on the potential for photochemically induced olefin isomerization, prompting conception of the pyridine ether chemotype represented by **116** which was designed based on the conformational analysis summarized in Fig. 23. ZK-807834 (**117**) is a potent factor Xa inhibitor, $K_i = 0.11$ nM, and an X-ray co-crystal structure confirmed the predicted topology for the acyclic amidine-substituted phenyl ether although the ring with the cyclic amidine moiety adopted the less stable conformation [173].

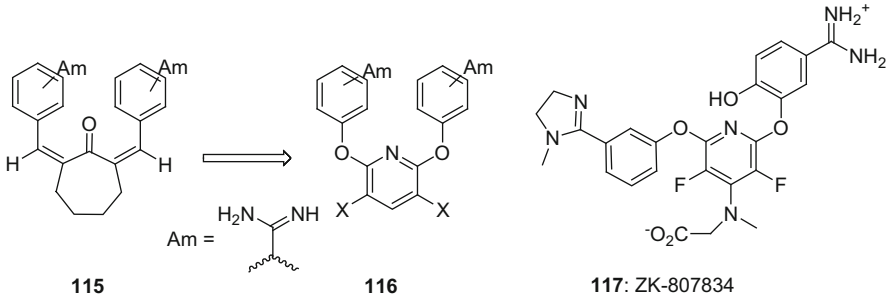

Two more recent examples where this phenomenon may be operative are provided by the corticotropin-releasing factor (CRF) antagonist **119**, which has potential for the treatment of depression and anxiety, and the GPR119 agonist **121** that promotes postprandial insulin secretion and may be useful for the treatment of diabetes [174, 175]. In both cases, a heteroaryl phenyl ether is employed to mimic the topology inherent to a fused heterocyclic ring system, the pyrrolo[2,3-*d*]pyrimidine **118** in the case of **119** and the pyrazolo[3,4-*d*]pyrimidine **120** in the case of **121**. In both examples, the favorable effect of the nonbonded lone pair-lone pair interactions may be augmented by intramolecular steric effects afforded by the heteroaryl CH_3 substituent that is manifested as allylic 1,3-strain [174, 175].

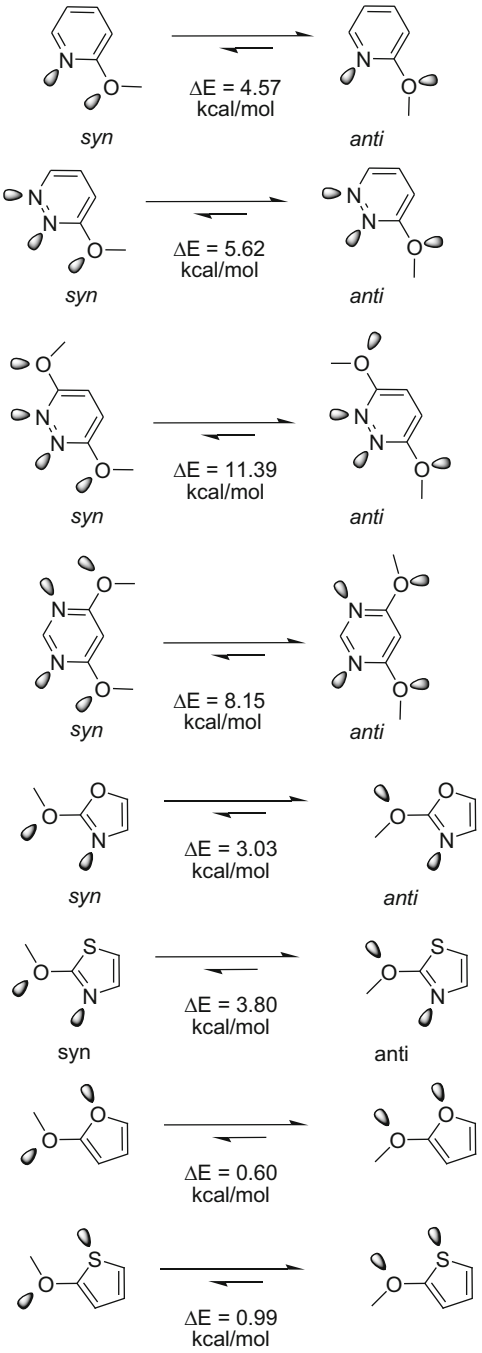

Fig. 22 Conformational preferences or heteroaryl ethers based on density functional calculations

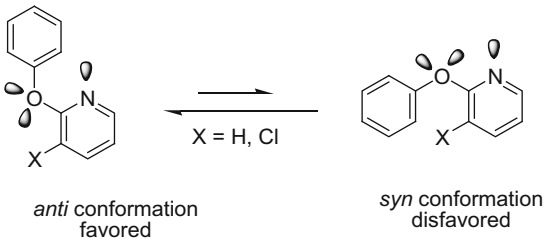

Fig. 23 Analysis of the topological equilibrium associated with the 2-phenoxy pyridines

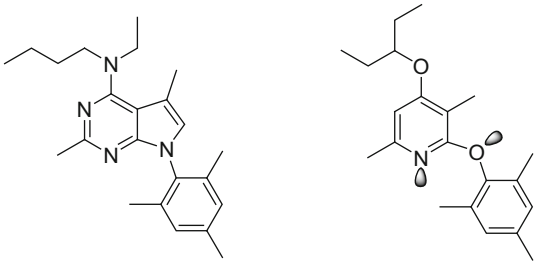

118
CRF IC_{50} = 5.5 nM

119
CRF IC_{50} = 6.8 nM

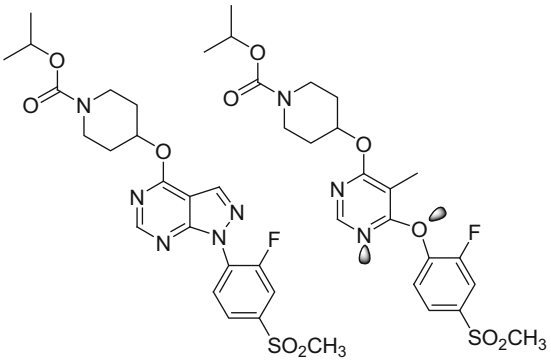

120
GPR119 EC_{50} = 2.7 nM
Emax = 89%

121
GPR119 EC_{50} = 9.7 nM
Emax = 59%

The conformational bias provided by an alkyl substituent bound to a phenyl ring has been used to advantage in the design of the factor Xa inhibitor **123** (Table 11) which is based on the biphenyl prototype **122**, in which improved physical properties (lower molecular weight and cLog*P*) were sought [176]. In this example, a cyclopropyl substituent was designed to replace the phenyl ring distal from the methoxyphenyl moiety that engages the enzyme S1 sub-pocket. A careful analysis of phenylcyclopropane conformation indicated that for compounds with a benzylic

Table 11 Potency and physical parameters of drug–target interactions associated with the factor Xa inhibitors **122** and **123**

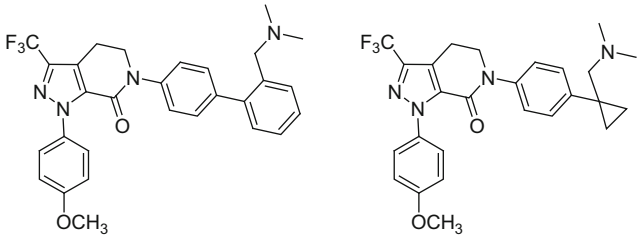

	122	**123**
K_i (nM)	0.3	0.035
Log*P*	5.94	4.99
MW	520.5	484.2
HAC	38	35
LE	0.34	0.41
LLE	3.58	5.47
LELP	17.47	12.35
Fsp^3	0.24	0.38

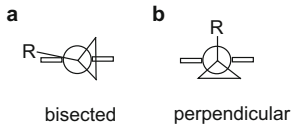

Fig. 24 Perpendicular and bisected conformations of phenylcyclopropane

H atom, the cyclopropane ring adopts a conformation designated as bisected (conformation A in Fig. 24) that is stabilized by electronic effects associated with overlap of the cyclopropyl carbon-carbon bond orbitals with the π system. However, the introduction of a benzylic substituent alters the preference to favor a perpendicular conformation (conformation B in Fig. 24), 0.7 kcal/mol more stable for CH_3, that would more effectively mimic that of the biphenyl moiety of **122** and project the dimethylamine into the enzyme S4 pocket. Reduction to practice revealed that the phenylcyclopropane **123** is close to an order of magnitude more potent than **122**, attributed to optimized hydrophobic interactions with the S4 pocket and slightly reduced strain in the bound geometry, as summarized in Table 11 [176]. In addition, the phenylcyclopropane **123** exhibits a reduced cLog*P* (1 $\log_{10}$) and a lower molecular weight that, when combined with the improved potency, affords significant improvements in ligand efficiency (LE), ligand-lipophilicity efficiency (LLE), lipophilicity-corrected ligand efficiency (LELP), and Fsp^3, the ratio of sp^3 C atoms to the total number of C atoms, all factors that are believed to be associated with increased drug durability in development [121, 177–182].

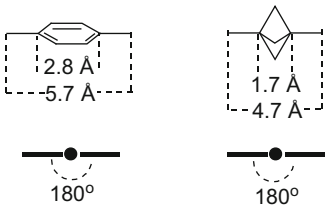

Fig. 25 Comparison of vectors and dimensions of a phenyl and bicyclo[1.1.1] pentane moiety

The bicyclo[1.1.1]pentane moiety is another isostere that mimics the conformation of a phenyl ring while simultaneously reducing lipophilicity and increasing Fsp^3. This moiety originally demonstrated value in the context of the glutamate antagonists **124**–**126** but more recently has found utility in inhibitors of the amyloid precursor protein processing enzyme γ-secretase **127** and **128** [183–186]. The presentation of the two key vectors by the bicyclo[1.1.1]pentane ring faithfully reproduces that of the *para*-substituents of a phenyl ring, but the dimensions are such that the distance between the substituents is ~1 Å shorter, as captured in Fig. 25 [186]. In the case of the glutamate antagonist **125**, a mimic of **124**, this could readily be compensated by deploying the larger tetrazole as a carboxylic acid isostere, although the result was less than impressive [183–185]. However, the propellane-based γ-secretase inhibitor **128** is an effective mimic of the phenyl analogue **127** without resort to additional structural adjustment and this compound offers improved solubility, membrane permeability, and metabolic stability in HLM than the progenitor, data summarized in Table 12 [186]. Moreover, **128** is less lipophilic, Elog$D$ = 3.8 compared to 4.7 for **127**, LLE increases from 4.76 to 6.55, and the introduction of five additional sp^3 carbon atoms more than doubles Fsp^3 from 0.25 to 0.53 [186].

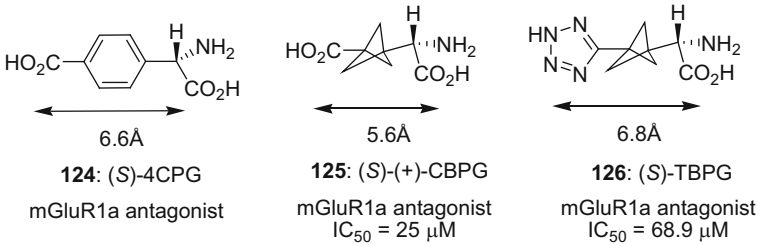

Table 12 Comparison of physical properties for the γ-secretase inhibitors **127** and **128**

Compound no.	Kinetic solubility, pH 6.5 (μM)	Thermodynamic solubility, pH 6.5 (μM)	Permeability: RRCK[a] P_{app} (A to B) [10^{-6} cm/s]	Human hepatocyte $CL_{int,app}$ (μL/min/million cells)	Elog*D*	LLE	LE	LELP	Fsp^3	Ar-sp^3
127	0.60	1.70	5.52	15.0	4.70	4.76	0.28	16.5	0.25	12
128	216	19.7	19.3	<3.80	3.80	6.55	0.30	12.5	0.53	1

[a]RRCK cells with low transporter activity were isolated from Madin–Darby canine kidney cells and were used to estimate intrinsic absorptive permeability

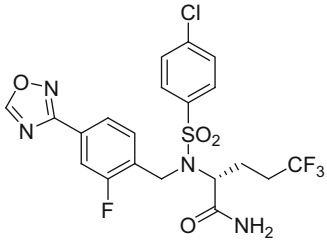

127
IC_{50} (Aβ42) = 0.225 nM

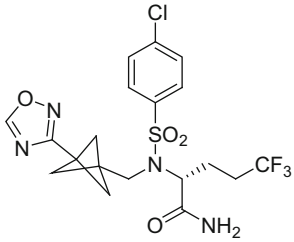

128
IC_{50} (Aβ42) = 0.178 nM

4 Bioisosteres to Modulate Drug Developability Properties

4.1 Isosteres to Modulate Permeability and P-Glycoprotein Recognition

The substitution of a H atom *ortho* to the anilide NH by a fluorine in the two closely related series of factor Xa inhibitors **129–132** and **133–135** resulted in improved Caco-2 cell permeability, as summarized in Table 13 [187, 188]. The observed increase in permeability for **130**, **132**, and **134** compared to the corresponding unsubstituted analogues **129**, **131**, and **133**, respectively, may be due to an effective masking of the H-bond donor properties of the anilide NH by association with the electronegative F atom in an electrostatic interaction [133, 189, 190]. In contrast, an *ortho* nitrile substituent in the aminobenzisoxazole chemotype afforded a compound **135** with significantly reduced permeability, presumably a function of increased acidity and H-bond donor capacity of the NH while geometrical constraints prevent the linear cyanide moiety from establishing an intramolecular H-bond.

The presence of a fluorine atom capable of engaging an amide or sulfonamide N–H in an electrostatic interaction has emerged as a common structural motif, particularly in kinase inhibitors, and may contribute to improved oral exposure, as illustrated by the matched pair comparisons between **136** and **137** and **138** and **139** that are compiled in Table 14 [191, 192].

Intramolecular H-bond capture by a pendent F atom was exploited to reduce P-glycoprotein (P-gp)-mediated brain efflux in a series of β-site amyloid precursor protein cleaving enzyme (BACE1) inhibitors [193–195]. The prototype BACE1 inhibitor **140** presented in Table 15 exhibited a large efflux ratio in cell lines expressing human or rat P-gp while analogues **141** and **142** show improved permeability properties, attributed to an intramolecular interaction between the F atom in the amide cap moiety and the NH, consistent with P-gp substrate recognition that relies upon protein–drug H-bonding [193–197].

Table 13 The effect of substituents *ortho* to an anilide on Caco-2 permeability in two series of factor Xa inhibitors

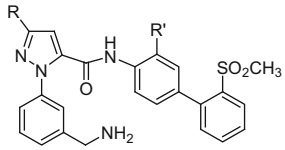

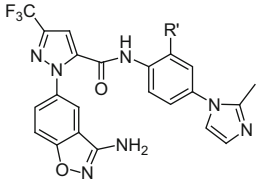

Compound no.	R	R′	Caco-2 permeability (cm/s)	Compound no.	R	Caco-2 permeability (cm/s)
129	CH_3	H	1.20×10^{-6}	**133**	H	0.82×10^{-6}
130	CH_3	F	3.14×10^{-6}	**134**	F	7.41×10^{-6}
131	CF_3	H	3.38×10^{-6}	**135**	CN	$<0.1 \times 10^{-6}$
132	CF_3	F	4.86×10^{-6}			

Table 14 Potency and oral bioavailability of Rho *kinase* (ROCK 1) inhibitors **136** and **137** and the *kinase* insert domain receptor (KDR) inhibitors **138** and **139**

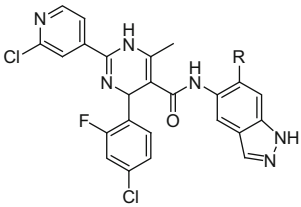

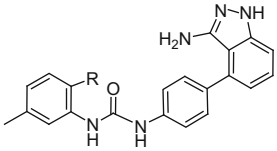

Compound no.	R	ROCK 1 IC_{50} (nM)	F (%)	Compound no.	R	KDR IC_{50} (nM)	F (%)
136	H	4	7	**138**	H	3	38
137	F	7	49	**139**	F	4	100

Table 15 Caco-2 permeability and efflux ratios for the series of BACE1 inhibitors **140–142**

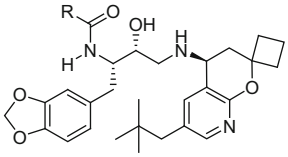

Compound no.	R	BACE1 IC_{50} (nM)	Caco-2 P_{app} (10^{-6} cm/s)	Human efflux ratio	Rat efflux ratio
140	CH_3	8	11	19	49
141		28.9	16	2	4
142	2-FC_6H_4	76.6	11	1	1

A similar tactical approach provided a solution to improved membrane in the series of CNS-penetrant bradykinin B1 antagonists **143–146** compiled in Table 16 which were explored as potential agents for the relief of pain [198]. The introduction of F atoms into the amide moiety resulted in improved passive permeability and reduced P-gp efflux ratios, attributed to a reduction in the strength of the

Table 16 Caco-2 permeability, efflux ratios, and H-bond strength for the series of bradykinin B1 antagonists **143–146**

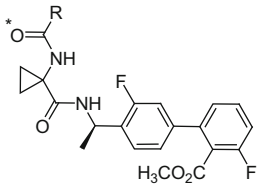

Compound no.	R	hBK1 K_i (nM)	Passive permeability P_{app} (nm/s)	P-gp efflux ratio	HBA (log) strength of C=O*
143	CH_3	0.93	210	8.6	2.12
144	CHF_2	0.40	310	3.2	1.63
145	CF_3	0.57	280	2.3	1.39
146	CF_3CF_2	1.6	310	1.4	1.35

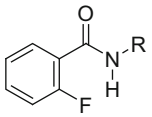

Fig. 26 The *ortho*-fluorinated benzamide motif

carbonyl marked with an asterisk (*) to act as a H-bond acceptor [198]. However, an intramolecular interaction between the F atoms and the NH may also be contributory.

The alternative topology depicted in Fig. 26 offers the potential for a similar electrostatic interaction between the *ortho*-F atom and the benzamide NH and this structural element is also prevalent in drug design [133, 189]. The potent tachykinin hNK_2 receptor antagonist **147** (Table 17) exhibited poor membrane permeability across a confluent Caco-2 cell layer, attributed to the polar amide NH moiety which was critical for potency and could not be modified by methylation or replaced by an isostere [199]. A halogen atom was introduced *ortho* to the amide carbonyl moiety to establish an intramolecular interaction with the NH, described as a H-bond with the fluoro derivative **149**, that resulted in improved permeability across a parallel artificial membrane (PAMPA) or a Caco-2 cell layer while a Cl substituent (**148**) was less effective but still superior to H. In this context, the *ortho*-F substituent in **149** performed somewhat similarly to the nitrogen atom of pyridine **151** which offers a more conventional H-bonding opportunity and markedly improved permeability in both assays compared to the analogous phenyl derivative **150** [199]. The *ortho*-F atom in the antiandrogen enzalutamide (**152**), which was approved for the treatment of castration-resistant prostate cancer by the FDA in August 2012, may contribute to its excellent pharmacokinetic profile [200, 201]. A similar motif is presented by ZD-9331 (**153**), a fluorinated methotrexate analogue which exhibits activity toward ovarian cancer cells resistant to classical thymidylate synthase inhibitors [202, 203].

Table 17 Structure, human NK2 receptor binding affinity, PAMPA, and Caco-2 permeability for a series of phenyl alanine-based antagonists

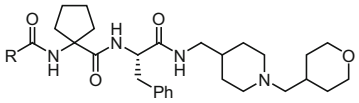

Compound no.	R	pK_i hNK$_2$	PAMPA P_{app} ($\times 10^{-6}$ cm/s)	Caco-2 P_{app} ($\times 10^{-6}$ cm/s)
147	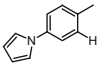	9.63	ND	<1
148	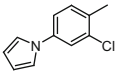	8.40	0.16	4.21
149	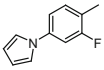	8.49	0.66	13.80
150	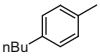	8.34	1.60	9.34
151	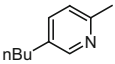	7.57	7.23	17.61

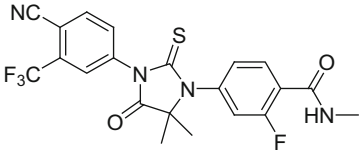

152 (enzalutamide, MDV-3100)

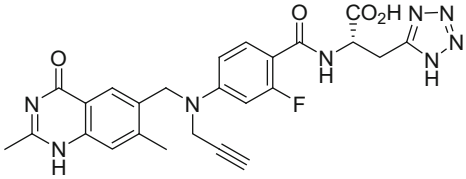

153 (ZD-9331)

Another productive F–NH relationship that exerts a beneficial effect on Caco-2 permeability and efflux ratio is provided by the series of cyclic benzamidine-based BACE1 inhibitors **154**–**157** (compiled in Table 18) [204]. The prototype compound **154** exhibited significant basicity, poor membrane permeability, and a high efflux ratio predictive of the molecule being a P-glycoprotein substrate which was anticipated to further contribute to reduced brain exposure. A key step toward solving the problem was the introduction of a fluorine atom *ortho* to the amidine moiety to afford **155**, a compound with a pK_a that is reduced by 1.3 units that exhibits improved Caco-2 permeability and a reduced efflux ratio while preserving BACE1 inhibitory activity. A similar effect was observed between the matched pairs **156** and **157** in which the F atom is believed to form a weak H-bond with the NH while calculations indicated that the solvation energy of the fluorinated derivative is less negative than for the H analogue, electronic and steric effects that shield the polar nitrogen atom which thus presents less than 2 H-bond donors to the environment [204].

Table 18 Caco-2 and pKa data associated with BACE1 inhibitors **154–157**

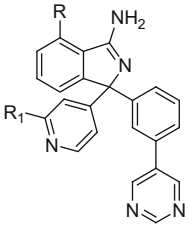

Compound no.	R	R_1	BACE1 IC_{50} (nM)	Caco-2 P_{app} (10^{-6} cm/s)	Caco-2 Efflux Ratio	pK_a
154	H	H	500	3.4	12	8.4
155	F	H	158	12	3.1	7.1
156	H	CF_3	134	0.13	>10	–
157	F	CF_3	241	39	0.6	6.9

4.2 Isosteres of Guanidines and Amidines

The high basicity associated with guanidine and amidine moieties limits the fraction of the more permeable unprotonated form that exists at physiological pH, providing an understanding for the generally poor permeability associated with molecules incorporating these structural elements [205, 206]. The prevalence of arginine as the P1 moiety of substrates of the serine protease enzymes that constitute the coagulation cascade has catalyzed the identification of guanidine and amidine surrogates as part of the effort to identify potent, selective, and orally bioavailable inhibitors that offer potential as antithrombotic agents [207–210]. The pK_a of a substituted guanidine moiety can be reduced significantly from the typical 13–14 range by modification to an acylguanidine, pK_a ~8, or an oxyguanidine, pK_a ~7–7.5, both of which represent isosteric replacements of a methylene moiety. However, these modifications have the potential to significantly affect molecular recognition that may be manifested as a reduction in potency, depending on the circumstance under study. Nevertheless, acylguanidines have been successfully deployed in a series of histamine H_2 agonists and NPY Y2 antagonists while an oxyguanidine moiety has proven to be an effective surrogate of arginine in thrombin inhibitors, with RWJ-671818 (**158**) a representative compound that was advanced into phase 1 clinical trials [211–218].

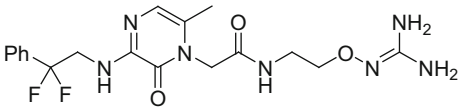

158 (RWJ-671818)

An extensive survey of benzamidine mimetics was conducted using the potent factor Xa inhibitor SN429 (**159**), $K_i = 13$ pM, as the basis for assessing the effect of this kind of structural variation on potency and oral bioavailability (Fig. 27) [219]. The study identified several neutral substituents that functioned as useful and effective amidine surrogates in this context, including the 3-chlorophenyl

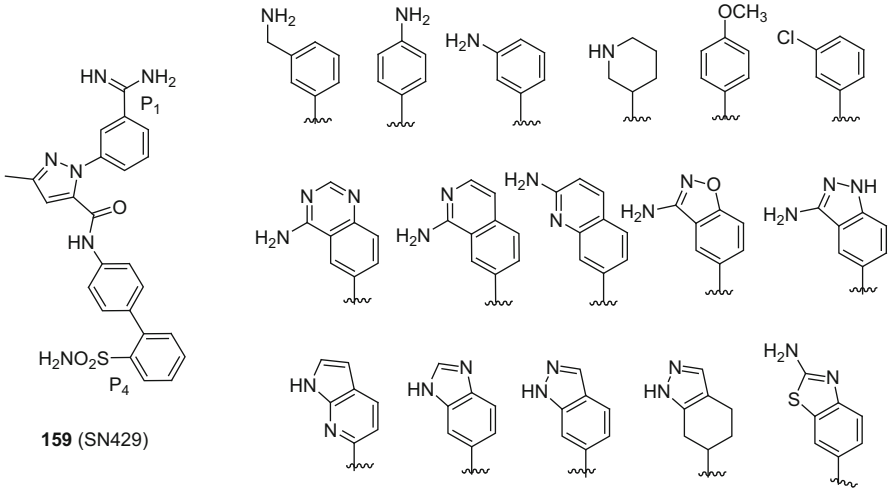

Fig. 27 The structure of the factor Xa inhibitor SN429 (**159**) and some of the benzamidine surrogates evaluated in an attempt to identify potent enzyme inhibitors with improved oral bioavailability

analogue which demonstrated a K_i of 37 nM, potency similar to that of the 3-aminophenyl derivative, which displays a K_i of 63 nM. However, both of these compounds are tenfold weaker than the more basic 3-aminomethyl compound, which exhibits a K_i of 2.7 nM, and are significantly less potent than the prototype **159**. However, the 4-methoxy analogue represented an acceptable compromise between potency ($K_i = 11$ nM) and pharmacokinetic properties and it is this P1 moiety that is found in the factor Xa inhibitor apixaban (**160**) which received marketing approval from the FDA in December 2012 as an agent for reducing the risk of blood clots and stroke in subjects experiencing atrial fibrillation that is not related to a heart valve problem [207, 220].

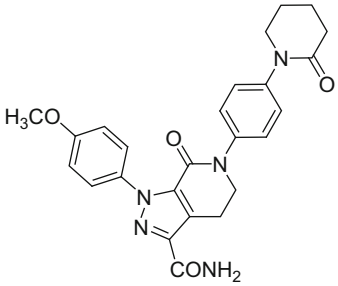

160 (apixaban)

4.3 Isosteres of Phosphates and Phosphonates

Phosphates and phosphonates are highly acidic elements, and the low pK_a associated with these moieties provides a significant limit to membrane permeability and, hence, oral bioavailability [221–223]. Monofluoro- and difluoromethylenebisphosphonic acids have been developed as useful chemically and enzymatically stable phosphate isosteres, but these rely upon preserving the inherently high acidity of the prototype and are not useful in the design of orally bioavailable drug candidates without resort to prodrug technology, which has been the most widely applied and successful tactic to deliver this kind of polar structural element [224–229]. Phosphate and phosphonate isosteres have been of particular interest in the design of nucleoside and nucleotide antiviral and anticancer agents and phosphatase inhibitors for which the design principles are based on substrate mimicry [230, 231]. However, the most notable success in the design of phosphate mimics has been accomplished in the arena of inhibitors of the strand transfer reaction catalyzed by HIV-1 integrase where the seminal identification of α,γ-diketo acids as phosphate transfer transition state mimics inspired the design of a wide range isosteres, summarized in Fig. 28, that are compatible with oral bioavailability [232–237].

The HIV-1 integrase inhibitors raltegravir (**161**), elvitegravir (**162**), and dolutegravir (**163**) have been licensed for marketing by the FDA for the treatment of HIV-1 infection [232–237].

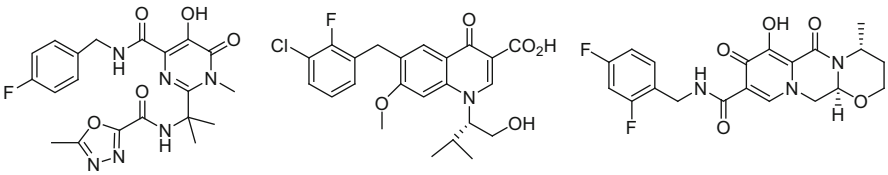

161 (raltegravir) **162** (elvitegravir) **163** (dolutegravir)

4.4 Isosteres to Modulate Basicity/Acidity and Solubility

The presence of a basic amine in a molecule can be associated with several problems including compound promiscuity, inhibition of the human *ether a go-go*-related gene type 1 (hERG) cardiac potassium channel, phospholipidosis, and recognition by P-glycoprotein [121, 238–246]. The basicity of an amine can readily be modulated by the introduction of proximal electron-withdrawing substituents or functionality, with the highly electronegative fluorine the most notable and one of the most widely utilized based on its metabolic stability and modest steric volume [247]. The pK_as of fluorinated ethylamines are summarized in

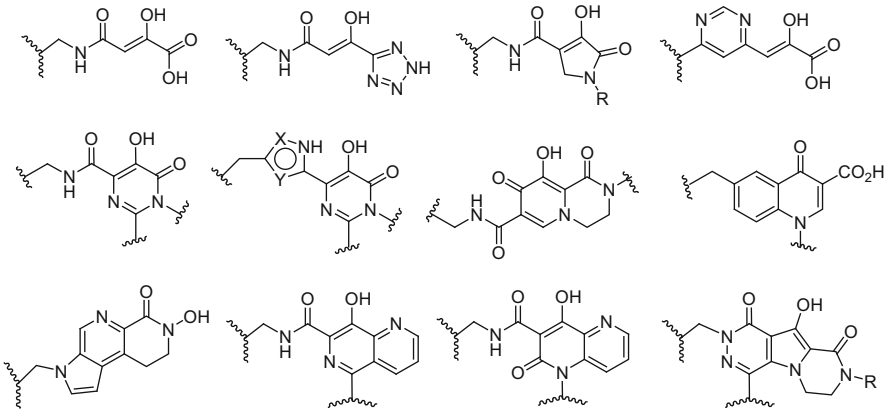

Fig. 28 A selection of HIV-1 integrase inhibiting motifs that mimic the transition state for phosphate transfer during integration of viral DNA into host chromosomal DNA

Table 19 The effect of proximal F atoms on the basicity of ethylamine

Amine	pK_a
$CH_3CH_2NH_3^+$	10.7
$CH_2FCH_2NH_3^+$	9.0
$CHF_2CH_2NH_3^+$	7.3
$CF_3CH_2NH_3^+$	5.7

Table 19 where the data indicate that the effect of introducing a F atom is additive in nature which allows the change in pK_a to be estimated with reasonable accuracy for aliphatic amines. Each fluorine atom introduced to a C atom β- to the amine reduces the pK_a by 1.7 units, an effect that is dependent on σ-transmission and therefore declines with increasing distance such that the effect at the γ-C is reduced to a shift of −0.7 units while a F at the δ-C reduces pK_a by 0.3 units, data that is reflected in Table 19.

An insightful example of the application of the effect of F to reduce amine basicity is provided by the design of inhibitors of the motor protein kinesin spindle protein (KSP) explored as a potential therapy for the treatment of taxane-refractory solid tumors [248]. The efficacy of this series of compounds was restricted by P-gp efflux which was determined experimentally to be minimized by adjusting the pK_a of the amine to a range between 6.5 and 8.0. The *N*-cyclopropyl derivative **164** represented an initial solution to this problem but was associated with time-dependent cytochrome P450 inhibition, a known liability of this structural element [249]. The β-fluoroethyl derivative **165** also satisfied the pK_a requirement but was found to be *N*-dealkylated in vitro and in vivo to release fluoroacetaldehyde which was oxidized to fluoroacetic acid, a toxin that is metabolized in vivo to a potent inhibitor of aconitase, an enzyme in the tricarboxylic acid cycle [139, 250]. This problem was solved by deploying the fluorine atom in the piperidine ring β- to the amine, an arrangement that produced the *cis* derivative **166**, in which the F atom is axially disposed as confirmed by single-crystal X-ray analysis, and the *trans*

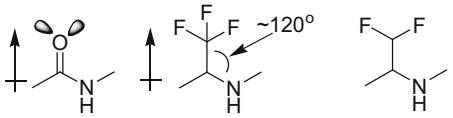

Fig. 29 Isosterism between an amide and trifluoroethylamine and difluoroethylamine moieties

analogue **167**, where the F atom adopts an equatorial disposition. The effect of this structural modification on the basicity of the piperidine was dependent on the stereochemical disposition of the F atom with the pK_a of **167** determined to be 6.6 while **168** was more basic with a pK_a of 7.6 and it was this compound, designated as MK-0371, that was selected for clinical evaluation [248].

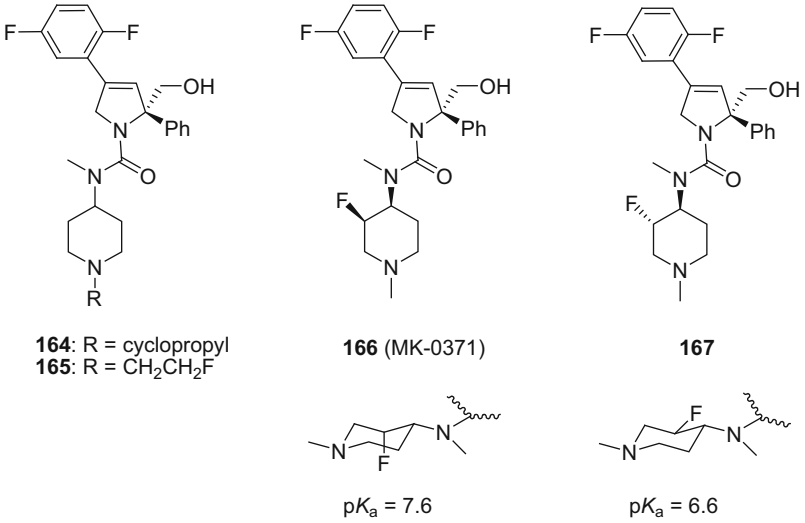

The electron-withdrawing properties of the CF_3 and CHF_2 deployed β- to an amine reduce basicity to an extent that these functionalities have found application as amide mimics, an isosteric relationship furthered by the similarity of dipoles and the geometry of the N-C-CF_3 and N-C-CF_2, which approximates the 120° associated with an amide moiety, as illustrated in Fig. 29 [251–254]. Although this bioisostere was originally conceived to replace the amide bonds of peptide derivatives, it has begun to find a similar application in drug design, with the most prominent example being the cathepsin K inhibitor odanacatib (**170**) which has completed phase 3 clinical trials for the treatment of osteoporosis. Cathepsin K is a lysosomal cysteine protease in osteoclasts that is responsible for bone degradation during remodeling and inhibitors prevent bone resorption. L-006235 (**168**), in which the nitrile moiety is presented to the enzyme as an electrophile to react reversibly with the catalytic cysteine thiol, emerged as a refined cathepsin K inhibitor that exhibited good pharmacokinetic properties. However, this compound has poor selectivity for cathepsin K versus the analogues enzymes cathepsin B, L, and S due to its strongly basic nature, which promoted accumulation in the acidic

environment of lysosomes [255]. L-873724 (**169**) offered good enzyme inhibitory selectivity but poor PK, with further optimization leading to odanacatib (**170**) which solved both problems by installing a F atom in the Ile residue to block hydroxylation while the cyclopropyl moiety reduced the propensity for amide hydrolysis [255, 256]. While odanacatib (**170**) has been quite successful clinically, with the phase 3 trial halted early due to the observation of good efficacy and safety, the pharmaceutical properties of this molecule are less than ideal [257–260]. Odanacatib (**170**) is highly crystalline and exhibits low aqueous solubility, properties that contribute to the $\leq$10% bioavailability across preclinical species after dosing the drug as a suspension in methocel. In an effort to overcome the dissolution-limited bioavailability, modification of the CF_3 moiety to a CHF_2 was explored as a means of improving the physical properties by increasing the pK_a of the amine [260]. This modification afforded **171** which preserved cathepsin K inhibitory potency and selectivity while decreasing log D by 3 units, attributed to the increased basicity, with the result that bioavailability from a 1% methocel suspension was improved fourfold from 6% with odanacatib (**170**) to 23% with **171** in the dog and 8–22% in the rat. The increase in basicity with **171** facilitated salt formation with strong acids like HCl although, interestingly, salts offered no advantage over the neutral form in rat PK studies [260].

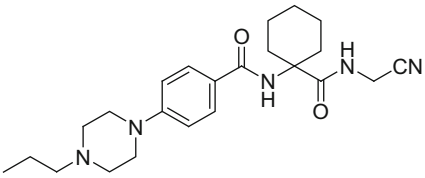

168: L-006235

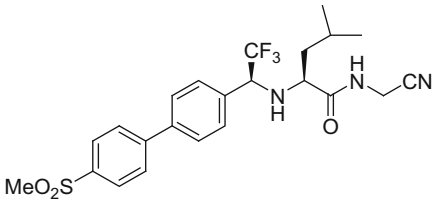

169: L-873724

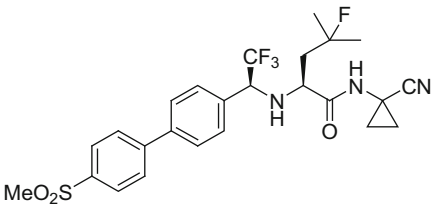

170: odanacatib (MK-0822)

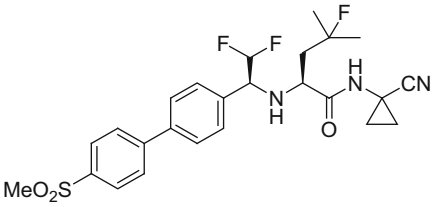

171

In a series of tetrahydroisoquinoline-based inhibitors of phenylethanolamine *N*-methyltransferase (PNMT), the enzyme that catalyzes the final step in epinephrine biosynthesis by methylating norepinephrine using *S*-adenosyl L-methionine as the cofactor, binding of these compounds to the α_2 adrenoreceptor was a significant issue. The prototypical 3-methyl derivative **172** is only modestly selective (Table 20) [261]. In an effort to address this problem, the effect of modulating the basicity of the amine by the successive introduction of F atoms into the

Table 20 Calculated basicity and inhibitory potency of a 3-substituted tetrahydroisoquinolines toward human PNMT and the α_2 adrenoreceptor

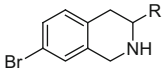

Compound no.	R	Calculated pK_a	K_i PNMT (μM)	K_i for α_2 adrenoreceptor (μM)	Selectivity: α_2/PNMT
172	CH_3	9.29	0.017	1.1	65
173	CH_2F	7.77	0.023	6.4	280
174	CHF_2	6.12	0.094	230	2,400
175	CF_3	4.33	3.2	>1,000	>310

3-methyl group was explored, an approach that proved to be both productive and informative. The monofluoro analogue **173** exhibited similar affinity for the enzyme as **172** while α_2 binding declined only modestly and this molecule was calculated to be less basic than the prototype by 1.5 pK_a units. The trifluoromethyl homologue **175** exhibited poor potency in both assays and is poorly basic; however, the difluoromethylated compound **174** provided the optimal balance of properties, retaining good affinity for PNMT while reducing α_2 adrenoreceptor binding by ~200-fold and providing the first example of fluorination of an amine modulating target selectivity [261].

A detailed analysis of the properties of 3-substituted oxetane rings and applications in the context of broader functionality have established this heterocycle as an advantageous structural element when utilized in a fashion that takes advantage of its electron-withdrawing properties and topographical isosterism with the carbonyl functionality [262–265]. These properties allow the oxetane ring to be deployed as a ketone or amide mimetic depending on the structural context with the electron-withdrawing effects reducing the basicity of an amine in a fashion that is strictly dependent on proximity [262]. As is evident from the homologous series presented in Table 21, the amino oxetane **177** is the weakest base while the aminomethyl and aminoethyl homologues **178** and **179**, respectively, exhibit progressively increased basicity which shows a correlation with solubility, with the exception of the parent molecule **176** which is poorly soluble despite being the most basic [262]. It is the weak basicity associated with **177** coupled with the structural mimicry of the carbonyl moiety by the oxetane ring which adopts a planar topography that has led to this motif being considered as a useful isostere of an amide functionality (Fig. 30).

4.5 Isosteres to Modulate Lipophilicity and sp^2 Atom Count

The oxetane ring has also been proposed as a useful replacement for the gem-dimethyl moiety that provides a similar vectorial presentation of the 2 substituents (Thorpe-Ingold effect) and a similar size while reducing the lipophilic

Table 21 Basicity and solubility of a series of oxetane-substituted phenylbutyl amines

Compound no.	Structure	pK_a of N	Solubility (mg/mL)
176	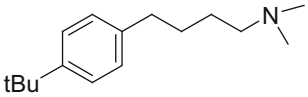	9.9	<1
177	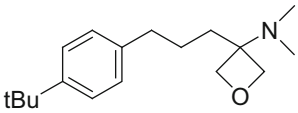	7.2	57
178	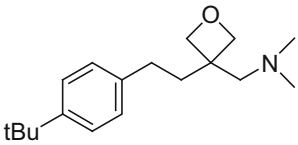	8.0	25
179	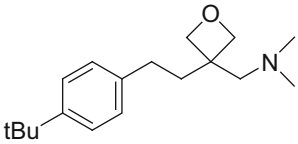	9.2	4,100

Fig. 30 Topographical similarity between the carbonyl and oxetane moieties

burden [121, 262–266]. This concept is particularly useful in an era where there is a considerable focus on the role of physical properties in drug design that has fostered the belief that contemporary practices relies far too heavily on lipophilicity to derive potency, a strategy that is based on taking advantage of entropic rather than enthalpic contributions to binding affinity [121, 177, 267–270]. The rising appreciation of the potential problems associated with this approach to drug design, referred to as molecular obesity, is beginning to be manifested in the description of strategies and tactics to identify scaffolds that replace sp^2 carbon centers by sp^3-based motifs [121, 181, 182, 238, 271–275]. One example of this is provided by studies of oxytocin antagonists of which **180** was the prototype, a compound potent receptor affinity, $K_i = 6$ nM, but poor aqueous solubility of 6 μg/mL and a low Fsp^3 of 0.18 [276]. The effect of replacing the pyrazine ring with piperidine, pyrrolidine, and azetidine was examined from which the azetidine **181** emerged as a preferred compound that bound to the oxytocin receptor with a K_i of 9.5 nM but which exhibited tenfold improved aqueous solubility of 59 μg/mL and a much increased Fsp^3 of 0.46 [276].

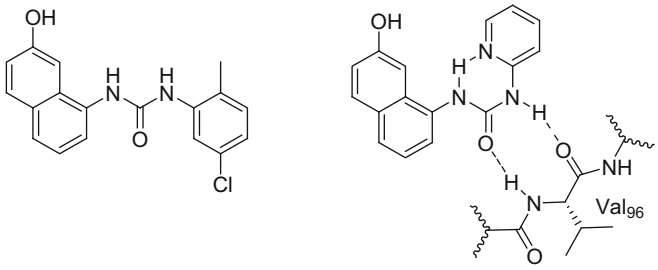

Fig. 31 Structure of the Cdk4 kinase inhibitor lead **182** and drug-target interactions for the analogue **185**

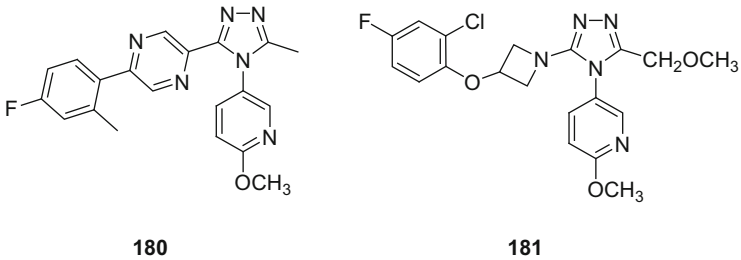

The establishment of an intramolecular H-bonding interaction can mimic the topology of an aromatic or heterocyclic ring in a fashion that reduces the dependence on sp^2 carbon centers, and this isosterism-based concept has found application in kinase inhibitor design. The Cdk4 inhibitor **182** (Fig. 31) was identified as a weak lead inhibitor, $IC_{50} = 44\ \mu M$, derived by structure-based scaffold generation using a model of Cdk4 and a proprietary modeling program [277]. The SAR associated with the homologous series of pyridine derivatives **183**–**185** is summarized in Table 22 and clearly reveals the importance of the topological deployment of the N atom, attributed to the formation of an intramolecular H-bond between the 2-pyridyl N atom of **185** and the distal urea NH that favors a *cis* amide topology. This hypothesis was subsequently confirmed by a co-crystal of the inhibitor with Cdk2 (Fig. 31) and the effect could be recapitulated with the thiazole **186** although this compound is threefold less potent than **185** [277].

PD-166285 (**187**) is a broad-acting kinase inhibitor that was used as a vehicle to explore the concept of replacing the pyridone ring with a mimic based on an intramolecular H-bond to favor the preferred topology [278, 279]. Ab initio calculations predicted that the *cis* urea is favored by 0.5 kcal/mol in H_2O and 3.2 kcal/mol in the gas phase, a contention supported by a search of the pyrimidinyl urea substructure in the CSD where seven molecules were found, all of which

Table 22 SAR associated with urea-based Cdk4 kinase inhibitors

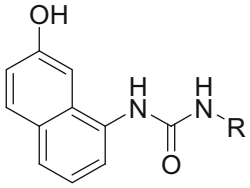

Compound no.	R	IC_{50} (μM)
183	4-Pyridyl	110
184	3-Pyridyl	340
185	2-Pyridyl	7.6
186	2-Thiazolyl	23

Fig. 32 Preferred conformation of 1-methyl-3-(pyrimidin-4-yl)urea

exhibited an intramolecular H-bond (Fig. 32). The urea **188** demonstrated broad-based kinase inhibitory activity with potency comparable to **187** and the derivative NVP-BGJ398 (**189**) was advanced into phase 1 clinical trials [278, 279].

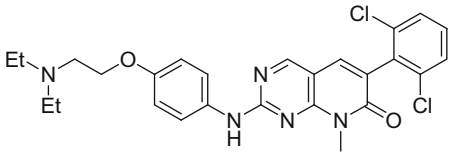

187

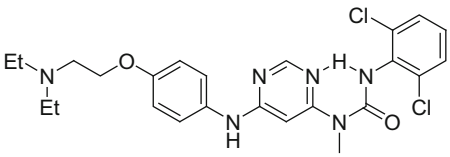

188

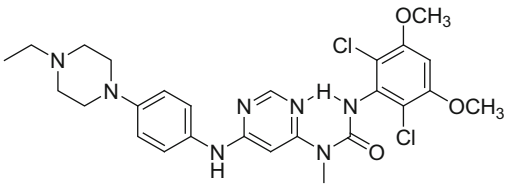

189

Another successful example of the application of this concept is provided by the anthranilamide **190** which mimics the phthalazine **191**, discovered as an inhibitor of the fibroblast growth factor receptor family of receptor tyrosine kinases by high-throughput screening [280]. The *anti* topology of the *para*-chlorophenyl ring depicted is calculated by *ab initio* methods to be 3.1 kcal/mol more stable than the *cis* conformer. This facilitated the design concept of replacing the pyridazine ring by an intramolecularly H-bonded moiety which led to compounds with potent kinase inhibitory properties [280].

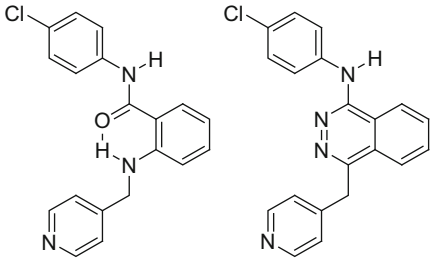

190 **191**

Other examples from the kinase inhibitor arena where this concept is well represented include the dual PI3Kα/mTOR inhibitor **193** which is derived from **192**, Lck inhibitors **194**, and the p38α MAP kinase inhibitor **195** [281–283]. The presence of intramolecular H-bonds in molecules of this type in an aqueous environment has recently been verified by NMR [284, 285].

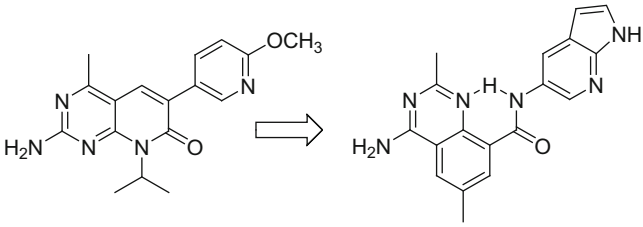

192
IC_{50} PI3Kα = 38 nM
IC_{50} mTOR = 15 nM

193
IC_{50} PI3Kα = 0.3 nM
IC_{50} mTOR = 17 nM

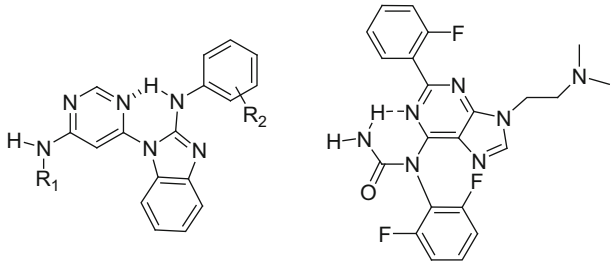

194

195
IC_{50} p38α MAP= 82 nM

An interesting application of the isosteric interplay between rings and H-bonded surrogates is provided by the design of the B-Raf^{V600E} kinase inhibitor **200** which has its origins in the benzamide derivative **196** [286]. The lead amide **196** exhibits poor solubility, 3–9 μg/mL, and a high melting point of 226°C and offers only a very weakly basic aminopyridine moiety, pK_a = 0.7, as a vehicle for salt formation, leading to a dependence on an amorphous dispersion-based formulation to deliver adequate oral exposure. The potency of **196** was improved markedly by modifying the aminopyridine moiety to the pyrazolopyridine found in **198** and both compounds were used as vehicles to explore the design of urea-based inhibitors that relied upon intramolecular H-bonding to correctly orient the pharmacophoric elements. This was successful in the context of the ureas **198** and **199**, but chemical instability led to further structural refinement with optimization ultimately focusing on the reverse amide series represented by **200**, a series with improved physical properties and robust antitumor activity in a B-Raf^{V600E} mouse xenograft model [286].

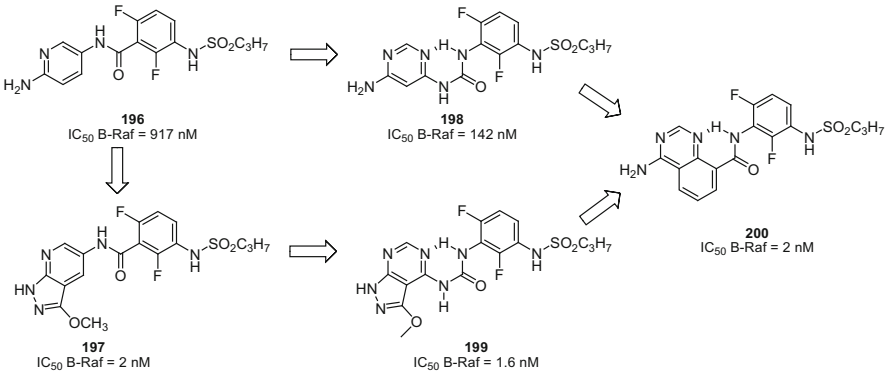

The sulfonamide moiety was developed as a useful phenol isostere in the context of β-adrenergic antagonists with advantage since the high polar surface area and H-bonding properties of this moiety frequently restrict blood–brain barrier penetration as a consequence of reduced permeability and recognition by P-gp [1–10, 196, 197, 287–292]. These physical properties have been exploited in restricting drug molecules to peripheral tissues, but the increased polarity may also reduce oral bioavailability due to poor membrane permeability and there are occasions where more lipophilic moieties are desirable [293, 294]. Although the 2,2-difluoro-2-(pyridin-2-yl)ethanamine moiety in the thrombin inhibitor **202** was introduced to interfere with benzylic oxidation by cyctochrome P450 (CYP 450), this moiety may, in essence, be functioning as a sulfonamide isostere based on analogy with the prototype **201** [216–218, 295–297]. In this context, not recognized in the design process, the two electronegative F atoms may be viewed as nonpolar mimics of the sulfone oxygen atoms that also reduce the basicity of the nitrogen atom and enhance the H-bonding donating properties of the NH to more effectively mimic the sulfonamide. The extra atom introduced with the phenethyl moiety may

Table 23 Structure and properties associated with the dual D2-receptor/β2-adrenoceptor agonists **203** and **204**

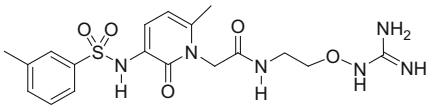

201
Ki = 4 nM

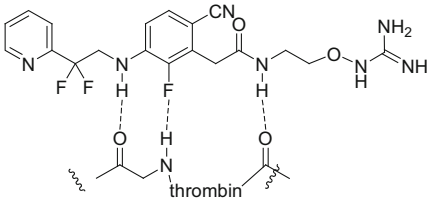

202
Ki = 1.2 nM

Compound no.	**203**	**204**
X	SO_2	CF_2
Log $D_{7.4}$	2.51	3.26
β2 $p[A]_{50}$	8.09	7.77
Intrinsic agonist activity	0.51	0.49
β2 duration (min)	146	>180
pK_a of the N atom	<8	>8

compensate to some extent for the longer bonds associated with the C–S bonds in a sulfonamide. However, the difluoroalkyl moiety has also been invoked as a heteroaryl ether isostere with the caveat that the geometry and topology of this moiety differs from that of an oxygen-based substituent; indeed, the difluoroalkyl substituent may more effectively mimic a fluoroalkyl ether which adopts an orthogonal disposition to the phenyl ring [298]. Interestingly, **202** also incorporates a fluorobenzene moiety to mimic the pyridone with a close interaction between the F atom and the thrombin peptide backbone NH observed in the co-crystal, indicative of isosterism between C–F and C=O bonds.

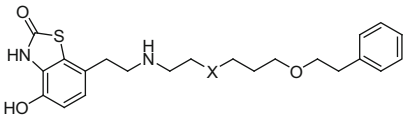

Another example where a difluoromethyl mimics a sulfone can be found in the matched pair of long-acting dual D2-receptor/β2-adrenoceptor agonists **203** and **204** captured in Table 23 [299]. The affinity of **203** and **204** for the β2-adrenergic receptor and the intrinsic agonistic properties are very similar, but the log $D_{7.4}$ and pK_a of the nitrogen atom for the 2 molecules differ, with the difluoromethyl analogue **204** more lipophilic but more basic. The design of **204** was based on the development of a model that identified secondary amines with a $pK_a > 8.0$ and a log $D_{7.4} > 2$ as molecules possessing an ultra-long duration of action [299].

5 Isosteres to Address Metabolism and Toxicity

5.1 Substitution of Hydrogen by Deuterium

The substitution of H by D is the most conservative form of bioisosteric replacement and this tactic has attracted considerable attention recently as a practical approach to drug design. The underlying premise relies upon the effect of deuterium substitution to influence pharmacokinetic properties when deployed in a strategic fashion that takes advantage of the kinetic isotope effect (KIE) associated with the heavier atom [300–304]. The differences between the isotopes are small but measurable, with deuterium 0.140 cm^3/mol per atom smaller than hydrogen, the C–D bond is 0.005 Å shorter than a C–H bond, and the log P_{oct} of D is 0.006 units less lipophilic, an effect that can be measured in per-deuterated alkanes and which has facilitated the chromatographic separation of enantiomers that are based solely on H/D isotopic substitution [305–307]. Deuteration slightly increases the basicity of proximal amines and reduces the acidity of phenols and carboxylic acid derivatives [308–311]. Following the discovery of the isotope, deuteration of drug molecules was quickly adopted as a useful structural modification for the study of metabolic pathways and the origins of toxicity, with the KIE playing the key role in this application [300, 312–314]. However, the study of the deuteration of drug candidates as an approach to improving pharmacokinetic properties by reducing the rate of metabolic modification at sites where H atom abstraction determines the rate of reaction has been adopted only recently, although the first demonstration of the practicality of the approach was described in 1961 [315]. The KIE for a D for H substitution is dependent on the circumstances but usually ranges from one- to sevenfold with calculations suggesting a seven- to tenfold difference; however, in specific cases, much higher isotope effects have been measured [316, 317]. D for H substitution has been shown to translate into meaningful changes in the clinical pharmacokinetic profiles of drugs, exemplified most effectively by CTP-347 (**205**), a dideuterated analogue of the antidepressant paroxetine, and SD-254 (**206**), a per-deuterated derivative of the dual serotonin/norepinephrine reuptake inhibitor venlafaxine that also finds utility for its antidepressant properties [303, 318, 319]. In CPT-347 (**205**), deuterium is introduced at the methylenedioxy moiety, the site of metabolic modification by CYP 2D6, which leads to mechanism-based inhibition of the enzyme through the intermediacy of a carbene-based metabolite, resulting in drug accumulation on repeat dosing due to autoinhibition and precipitating drug–drug interactions [303, 320–322]. CPT-347 (**205**) does not exhibit significant mechanism-based inhibition of CYP 2D6 in vitro and a phase 1 clinical study demonstrated that subjects dosed with the deuterated drug were able to metabolize the CYP 2D6 substrate dextromethorphan more effectively when compared to historical data for paroxetine [303]. In a phase 1 clinical trial in normal healthy volunteers, SD-254 (**206**) was reported to be metabolized more slowly than venlafaxine which is O-demethylated by CYP 2D6 [303].

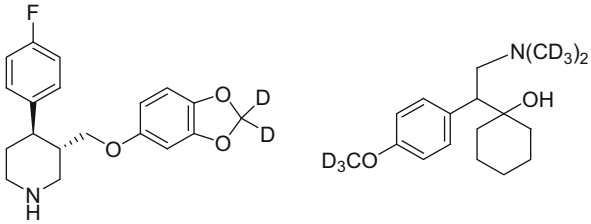

205: CTP-347 **206**: SD-254

However, selective deuteration at a site of metabolism does not always lead to enhanced pharmacokinetic properties, illustrated by a study of the tyrosine kinase inhibitor imatinib (**207**) for which *N*-demethylation to the less active piperazine **208** is a major metabolic pathway [323–325]. The tri-deuterio analogue **209** exhibited increased stability toward *N*-demethylation in rat and human liver microsomes, as anticipated, but intravenous administration of the compound to rats was not associated with increased exposure and the rate of demethylation of **209** was similar to **207**, attributed to a relatively low rate of demethylation of the parent in rat liver microsomes and the low rate clearance of both compounds in rats [323].

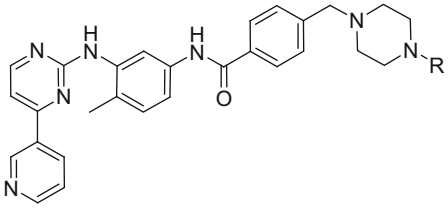

207: R = CH_3
208: R = H
209: R = CD_3

An alternative application of deuterium incorporation that led to improved pharmacokinetic properties is illustrated by the HCV NS3 protease inhibitor telaprevir (**210**) which suffers facile racemization at the P1 residue at higher pH and in human plasma [326]. The (*R*)-diastereomer is the major metabolite of telaprevir in vivo but is 30-fold weaker than the (*S*)-isomer which contributes to the need for this drug to be dosed on a TID schedule. Installing a deuterium atom at the configurationally labile carbon atom gave a compound that inhibited HCV NS3 protease with a $K_i = 20$ nM, approximately twofold more potent than the telaprevir (**210**), and reduced the propensity for racemization in human plasma: the deuterated compound produced only 10% of the epimer over 1 h of incubation compared to 35% with the protio homologue. Although the stability of the deuterio derivative in rat plasma was lower, this compound exhibited a 13% increased AUC following oral administration to rats when compared to telaprevir (**210**) [326].

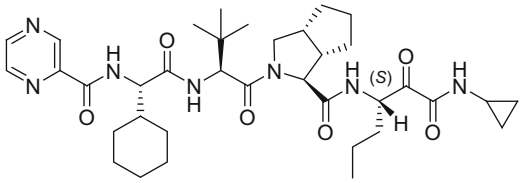

210: telaprevir

Deuteration at metabolically labile sites can redirect metabolism away from a toxic species, as in the case of the HIV-1 non-nucleoside reverse transcriptase inhibitor efavirenz (**211**), or enhance bioactivation of prodrugs, as illustrated by the platelet aggregation inhibitor clopidogrel (**214**) [327, 328]. In rats, the metabolism of efavirenz (**211**) is complex, with the initial step hydroxylation of the aromatic ring to afford a phenol that is a substrate for sulfation. Subsequent hydroxylation at the propargylic position affords a cyclopropylcarbinol that facilitates the addition of glutathione to the alkyne to afford an adduct from which the glutamate is subsequently cleaved, a process blocked by acivicin, to afford **213**, which was determined to be the source of kidney toxicity seen uniquely in rats. As part of this investigation, deuteration at the propargylic position was designed to slow the hydroxylation step and reduce the amount of **213** produced, a successful enterprise since **212** exhibits less severe nephrotoxicity of lower frequency [327].

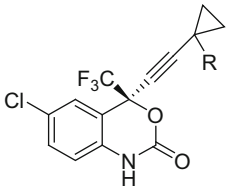

211: R = H, efavirenz
212: R = D

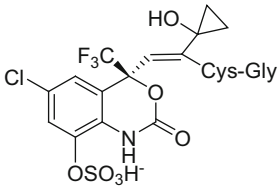

213

Clopidogrel (**214**) requires metabolic activation in order to express its antithrombotic effects, a process that is initiated by oxidation of the thiophene ring by CYP 450 enzymes to produce the thiolactone **215** [328, 329]. Thiolactone **215** is further oxidized to the acylated sulfoxide **216**, a species that is readily hydrolyzed to the highly reactive sulfenic acid **217**, considered to be the ultimate active principle of the drug that reacts covalently with and blocks the $P2Y_{12}$ receptor that is activated by adenosine diphosphate (ADP) [328, 329]. However, the metabolism of clopidogrel (**214**) into the active species is limited, complicated by alternative pathways that involve cleavage of the ester moiety to afford an inactive acid and CYP-mediated oxidation of the piperidine ring [328]. In an effort to direct metabolic activation toward the thiophene ring and enhance the antiplatelet activity of clopidogrel (**214**) in vivo, the effect of deuteration of the piperidine was examined. The d_6 derivative **218** exhibited similar metabolic

stability to clopidogrel (**214**) in rat and human liver microsomes but improved conversion to the thiolactone **215**, an effect that manifested in vivo in rats as enhanced ex vivo inhibition of ADP-induced platelet aggregation following oral administration of **218** [328].

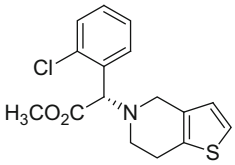

214

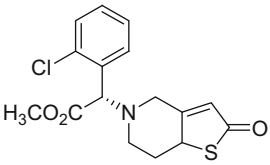

215

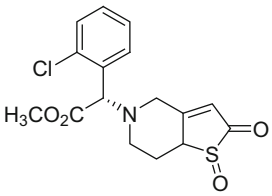

216

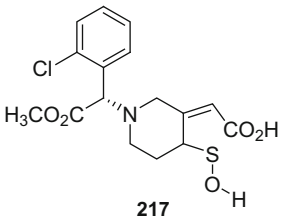

217

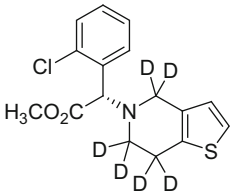

218

5.2 Substitution of Carbon by Silicon

The replacement of carbon atoms by silicon has attracted attention as a drug design principle that may offer advantage in specific circumstances where the unique properties of silicon can be exploited [330, 331]. A particularly compelling example of the application of deploying silicon in a tactical sense is provided by studies with the antipsychotic agent haloperidol (**219**), a dopamine D_2 antagonist, in which the replacement of the carbinol carbon by silicon was examined as a means of eliminating a problematic metabolic pathway [332, 333]. Haloperidol (**219**) is metabolized, in part, by dehydration of the piperidinol which affords the

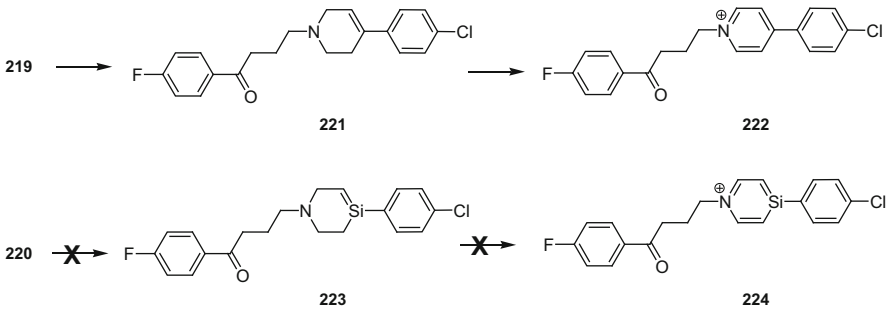

Fig. 33 Metabolism of haloperidol (**219**) to a pyridinium

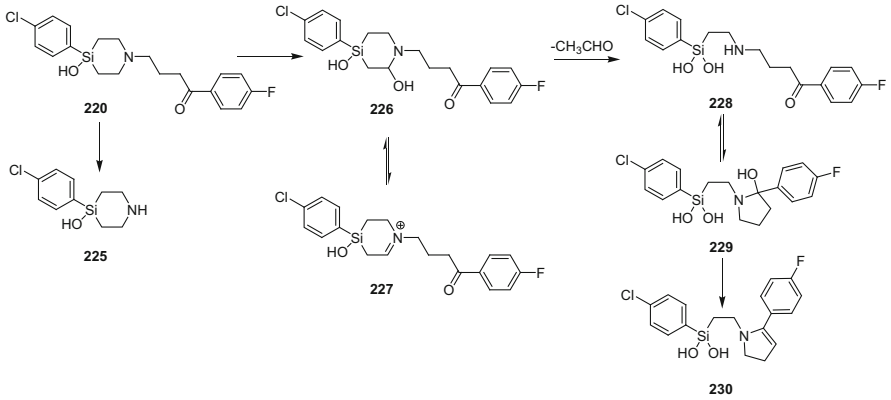

Fig. 34 Metabolism of sila-haloperidol (**220**)

tetrahydropiperidine **221**, a precursor to the pyridinium **222** which is neurotoxic, as summarized in Fig. 33. Sila-haloperidol (**220**) exhibits biological properties that are quite similar to the progenitor **219**, but this compound cannot be metabolized by dehydration to **223** and further oxidized to **224** due to the inherent instability of carbon-silicon double bonds [332]. Indeed, the metabolism of sila-haloperidol (**220**) follows more conventional pathways associated with the piperidine moiety in which oxidative metabolism occurs adjacent to the N atom leading to dealkylation of the fluorophenyl-containing side chain to afford **225** and ring hydroxylation that produces **228** and **230** (Fig. 34) [334].

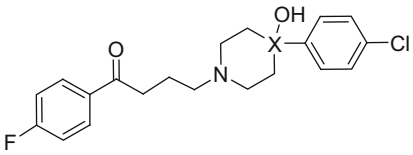

219: X = C - haloperidol
220: X = Si - sila-haloperidol

5.3 Isosteres of Alkyl Groups and Alkylene Moieties

tert-Butyl moieties are susceptible to metabolic oxidation of the methyl groups and this pathway can be a source of poor pharmacokinetic properties. Replacing a single methyl group with CF_3 in the context of the NK1 receptor antagonist **231** and the vanilloid receptor antagonist **233** afforded **232** and **234**, respectively, as compounds that demonstrate enhanced metabolic stability in human liver microsomes compared to the prototypes [335]. A further refinement of this approach identified the trifluoromethylcyclopropyl as a metabolically more stable *tert*-butyl isostere, exemplified in the type II 5α-reductase inhibitor finasteride (**235**) where this substitution provided **236** which exhibits a half-life in human liver microsomes of 114 min, a substantial improvement on the 63-min half-life measured for the progenitor [336]. The potent respiratory syncytial virus fusion inhibitor **237** exhibits poor stability in human liver microsomes with a $t_{1/2}$ of just 4 min, similar to the isopropyl- and cyclobutyl-substituted homologues while the cyclopropyl derivative **238** uniquely addressed this deficiency exhibiting a tenfold improved $t_{1/2}$ of 39 min [337].

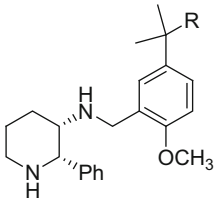

231: R = CH_3
232: R = CF_3

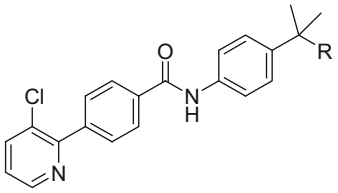

233: R = CH_3
234: R = CF_3

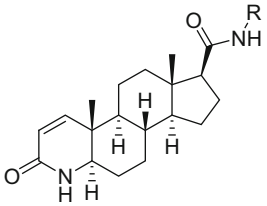

235: R = tBu

236: R =

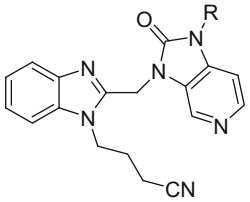

237: R = tBu
238: R = cyclopropyl

Alkanoic acid derivatives can be metabolized by β-oxidation that can lead to poor pharmacokinetic properties in vivo, a problem encountered with iloprost (**240**), an analogue of prostacyclin (**239**) in which the chemically labile bicyclic enol ether oxygen atom is replaced with a CH_2 isostere [338]. β-Oxidation of fatty acids is a degradative pathway that proceeds mechanistically as depicted in Fig. 35

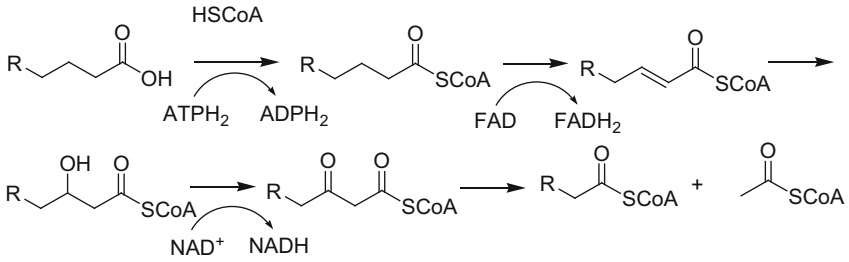

Fig. 35 The β-oxidation pathway for alkanoic carboxylic acids

and involves the initial formation of a CoA ester as a substrate for oxidation to an α,β-unsaturated CoA ester that is further metabolized to a CoA ester with two fewer carbon atoms [339, 340]. The essential formation of the α,β-unsaturated CoA ester provides opportunity for rational structural modification of xenobiotic carboxylic acids to block this pathway. The introduction of germinal substitution at the α- or β-positions and replacing the β-carbon with a heteroatom are effective tactics that prevent olefin formation and it was the latter that was successfully applied to iloprost (**240**) leading to the design of cicaprost (**241**), a compound with longer-lasting hypotensive effects in rats following oral administration [338].

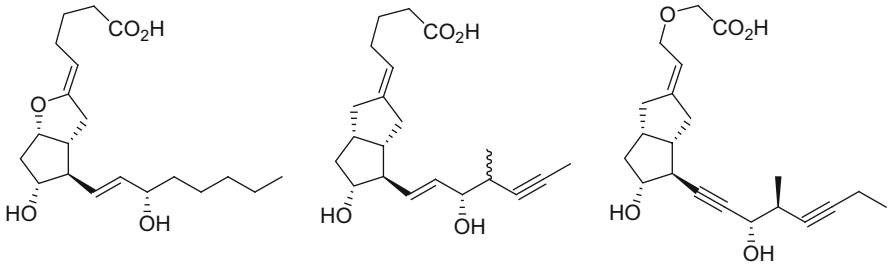

239: prostacyclin **240**: iloprost **242**: cicaprost

5.4 *Isosteres of Carboxylic Acids to Reduce Reactive Metabolite Formation*

Acyl-CoA esters have been shown to be inherently electrophilic acylating agents, providing further impetus to replace the carboxylic acid moiety with an isostere that cannot engage in this metabolic pathway [10, 341–345]. Carboxylic acids are also readily conjugated with glucuronic acid in vivo to afford acyl glucuronides that can undergo sequential rearrangement of the acyl moiety to the adjacent hydroxyl substituents on the pyranose ring, a process summarized in Fig. 36. This becomes problematic when the pyran ring opens to reveal an unnatural aldehyde which can react with amine moieties of proteins, lysine, for example, to generate an imine

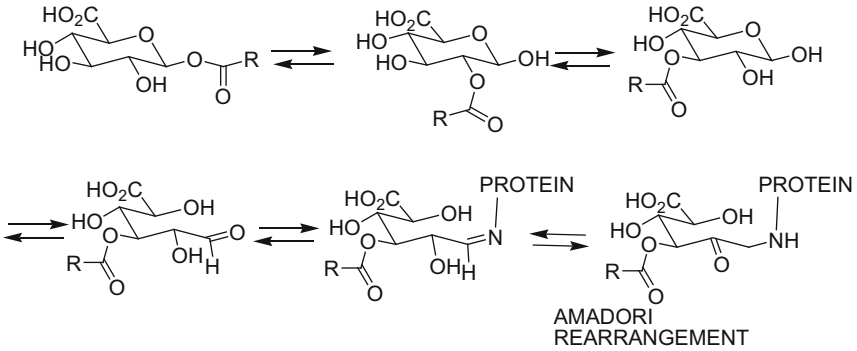

Fig. 36 Rearrangement of acyl glucuronides and exposure of an electrophilic aldehyde moiety

[346, 347]. The imine intermediate can be trapped with $NaB^3[H]_4$, but this functionality can also undergo an Amadori rearrangement to afford the corresponding aminomethyl ketone, resulting in an irreversible protein modification that may create a hapten. Insights have been gleaned into the properties of a carboxylic acid that promote this rearrangement which has been shown to be more facile for electron-deficient acids but slowed by bulky substituents at the α-carbon atom [348–350]. Guidelines have been developed that attempt to equate the propensity of rearrangement with the potential for idiosyncratic toxicity, with the half-life of the acyl glucuronide in buffer that separated safe from problematic acids estimated to be 3.6 h [351]. The level of mechanistic understanding underlying the potential toxicity of carboxylic acid provides a rationale for structural modification to avoid this metabolic pathway by deploying an acid isostere incapable of undergoing rearrangement after glucuronidation. Figure 37 captures the range of acidic functionality that has been examined to address problems across a wide variety of medicinal chemistry campaigns [10, 344, 345, 352, 353].

5.5 *Isosteres of Thiols and Alcohols*

The thiol moiety is relatively uncommon in drugs and drug candidates due to potential problems arising from metabolic lability or chemical reactivity, with the angiotensin-converting enzyme inhibitor captopril (**243**) and penicillamine (**244**), a chelator used to promote heavy metal excretion, the most prominent exceptions [354, 355].

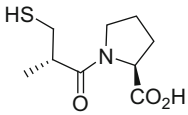

243

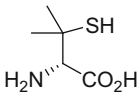

244

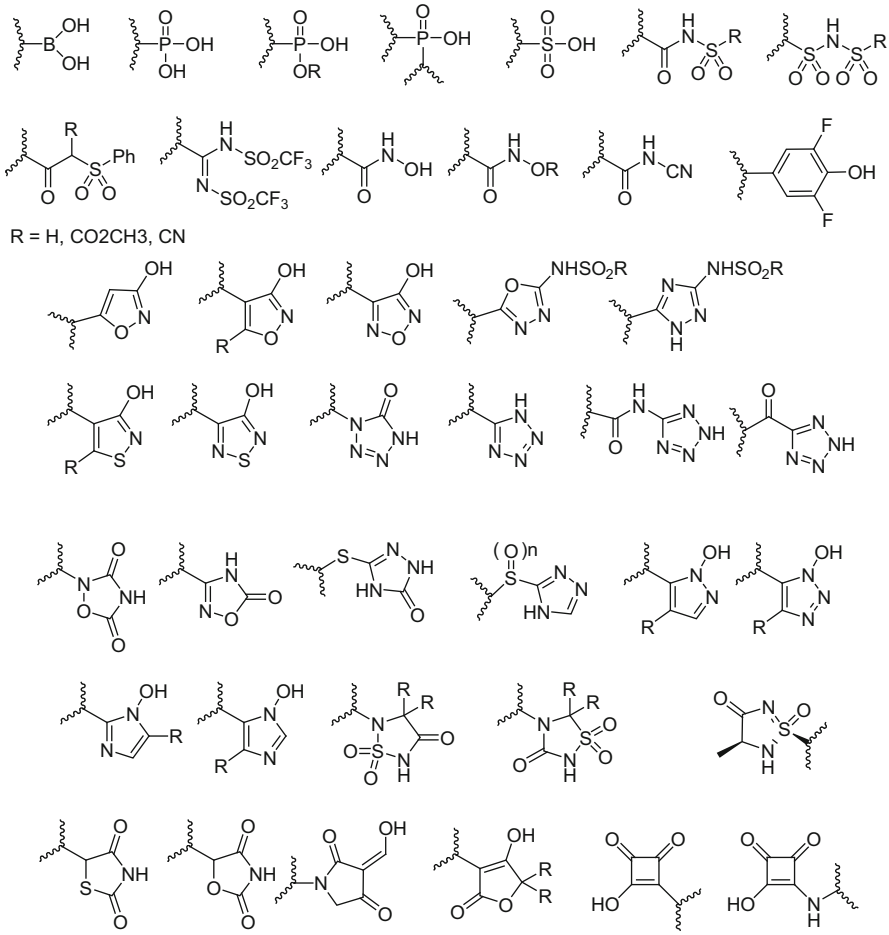

Fig. 37 A sampling of carboxylic acid isosteres

A useful although somewhat underutilized isostere of a thiol is the CHF_2 moiety which has been applied in an elegant fashion to the design of HCV NS3 protease inhibitors where the P1 cysteine moiety of hexapeptide, substrate-based inhibitors, was considered to be a liability [356]. Capitalizing on earlier observations of the intramolecular H-bonding properties of the CHF_2 moiety in **248**, this element was examined as a thiol surrogate in the context of the potent NS3 inhibitor **245** which exhibited a $K_i = 40$ nM [356, 357]. Replacing the P1 SH with CH_3 led to an almost 20-fold erosion of potency and **246** inhibited the enzyme with a $K_i = 700$ nM. However, a CHF_2 terminus at P1 proved to be very effective, fully restoring the potency of **247** to that of the cysteine progenitor, with a $K_i = 30$ nM [356]. This amino acid, referred to as difluoro-Abu, was conceived to be suitable for this context after an insightful analysis of its properties which suggested considerable potential to mimic the cysteine. Mimicry between a SH and a CHF_2 was based on

several observations that included the similarity of the van der Waals surfaces of the two structural elements, 46.7 Å for HCF_2CH_3 compared to 47.1 Å for $HSCH_3$ and electrostatic potential maps, which revealed that the negative potential around the sulfur lone pairs of electrons was similar to that of the two fluorine atoms while there was positive potential around both the SH and CF_2H hydrogen atoms, suggestive of H-bonding capability. Indeed, an X-ray co-crystal structure of a related inhibitor revealed that the CF_2H moiety donated a H-bond to the C=O of Lys_{136} while one of the fluorine atoms was close enough to the C-4-hydrogen atom of Phe_{154} to suggest the presence of a weak C–H to F H-bond [356].

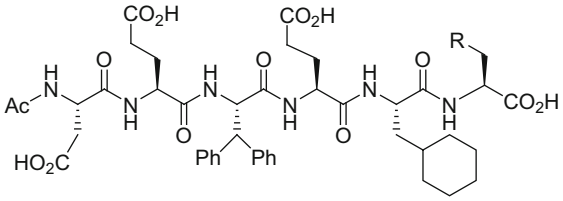

245: R = SH
246: R = CH_3
247: R = CHF_2

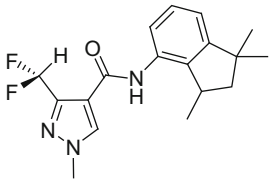

248

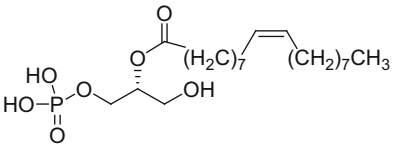

249

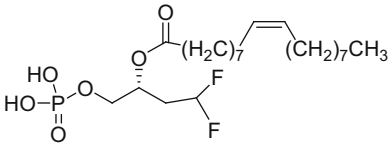

250

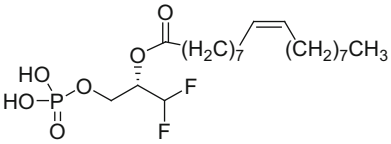

251

Lysophosphatidic acid (**249**) is a mitogen that has been shown to interact with four G protein-coupled receptors designated LPA 1–4 in addition to being an agonist at the peroxisome proliferator-activated receptor γ (PPARγ), a nuclear hormone receptor, and antagonists offer potential in a range of clinical conditions including the treatment of liver and lung fibrosis, several cancers, and neuropathic pain [358, 359]. The acyl moiety in lysophosphatidic acid (**249**) can migrate to the primary alcohol, stimulating the design of analogues that are functionally incapable of entering this rearrangement pathway [360, 361]. In this context the CHF_2 moieties of **250** and **251** were conceived as potential mimics of the OH moiety of **249** that would be chemically stable. Neither compound was recognized by LPA receptors 1, 2, or 3, with both agonistic and antagonistic properties evaluated, but **250** was found to stimulate luciferase production in CV-1 cells transfected with luciferase under the control of a PPARγ-responsive element [360, 361].

5.6 Substitution of C–H by N in Phenyl Rings and C by N in Dihydropyridines

The substitution of the C–H moiety of a phenyl ring by nitrogen is a useful and well-established tactic for mitigating metabolic activation to chemically reactive and potentially toxic species that has found broad-based application and is captured in synoptic form by several illustrative examples [362–367]. The 4,7-dimethoxy indole derivative **252** is a potent HIV-1 attachment inhibitor, but the observation of O-demethylation as a metabolic pathway in HLM gave rise to the concern that the chemically electrophilic quinone **253** could be formed in vivo [362]. The 4,7-dimethoxy-6-azaindole **254** analogue largely preserved the antiviral activity of **252** but, in contrast, would afford the far less electrophilic **255** upon dealkylative metabolism, and it was this compound, designated BMS-488043, that was advanced into proof-of-concept clinical studies [362]. In addition, the mild basicity associated with the azaindole ring of **254** led to improved aqueous solubility.

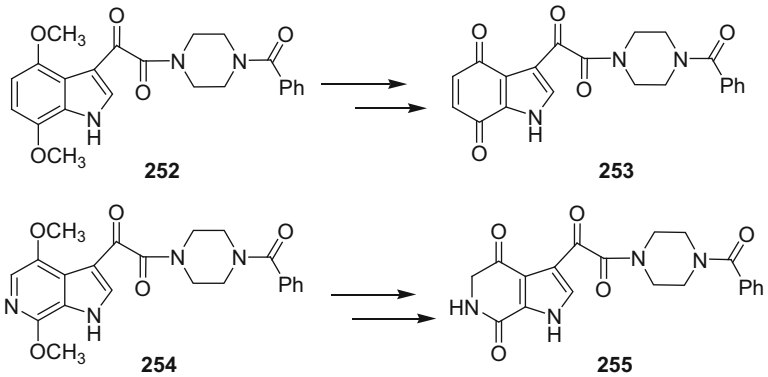

The phenol **256** is a short-acting calcium-sensing receptor antagonist that was examined for its potential as a treatment for osteoporosis [363, 364]. However, CYP 3A4-mediated oxidation of the phenol ring of **256** afforded the catechol **257** which underwent further oxidation to the corresponding *ortho* quinone, a metabolite identified as the source of GSH adducts in both human and rat liver microsomes. The strategic introduction of a nitrogen atom into the phenol ring of **256** to give **258** was anticipated to reduce the rate of metabolic activation of the catechol based on quantum chemistry calculations which indicated that oxidation of the aza-catechol derived from **258** to the corresponding quinone was energetically less favorable than for **257**. This was confirmed experimentally with a 50-fold reduction in the formation of GSH adducts compared to **256** when **258** was incubated in liver microsomes [363, 364].

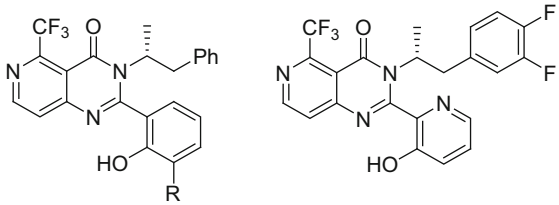

256: R = H
257: R = OH

258

The CRF antagonist **259** was found to undergo metabolic activation following dosing to rats followed by trapping of the reactive species by GSH which afforded adducts amounting to 25% of the dose, with **260** identified as the major species produced in vivo [365–367]. This metabolic process was postulated to proceed via iminoquinone formation, providing a rationale for studying the effect of replacing the electron-rich phenyl ring with a pyridine, an approach that, after additional optimization, led to the identification of **261** as a compound with targeted biological and pharmacokinetic properties. As part of the structural refinement of **259**, the pyrazinone chlorine substituent was replaced with an electron-withdrawing nitrile moiety in order to reduce metabolic activation of the olefin while the methoxy was introduced into the side chain to redirect metabolism to an alternative site that would provide benign products [365–367].

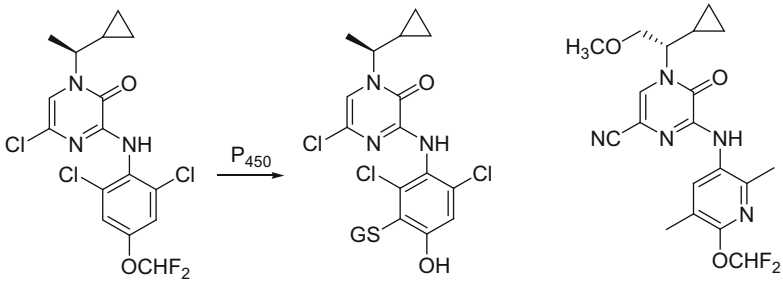

GS = glutathione

259 **260** **261**

Another example of the beneficial effect of replacing a C atom with N to interfere with metabolism is provided by the bioisosteric replacement of the dihydropyridine (DHP) ring of the Ca^{2+} channel blocker class of smooth muscle relaxant exemplified by nifedipine (**262**, R=*ortho*-NO_2) with a pyrimidinone heterocycle [368–371]. The dihydropyridine ring is subject to rapid first-pass oxidative metabolism in vivo to give the corresponding pyridine **263** which is an inactive metabolite. This led to the design of the pyrimidinone **264** as a probe of the idea that this ring system would be an effective substitute of the DHP ring. The design concept was based on the premise that the amide NH of **264** would mimic the H-bond donor properties of the dihydropyridine NH of **262** while the second nitrogen atom of the ring would provide a site for the introduction of the important carbonyl moiety, initially examined in the context of the methoxycarbonyl derivative **264**, as well as providing resistance toward facile oxidation of the heterocycle. However, as an acylated urea derivative, **264** suffered from chemical instability, necessitating replacement by the more robust ureido moiety found in **265**. In this analogue, the orientation of the exocyclic carbonyl group is as depicted in **265**, favored by both dipole–dipole interactions and an intramolecular H-bond that projects the R substituent in a vector compatible with vasodilatory activity [368–371].

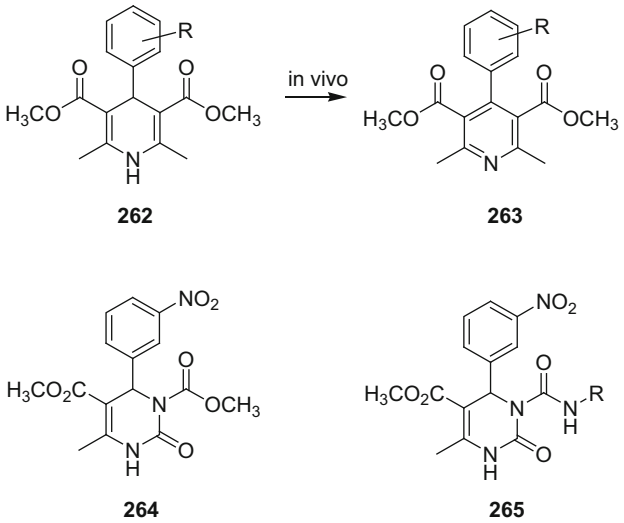

5.7 *Isosteres of Heterocycles to Reduce Metabolic Activation*

The potent bradykinin B_1 antagonist **266**, $K_i = 11.8$ nM, developed as a potential treatment for pain, was found to produce glutathione adducts when incubated in rat and human liver microsomal preparations, a metabolic pathway also observed

in vivo following oral administration of the drug to rats with GSH adducts derived from the drug identified in bile [372]. The site of GSH adduction was determined to be the pyridine ring, characterized as **268** and hypothesized to arise either from the diiminoquinone **267** or the epoxide **270**, while the pyridine N-oxide **269** was determined to be a minor contributory pathway.

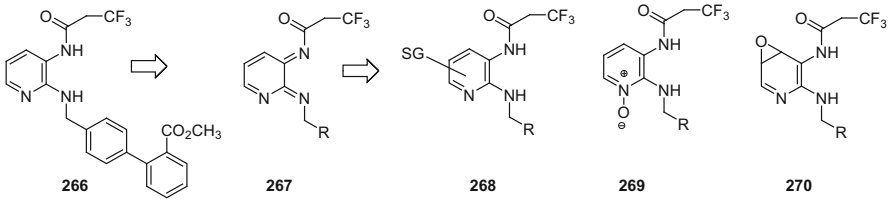

The design of a suitable isostere of the diaminopyridine ring was based upon the assumption that both NHs were of importance while the pyridine N atom was considered to function as a H-bond acceptor, an analysis that anticipated the simple glycine derivative **271** as the most rudimentary mimic. In order to influence the conformation of **271** in a fashion that allowed mimicry of the topology of the *ortho*-disposed substituents of **266**, the gem-dimethyl derivative **272** was prepared, but this compound expressed only modest affinity for the bradykinin B_1 receptor, $K_i = 3.5$ μM [372]. Further refinement to the cyclopropyl analogue **273** led to a more than 50-fold increase in potency, attributed to conformational constraint due to π–π hyperconjugation between the cyclopropyl C–C bond and the amide C=O that favors the two conformations depicted in Fig. 38, with that represented by A mimicking the topology associated with **266**. In addition, it was noted that the 116° bond angle associate with the cyclopropane ring substituents more closely matches the 120° vectors projected by the pyridine ring.

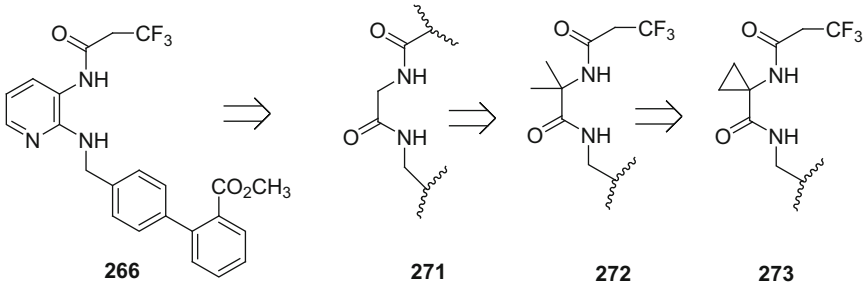

Amide and ester isosteres are susceptible to protease and/or esterase-mediated degradation in vivo while alkyl esters can be degraded by oxidative dealkylation by CYP 450 enzymes to afford the corresponding carboxylic acids, providing an impetus to identify surrogates with resistance to metabolic modification [373–377]. Pioneering studies in this area were focused on the design of heterocycles as ester replacements in the context of benzodiazepine derivatives of general

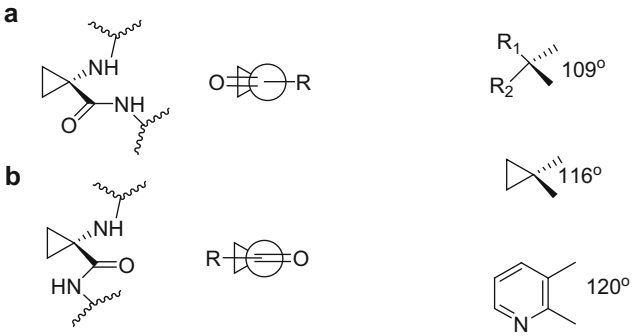

Fig. 38 Conformational topology and bond angles of spirocyclopropyl glycinamides

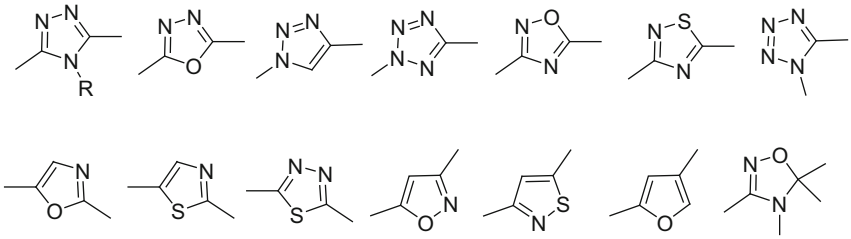

Fig. 39 Azole isosteres of esters and amides

structure **274** and **275** and muscarinic agonists based on the naturally occurring arecoline (**276**) [378–380]. Azole heterocycles are the most common amide and ester replacements that have been explored, captured in synoptic fashion in Fig. 39. This tactic remains an approach of contemporary interest although there can be marked differences between heterocycles in the ability to emulate carbonyl-based functionality dependent on context that may be attributed to subtle effects associated with the underlying electronic properties of a heterocycle that are not always understood [2, 3, 9, 10, 71, 381–387].

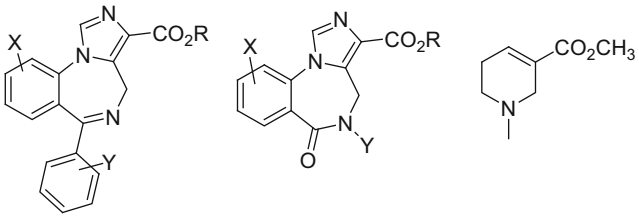

274 **275** **276**

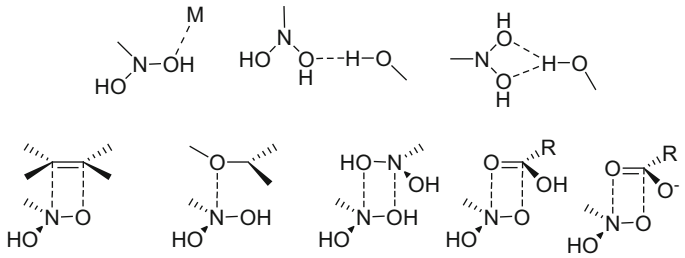

Fig. 40 Intermolecular interactions of nitro groups from the Cambridge Structural Database

5.8 Isosteres of the NO_2 Moiety

The unique properties of the nitro group have often made this a difficult structural motif to emulate by isosteric replacement [388, 389]. For example, the nitrophenyl moiety of **277**, an inhibitor of the protein–protein interaction between murine double minute 2 (MDM2) and p53, offers the optimal potency from an extensive survey of potential substitutes [389]. These observations were suggested to be a function of a lipophilic and strongly directional interaction between the nitro group and the MDM2 protein that is also dependent on the electron-withdrawing properties. Where the latter effect is of importance for drug–target interactions, several electron-withdrawing functional groups can substitute for the nitro, including pyridine, pyridine N-oxide, sulfonyl, trifluoromethyl, amide, and a carboxylic acid moiety that is considered to be an exact isostere [104, 390–395]. Intermolecular interactions for the nitro moiety as collected from the Cambridge Structural Database of small molecules are summarized in Fig. 40 [387].

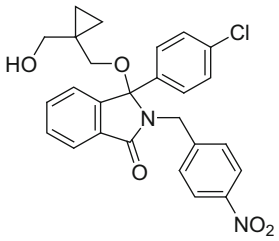

277

6 Epilogue

The design of bioisosteres is a powerful and effective concept in drug design that has been applied to solve a wide range of problems encountered in drug discovery campaigns. This chapter has focused on the practical utility of applying bioisosteric

substitution to solve contemporary developability challenges that are encountered almost routinely by the practicing medicinal chemistry. The creativity and ingenuity of medicinal chemists is quite clear from this synopsis which captures many insightful and elegant examples of drug design. The most successful and creative designs are frequently based on a careful analysis of not only the chemistry underlying a particular problem but also a deep and detailed understanding of the physicochemical properties of the atoms and structural elements that are selected to address an issue. While medicinal chemists have developed a broad toolbox of useful structural elements to draw upon to emulate a range of commonly encountered functionalities, it is anticipated that the challenges in drug design that lie ahead will continue to provide a stimulus for creativity that will expand the range of bioisosteric replacements.

References

1. Burger A (1991) Isosterism and bioisosterism in drug design. Progress Drug Res 37:288–362
2. Patani GA, LaVoie EJ (1996) Bioisosterism: a rational approach in drug design. Chem Rev 96:3147–3176
3. Thornber CW (1979) Isosterism and molecular modification in drug design. Chem Soc Rev 8:563–580
4. Lipinski CA (1986) Bioisosterism in drug design. Ann Rep Med Chem 21:283–291
5. Wermuth CG, Bourguignon J-J (2003) In: Wermuth CG (ed) The practice of medicinal chemistry, 2nd edn. Chaps 12–16, Academic, London, pp 181–310. ISBN: 0-12-744640-0
6. Olsen PH (2001) The use of bioisosteric groups in lead optimization. Curr Opin Drug Discov Devel 4:471–478
7. Sheridan RP (2002) The most common chemical replacements in drug-like compounds. J Chem Inf Comput Sci 42:103–108
8. Wermuth CG (2005) Similarity in drugs: reflections on analogue design. Drug Discov Today 11:348–354
9. Lima LM, Barriero EJ (2005) Bioisosterism: a useful strategy for molecular modification in drug design. Curr Med Chem 12:23–49
10. Meanwell NA (2011) Synopsis of some recent tactical applications of bioisosteres in drug design. J Med Chem 54:2529–2591
11. Langmuir I (1919) Isomorphism, isosterism and covalence. J Am Chem Soc 41:1543–1559
12. Erlenmeyer H, Berger E (1932) Studies on the significance of structure of antigens for the production and the specificity of antibodies. Biochem Z 252:22–36
13. Erlenmeyer H, Berger E, Leo M (1933) Relationship between the structure of antigens and the specificity of antibodies. Helv Chim Acta 16:733–738
14. Friedman HL (1951) Influence of isosteric replacements upon biological activity. NASNRS 206:295–358
15. Bégué J-P, Bonnet-Delpon D (2008) Bioorganic and medicinal chemistry of fluorine. Wiley, Hoboken
16. Böhm H-J, Banner D, Bendels S, Kansy M, Kuhn B, Müller K, Obst-Sander U, Stahl M (2004) Fluorine in medicinal chemistry. ChemBioChem 5:637–643
17. Müller K, Faeh C, Diederich F (2007) Fluorine in pharmaceuticals: looking beyond intuition. Science 317:1881–1886
18. Hagman WK (2008) The many roles for fluorine in medicinal chemistry. J Med Chem 51:4359–4369

19. Shah P, Westwell AD (2007) The role of fluorine in medicinal chemistry. J Enzyme Inhib Med Chem 22:527–540
20. Purser S, Moore PR, Swallow S, Gouverneur V (2008) Fluorine in medicinal chemistry. Chem Soc Rev 37:320–330
21. O'Hagan D (2008) Understanding organofluorine chemistry. An introduction to the C–F bond. Chem Soc Rev 37:308–319
22. O'Hagan D (2010) Fluorine in health care: organofluorine containing blockbuster drugs. J Fluorine Chem 131:1071–1081
23. Hodgetts KJ, Combs KJ, Elder AM, Harriman GC (2010) The role of fluorine in the discovery and optimization of CNS agents: modulation of drug-like properties. Ann Rep Med Chem 45:429–448
24. Smart BE (2001) Fluorine substituent effects (on bioactivity). J Fluorine Chem 109:3–11
25. Schinazi RF, McMillan A, Cannon D, Mathis R, Loyd RM, Peck A, Sommadossi J-P, St. Clair M, Wilson J, Furman PA, Painter G, Choi W-B, Liotta DC (1992) Selective inhibition of human immunodeficiency viruses by racemates and enantiomers of cis-5-fluoro-1-[2-(hydroxymethyl)-1,3-oxathiolan-5-yl]cytosine. Antimicrob Agents Chemother 36:2423–2431
26. Wang LH, Begley J, St. Claire RL, III, Harris J, Wakeford C, Rousseau FS (2004) Pharmacokinetic and pharmacodynamic characteristics of emtricitabine support its once daily dosing for the treatment of HIV infection. AIDS Res Human Retroviruses 20:1173–1182
27. Feng JY, Shi J, Schinazi RF, Anderson KS (1999) Mechanistic studies show that (−) FTC-TP is a better inhibitor of HIV-1 reverse transcriptase than 3TC-TP. FASEB J 13:1511–1517
28. Domagala JM, Hanna LD, Heifetz CL, Hutt MP, Mich TF, Sanchez JP, Solomon M (1986) New structure–activity relationships of the quinolone antibacterials using the target enzyme. The development and application of a DNA gyrase assay. J Med Chem 29:394–404
29. Barbachyn MR, Ford CW (2003) Oxazolidinone structure–activity relationships leading to linezolid. Angew Chem Int Ed 42:2010–2023
30. Meanwell NA, Wallace OB, Fang H, Wang H, Deshpande M, Wang T, Yin Z, Zhang Z, Pearce BC, James J, Yeung K-S, Qiu Z, Wright JJK, Yang Z, Zadjura L, Tweedie DL, Yeola S, Zhao F, Ranadive S, Robinson BA, Gong Y-F, Wang H-GH, Blair WS, Shi P-Y, Colonno RJ, P-f L (2009) Inhibitors of HIV-1 attachment. Part 2: an initial survey of indole substitution patterns. Bioorg Med Chem Lett 19:1977–1981
31. Kitas EA, Galley G, Jakob-Roetne R, Flohr A, Wostl W, Mauser H, Alker AM, Czech C, Ozmen L, David-Pierson P, Reinhardt D, Jacobsen H (2008) Substituted 2-oxo-azepane derivatives are potent, orally active γ-secretase inhibitors. Bioorg Med Chem Lett 18:304–308
32. Olsen JA, Banner DW, Seiler P, Wagner B, Tschopp T, Obst-Sander U, Kansy M, Müller K, Diederich F (2004) Fluorine interactions at the thrombin active site: protein backbone fragments H-Cα-C=O comprise a favorable C-F environment and interactions of C-F with electrophiles. ChemBioChem 5:666–675
33. Olsen JA, Banner DW, Seiler P, Sander UO, D'Arcy A, Stihle M, Muller K, Diederich F (2003) A fluorine scan of thrombin inhibitors to map the fluorophilicity/fluorophobicity of an enzyme active site: evidence for C-F•••C=O interactions. Angew Chem Int Ed 42:2507–2511
34. Carini DJ, Christ DD, Duncia JV, Pierce ME (1989) The discovery and development of angiotensin II antagonists. Pharmaceutical Biotechnol 11:29–56
35. Duncia JV, Carini DJ, Chiu AT, Johnson AL, Price WA, Wong PC, Wexler RR, Timmermans PBMWM (1992) The discovery of DuP 753, a potent, orally active nonpeptide angiotensin II receptor antagonist. Med Res Rev 12:149–191
36. Duncia JV, Chiu AT, Carini DJ, Gregory GB, Johnson AL, Price WA, Wells GJ, Wong PC, Calabrese JC, Timmermans PBMWM (1990) The discovery of potent nonpeptide angiotensin II receptor antagonists: a new class of potent antihypertensives. J Med Chem 33:1312–1329

37. Carini DJ, Duncia JV, Johnson AL, Chiu AT, Price WA, Wong PC, Timmermans PBMWM (1990) Nonpeptide angiotensin II receptor antagonists: *N*-[(benzyloxy)benzyl]imidazoles and related compounds as potent antihypertensives. J Med Chem 33:1330–1336
38. Carini DJ, Duncia JV, Aldrich PE, Chiu AT, Johnson AL, Pierce ME, Price WA, Santella JB III, Wells GJ, Wexler RR, Wong PC, Yoo S-E, Timmermans PBMWM (1991) Nonpeptide angiotensin II receptor antagonists: the discovery of a series of *N*-(biphenylylmethyl)imidazoles as potent, orally active antihypertensives. J Med Chem 34:2525–2547
39. Herr RJ (2002) 5-Substituted-1*H*-tetrazoles as carboxylic acid isosteres: medicinal chemistry and synthetic methods. Bioorg Med Chem 10:3379–3393
40. Allen FH, Groom CR, Liebeschuetz JW, Bardwell DA, Olsson TSG, Wood PA (2012) The hydrogen bond environments of 1*H*-tetrazole and tetrazolate rings: the structural basis for tetrazole−carboxylic acid bioisosterism. J Chem Inf Model 52:857–866
41. Noda K, Saad Y, Kinoshita A, Boyle TP, Graham RM, Husain A, Karnik SS (1995) Tetrazole and carboxylate groups of angiotensin receptor antagonists bind to the same subsite by different mechanisms. J Biol Chem 270:2284–2289
42. Naylor EM, Chakravarty PK, Costello CA, Chang RS, Chen T-B, Faust KA, Lotti VJ, Kivlighn SD, Zingaro GJ, Siegl PKS, Wong PC, Carini DJ, Wexler RR, Patchett AA, Greenlee WJ (1993) Potent imidazole angiotensin II antagonists: acyl sulfonamides and acyl sulfamides as tetrazole replacements. Bioorg Med Chem Lett 3:69–74
43. Lamarre D, Anderson PC, Bailey M, Beaulieu P, Bolger G, Bonneau P, Boes M, Cameron DR, Cartier M, Cordingley MG, Faucher A-M, Goudreau N, Kawai SH, Kukolj G, Lagace L, LaPlante SR, Narjes H, Poupart M-A, Rancourt J, Sentjens R,E, St. George R, Simoneau B, Steinmann G, Thibeault D, Tsantrizos YS, Weldon SM, Yong C-L, Llinas-Brunet M (2003) An NS3 protease inhibitor with antiviral effects in humans infected with hepatitis C virus. Nature 426:186–189
44. Llinas-Brunet M, Bailey MD, Bolger G, Brochu C, Faucher A-M, Ferland JM, Garneau M, Ghiro E, Gorys V, Grand-Maitre C, Halmos T, Lapeyre-Paquette N, Liard F, Poirier M, Rheaume M, Tsantrizos YS, Lamarre D (2004) Structure-activity study on a novel series of macrocyclic inhibitors of the hepatitis C virus NS3 protease leading to the discovery of BILN 2061. J Med Chem 47:1605–1608
45. Stoltz JH, Stern JO, Huang Q, Seidler RW, Pack FD, Knight BL (2011) A twenty-eight-day mechanistic time course study in the rhesus monkey with hepatitis C virus protease inhibitor BILN 2061. Toxicol Pathol 39:496–501
46. Campbell JA, Good A (2002) Preparation of tripeptides as hepatitis C inhibitors. PCT Int. Appl. WO 2002/060,926
47. Scola PM, Sun L-Q, Chen J, Wang AX, Sit S-Y, Chen Y, D'Andrea SV, Zheng Z, Sin N, Venables BL, Cocuzza A, Bilder D, Carini D, Johnson B, Good AC, Rajamani R, Klei HE, Friborg J, Barry D, Levine S, Chen C, Sheaffer A, Hernandez D, Falk P, Yu F, Zhai G, Knipe JO, Mosure K, Shu Y-Z, Phillip T, Arora VK, Loy J, Adams S, Schartman R, Browning M, Levesque PC, Li D, Zhu JL, Sun H, Pilcher G, Bounous D, Lange RW, Pasquinelli C, Eley T, Colonno R, Meanwell NA, McPhee F (2010) Discovery of BMS-650032, an NS3 protease inhibitor for the treatment of Hepatitis C. In: 239th ACS national meeting and exposition, March 21–25, 2010, San Francisco. Abstract: MEDI-38
48. Liverton NJ, Holloway MK, McCauley JA, Rudd MT, Butcher JW, Carroll SS, DiMuzio J, Fandozzi C, Gilbert KF, Mao S-S, McIntyre CJ, Nguyen KT, Romano JJ, Stahlhut M, Wan B-L, Olsen DB, Vacca JP (2008) Molecular modeling based approach to potent P2-P4 macrocyclic inhibitors of hepatitis C NS3/4A protease. J Am Chem Soc 130:4607–4609
49. Cummings MD, Lindberg J, Lin T-I, de Kock H, Lenz O, Lilja E, Fellander S, Baraznenok V, Nystrom S, Nilsson M, Vrang L, Edlund M, Rosenquist A, Samuelsson B, Raboisson P, Simmen K (2010) Induced-fit binding of the macrocyclic noncovalent inhibitor TMC435 to its HCV NS3/NS4A protease target. Angew Chemie Int Ed 49:1652–1655
50. Wendt MD (2008) Discovery of ABT-263, a Bcl-family protein inhibitor: observations on targeting a large protein–protein interaction. Exp Opin Drug Discov 3:1123–1143

51. Petros AM, Dinges J, Augeri DA, Baumeister SA, Betebenner DA, Bures MG, Elmore SW, Hajduk PJ, Joseph MK, Landis SK, Nettesheim DG, Rosenberg SH, Shen W, Thomas S, Wang X, Zanze I, Zhang H, Fesik SW (2006) Discovery of a potent inhibitor of the antiapoptotic protein Bcl-xL from NMR and parallel synthesis. J Med Chem 49:656–663
52. Park C-M, Bruncko M, Adickes J, Bauch J, Ding H, Kunzer A, Marsh KC, Nimmer P, Shoemaker AR, Song X, Tahir SK, Tse C, Wang X, Wendt MD, Yang X, Zhang H, Fesik SW, Rosenberg SH, Elmore SW (2008) Discovery of an orally bioavailable small molecule inhibitor of prosurvival B-cell lymphoma 2 proteins. J Med Chem 51:6902–6915
53. Laurence C, Berthelot M (2000) Observations on the strength of hydrogen bonding. Perspect Drug Discov Des 18:39–60
54. Laurence C, Brameld KA, Graton J, Le Questel J-Y, Renault E (2009) The pK_{BHX} database: toward a better understanding of hydrogen-bond basicity for medicinal chemists. J Med Chem 52:4073–4086
55. Abraham MH, Duce PP, Prior DV (1989) Hydrogen bonding. Part 9. Solute proton donor and proton acceptor scales for use in drug design. J Chem Soc Perkin Trans 2 1355–1375
56. Graton J, Berthelot M, Gal J-F, Laurence C, Lebreton J, Le Questel J-Y, Maria P-C, Robins R (2003) The nicotinic pharmacophore: thermodynamics of the hydrogen-bonding complexation of nicotine, nornicotine, and models. J Org Chem 68:8208–8221
57. Arnaud V, Le Questel J-Y, Mathé-Allainmat M, Lebreton J, Berthelot M (2004) Multiple hydrogen-bond accepting capacities of polybasic molecules: the case of cotinine. J Phys Chem A 108:10740–10748
58. Locati A, Berthelot M, Evain M, Lebreton J, Le Questel J-Y, Mathé-Allainmat M, Planchat A, Renault E, Graton J (2007) The exceptional hydrogen-bond properties of neutral and protonated lobeline. J Phys Chem A 111:6397–6405
59. Arnaud V, Berthelot M, Evain M, Graton J, Le Questel J-Y (2007) Hydrogen-bond interactions of nicotine and acetylcholine salts: a combined crystallographic, spectroscopic, thermodynamic and theoretical study. Chem Eur J 13:1499–1510
60. Arnaud V, Berthelot M, Le Questel J-Y (2005) Hydrogen-bond accepting strength of protonated nicotine. J Phys Chem A 109:3767–3770
61. Arnaud V, Berthelot M, Felpin F-X, Lebreton J, Le Questel J-Y, Graton J (2009) Hydrogen-bond accepting strength of five-membered *N*-heterocycles: the case of substituted phenylpyrrolines and myosmines. Eur J Org Chem 4939–4948
62. Graton J, Berthelot M, Gal J-F, Girard S, Laurence C, Lebreton J, Le Questel J-Y, Maria P-C, Naus P (2002) Site of protonation of nicotine and nornicotine in the gas phase: pyridine or pyrrolidine nitrogen? J Am Chem Soc 124:10552–10562
63. Wermuth CG (2012) Are pyridazines privileged structures? Med Chem Commun 2:935–941
64. Taft RW, Anvia F, Taagpera M, Catalán J, Elguero J (1986) Electrostatic proximity effects in the relative basicities and acidities of pyrazole, imidazole, pyridazine, and pyrimidine. J Am Chem Soc 108:3237–3239
65. Meanwell NA, Romine JL, Seiler SM (1994) Non-prostanoid prostacyclin mimetics. Drugs Future 19:361–385
66. Meanwell NA, Rosenfeld MJ, Trehan AK, Wright JJK, Brassard CL, Buchanan JO, Federici ME, Fleming JS, Gamberdella M, Zavoico GB, Seiler SM (1992) Nonprostanoid prostacyclin mimetics. 2. 4,5-Diphenyloxazole derivatives. J Med Chem 35:3483–3497
67. Meanwell NA, Rosenfeld MJ, Wright JJK, Brassard CL, Buchanan JO, Federici ME, Fleming JS, Gamberdella M, Hartl KS, Zavoico GB, Seiler SM (1993) Nonprostanoid prostacyclin mimetics. 4. Derivatives of 2-[3-[2-(4,5-diphenyl-2-oxazolyl)ethyl]phenoxy]acetic acid substituted α- to the oxazole ring. J Med Chem 36:3871–3883
68. Meanwell NA, Romine JL, Rosenfeld MJ, Martin SW, Trehan AK, Wright JJK, Malley MF, Gougoutas JZ, Brassard CL, Buchanan JO, Federici ME, Fleming JS, Gamberdella M, Hartl KS, Zavoico GB, Seiler SM (1992) Nonprostanoid prostacyclin mimetics. 5. Structure–activity relationships associated with [3-[4-(4,5-diphenyl-2-oxazolyl)-5-oxazolyl]phenoxy] acetic acid. J Med Chem 36:3884–3903

69. Böhm H-J, Klebe G, Brode S, Hesse U (1996) Oxygen and nitrogen in competitive situations: which is the hydrogen-bond acceptor? Chem Eur J 2:1509–1513
70. Nobeli I, Price SL, Lommerse JPM, Taylor R (1997) Hydrogen bonding properties of oxygen and nitrogen acceptors in aromatic heterocycles. J Comput Chem 18:2060–2074
71. Kumar DV, Rai R, Brameld KA, Riggs J, Somoza JR, Rajagopalan R, Janc JW, Xia YM, Ton TL, Hu H, Lehoux I, Ho JD, Young WB, Hart B, Green MJ (2012) 3-Heterocyclyl quinolone inhibitors of the HCV NS5B polymerase. Bioorg Med Chem Lett 22:300–304
72. Boström J, Hogner A, Llinàs A, Wellner E, Plowright AT (2012) Oxadiazoles in medicinal chemistry. J Med Chem 55:1817–1830
73. Jones ED, Vandegraaff N, Le G, Choi N, Issa W, MacFarlane K, Thienthong N, Winfield LJ, Coates JAV, Lu L, Li X, Feng X, Yu C, Rhodes DI, Deadman JJ (2010) Design of a series of bicyclic HIV-1 integrase inhibitors. Part 1: selection of the scaffold. Bioorg Med Chem Lett 20:5913–5917
74. Le G, Vandegraaff N, Rhodes DI, Jones ED, Coates JAV, Thienthong N, Winfield LJ, Lu L, Li X, Yu C, Feng X, Deadman JJ (2010) Design of a series of bicyclic HIV-1 integrase inhibitors. Part 2: azoles: effective metal chelators. Bioorg Med Chem Lett 20:5909–5912
75. Le G, Vandegraaff N, Rhodes DI, Jones ED, Coates JAV, Lu L, Li X, Yu C, Feng X, Deadman JJ (2010) Discovery of potent HIV integrase inhibitors active against raltegravir resistant viruses. Bioorg Med Chem Lett 20:5013–5018
76. Johns BA, Weatherhead JG, Allen SH, Thompson JB, Garvey EP, Foster SA, Jeffrey JL, Miller WH (2009) The use of oxadiazole and triazole substituted naphthyridines as HIV-1 integrase inhibitors. Part 1: establishing the pharmacophore. Bioorg Med Chem Lett 19:1802–1806
77. Johns BA, Weatherhead JG, Allen SH, Thompson JB, Garvey EP, Foster SA, Jeffrey JL, Miller WH (2009) 1,3,4-Oxadiazole substituted naphthyridines as HIV-1 integrase inhibitors. Part 2: SAR of the C5 position. Bioorg Med Chem Lett 19:1807–1810
78. Kalgutkar AS, Jones R, Sawant A (2010) Sulfonamide as an essential functional group in drug design. In: Smith DA (ed) Metabolism, pharmacokinetics and toxicity of functional groups. RSC drug discovery series 1. Chap 5, Royal Society of Chemistry, London, pp 210–274
79. Hedstrom L (2002) Serine protease mechanism and specificity. Chem Rev 102:4501–4523
80. Long JZ, Cravatt BF (2011) The metabolic serine hydrolases and their functions in mammalian physiology and disease. Chem Rev 111:6022–6063
81. Otrubova K, Boger DL (2012) α-Ketoheterocycle-based inhibitors of fatty acid amide hydrolase (FAAH). ACS Chem Neurosci 3:340–348
82. Bradamante S, Pagani GA (1996) Benzyl and heteroarylmethyl carbanions: structure and substituent effects. Adv Carbanion Chem 2:189–263
83. Abbotto A, Bradamante S, Pagani GA (1993) Charge mapping in carbanions. Weak charge demand of the cyano group as assessed from a ^{13}C-NMR study of carbanions of α-activated acetonitriles and phenylacetonitriles: breakdown of a myth. J Org Chem 58:449–455
84. Abbotto A, Bradamante S, Pagani GA (1996) Diheteroarylmethanes. 5. *E-Z* isomerism of carbanions substituted by 1,3-azoles: ^{13}C and ^{15}N δ-charge/shift relationships as source for mapping charge and ranking the electron-withdrawing power of heterocycles. J Org Chem 61:1761–1769
85. Abbotto A, Bradamante S, Facchetti A, Pagani GA (1999) Diheteroarylmethanes. 8. Mapping charge and electron-withdrawing power of the 1,2,4-triazol-5-yl substituent. J Org Chem 64:6756–6763
86. Imperiali B, Abeles RH (1986) Inhibition of serine proteases by peptidyl fluoromethyl ketones. Biochemistry 25:3760–3767
87. Imperiali B, Abeles RH (1987) Extended binding inhibitors of chymotrypsin that interact with leaving group subsites S1′–S3′. Biochemistry 26:4474–4477
88. Edwards PD, Meyer EF Jr, Vijayalakshmi J, Tuthill PA, Andisik DA, Gomes B, Strimplerg A (1992) Elastase inhibitors, the peptidyl α-ketobenzoxazoles, and the X-ray crystal structure of

the covalent complex between porcine pancreatic elastase and Ac-Ala-Pro-Val-2-benzoxazole. J Am Chem Soc 114:1854–1863
89. Edwards PD, Wolanin DJ, Andisik DA, David MW (1995) Peptidyl α-ketoheterocyclic inhibitors of human neutrophil elastase. 2. Effect of varying the heterocyclic ring on in vitro potency. J Med Chem 38:76–85
90. Edwards P, Zottola MA, Davis M, Williams J, Tuthill PA (1995) Peptidyl α-ketoheterocyclic inhibitors of human neutrophil elastase. 3. In vitro and in vivo potency of a series of peptidyl α-ketobenzoxazoles. J Med Chem 38:3972–3982
91. Ohmoto K, Yamamoto T, Horiuchi T, Imanishi H, Odagaki Y, Kawabata K, Sekioka T, Hirota Y, Matsuoka S, Nakai H, Toda M, Cheronis JC, Spruce LW, Gyorkos A, Wieczorek M (2000) Design and synthesis of new orally active nonpeptidic inhibitors of human neutrophil elastase. J Med Chem 43:4927–4929
92. Ohmoto K, Yamamoto T, Okuma M, Horiuchi T, Imanishi H, Odagaki Y, Kawabata K, Sekioka T, Hirota Y, Matsuoka S, Nakai H, Toda M, Cheronis JC, Spruce LW, Gyorkos A, Wieczorek M (2001) Development of orally active nonpeptidic inhibitors of human neutrophil elastase. J Med Chem 44:1268–1285
93. Costanzo MJ, Almond HR Jr, Hecker LR, Schott MR, Yabut SC, Zhang H-C, Andrade-Gordon P, Corcoran TW, Giardino EC, Kauffman JA, Lewis JM, de Garavilla L, Haertlein BJ, Maryanoff BE (2005) In-depth study of tripeptide-based α-ketoheterocycles as inhibitors of thrombin. Effective utilization of the S1' subsite and its implications to structure-based drug design. J Med Chem 48:1984–2008
94. Maryanoff BE, Costanzo MJ (2008) Inhibitors of proteases and amide hydrolases that employ α-ketoheterocycles as a key enabling functionality. Bioorg Med Chem 16:1562–1595
95. Romero FA, Hwang I, Boger DL (2006) Delineation of a fundamental α-ketoheterocycle substituent effect for use in the design of enzyme inhibitors. J Am Chem Soc 128:14004–14005
96. Mileni M, Garfunkle J, DeMartino JK, Cravatt BF, Boger DL, Stevens RC (2009) Binding and inactivation mechanism of a humanized fatty acid amide hydrolase by α-ketoheterocycle inhibitors revealed from cocrystal structures. J Am Chem Soc 131:10497–10506
97. Boger DL, Miyauchi H, Du W, Hardouin C, Fecik RA, Cheng H, Hwang I, Hedrick MP, Leung D, Acevedo O, Guimarães CRW, Jorgensen WL, Cravatt BF (2005) Discovery of a potent, selective, and efficacious class of reversible α-ketoheterocycle inhibitors of fatty acid amide hydrolase effective as analgesics. J Med Chem 48:1849–1856
98. Hardouin C, Kelso MJ, Romero FA, Rayl TJ, Leung D, Hwang I, Cravatt BF, Boger DL (2007) Structure–activity relationships of α-ketooxazole inhibitors of fatty acid amide hydrolase. J Med Chem 50:3359–3368
99. DeMartino JK, Garfunkle J, Hochstatter DG, Cravatt BF, Boger DL (2008) Exploration of a fundamental substituent effect of α-ketoheterocycle enzyme inhibitors: potent and selective inhibitors of fatty acid amide hydrolase. Bioorg Med Chem Lett 18:5842–5846
100. Garfunkle J, Ezzili C, Ray TJ, Hochstatter DG, Hwang I, Boger DL (2008) Optimization of the central heterocycle of α-ketoheterocycle inhibitors of fatty acid amide hydrolase. J Med Chem 51:4392–4403
101. Mileni M, Garfunkle J, Ezzili C, Kimball FS, Cravatt BF, Stevens RC, Boger DL (2009) X-ray crystallographic analysis of α-ketoheterocycle inhibitors bound to a humanized variant of fatty acid amide hydrolase. J Med Chem 53:230–240
102. Mileni M, Garfunkle J, Ezzili C, Cravatt BF, Stevens RC, Boger DL (2011) Fluoride-mediated capture of a noncovalent bound state of a reversible covalent enzyme inhibitor: X-ray crystallographic analysis of an exceptionally potent α-ketoheterocycle inhibitor of fatty acid amide hydrolase. J Am Chem Soc 133:4092–4100
103. Otrubova K, Ezzili C, Boger DL (2011) The discovery and development of inhibitors of fatty acid amide hydrolase (FAAH). Bioorg Med Chem Lett 21:4674–4685
104. Hansch C, Leo A, Unger SH, Kim KH, Nikaitani D, Lien EJ (1973) Aromatic substituent constants for structure-activity correlations. J Med Chem 16:1207–1216

105. Cai J, Fradera X, van Zeeland M, Dempster M, Cameron KS, Bennett DJ, Robinson J, Popplestone L, Baugh M, Westwood P, Bruin J, Hamilton W, Kinghorn E, Long C, Uitdehaag JCM (2010) 4-(3-Trifluoromethylphenyl)-pyrimidine-2-carbonitrile as cathepsin S inhibitors: N3, not N1 is critically important. Bioorg Med Chem Lett 20:4507–4510
106. Salonen LM, Holland MC, Kaib PSJ, Haap W, Benz J, Mary J-L, Kuster O, Schweizer WB, Banner DW, Diederich F (2012) Molecular recognition at the active site of factor Xa: cation–π interactions, stacking on planar peptide surfaces, and replacement of structural water. Chem Eur J 18:213–222
107. Harder M, Kuhn B, Diederich F (2013) Efficient stacking on protein amide fragments. ChemMedChem 8:397–404
108. Michel J, Tirado-Rives J, Jorgensen WL (2009) Energetics of displacing water molecules from protein binding sites: consequences for ligand optimization. J Am Chem Soc 131:15403–15411
109. Lam PYS, Jadhav PK, Eyermann CJ, Hodge CN, Ru Y, Bacheler LT, Meek JL, Otto MJ, Rayner MM, Wong YN, Chang C-H, Weber PC, Jackson DA, Sharpe TR, Erikson-Viitanen S (1994) Rational design of potent, bioavailable, nonpeptide cyclic ureas as HIV protease inhibitors. Science 263:380–384
110. Lam PYS, Ru Y, Jadhav PK, Aldrich PE, DeLucca GV, Eyermann CJ, Chang C-H, Emmett G, Holler ER, Daneker WF, Li L, Confalone PN, McHugh RJ, Han Q, Li R, Markwalder JA, Seitz SP, Sharpe TR, Bacheler LT, Rayner MM, Klabe RM, Shum L, Winslow DL, Kornhauser DM, Jackson DA, Erickson-Viitanen S, Hodge CN (1996) Cyclic HIV protease inhibitors: synthesis, conformational analysis, P2/P2' structure–activity relationship, and molecular recognition of cyclic ureas. J Med Chem 39:3514–3525
111. De Lucca GV, Erickson-Viitanen S, Lam PYS (1997) Cyclic HIV protease inhibitors capable of displacing the active site structural water molecule. Drug Discov Today 2:6–18
112. Nalam MNL, Peeters A, Jonckers TMH, Dierynck I, Schiffer CA (2007) Crystal structure of lysine sulfonamide inhibitor reveals the displacement of the conserved flap water molecule in human immunodeficiency virus type 1 protease. J Virol 81:9512–9518
113. Canan Koch SS, Thoresen LH, Tikhe JG, Maegley KA, Almassy RJ, Li J, Yu X-H, Zook SE, Kumpf RA, Zhang C, Boritzki TJ, Mansour RN, Zhang KE, Ekker A, Calabrese CR, Curtin NJ, Kyle S, Thomas HD, Wang L-Z, Calvert AH, Golding BT, Griffin RJ, Newell DR, Webber SE, Hostomsky Z (2002) Novel tricyclic poly(ADP-ribose) polymerase-1 inhibitors with potent anticancer chemopotentiating activity: design, synthesis, and X-ray cocrystal structure. J Med Chem 45:4961–4974
114. Tikhe JG, Webber SE, Hostomsky Z, Maegley KA, Ekkers A, Li J, Yu X-H, Almassy RJ, Kumpf RA, Boritzki TJ, Zhang C, Calabrese CR, Curtin NJ, Kyle S, Thomas HD, Wang L-Z, Calvert AH, Golding BT, Griffin RJ, Newell DR (2004) Design, synthesis, and evaluation of 3,4-dihydro-2*H*-[1,4]diazepino[6,7,1-*hi*]indol-1-ones as inhibitors of poly(ADP-Ribose) polymerase. J Med Chem 47:5467–5481
115. García-Sosa AT, Firth-Clark S, Mancera RL (2005) Including tightly-bound water molecules in de novo drug design. Exemplification through in silico generation of poly(ADP-ribose) polymerase inhibitors. J Chem Inf Model 45:624–633
116. Chen JM, Xu SL, Wawrzak Z, Basarab GS, Jordan DB (1998) Structure-based design of potent inhibitors of scytalone dehydratase: displacement of a water molecule from the active site. Biochemistry 37:17735–17744
117. Liu C, Wrobleski ST, Lin J, Ahmed G, Metzger A, Wityak J, Gillooly KM, Shuster DJ, McIntyre KW, Pitt S, Shen DR, Zhang RF, Zhang H, Doweyko AM, Diller D, Henderson I, Barrish JC, Dodd JH, Schieven GL, Leftheris K (2005) 5-Cyanopyrimidine derivatives as a novel class of potent, selective, and orally active inhibitors of p38α MAP kinase. J Med Chem 48:6261–6270
118. Wissner A, Berger DM, Boschelli DH, Floyd MB Jr, Greenberger LM, Gruber BC, Johnson BD, Mamuya N, Nilakantan R, Reich MF, Shen R, Tsou H-R, Upeslacis E, Wang YF, Wu B, Ye F, Zhang N (2000) 4-Anilino-6,7-dialkoxyquinoline-3-carbonitrile inhibitors of epidermal

growth factor receptor kinase and their bioisosteric relationship to the 4-anilino-6,7-dialkoxy-quinazoline inhibitors. J Med Chem 43:3244–3256
119. Davies NGM, Browne H, Davis B, Drysdale MJ, Foloppe N, Geoffrey S, Gibbons B, Hart T, Hubbard R, Rugaard Jensen M, Mansell H, Massey A, Matassova N, Moore JD, Murray J, Pratt R, Ray S, Robertson A, Roughley SD, Schoepfer J, Scriven K, Simmonite H, Stokes S, Surgenor A, Webb P, Wood M, Wright L, Brough P (2012) Targeting conserved water molecules: design of 4-aryl-5-cyanopyrrolo[2,3-*d*]pyrimidine Hsp90 inhibitors using fragment-based screening and structure-based optimization. Bioorg Med Chem 20:6770–6789
120. Trujillo JI, Kiefer JR, Huang W, Day JE, Moon J, Jerome GM, Bono CP, Kornmeier CM, Williams ML, Kuhn C, Rennie GR, Wynne TA, Carron CP, Thorarensen A (2012) Investigation of the binding pocket of human hematopoietic prostaglandin (PG) D2 synthase (hH-PGDS): a tale of two waters. Bioorg Med Chem Lett 22:2795–3799
121. Meanwell NA (2011) Improving drug candidates by design: a focus on physicochemical properties as a means of improving compound disposition and safety. Chem Res Toxicol 24:1420–1456
122. Johnson F (1968) Allylic strain in six membered rings. Acc Chem Res 68:375–413
123. Yamazaki T, Taguchi T, Ojima I (2009) Unique properties of fluorine and their relevance to medicinal chemistry and chemical biology. In: Ojima I (ed) Fluorine in medicinal chemistry and chemical biology. Chap 1, Wiley, Chichester, UK pp 1–46
124. Hunter L (2010) The C–F bond as a conformational tool in organic and biological chemistry. Beilstein J Org Chem 6. doi:10.3762/bjoc.6.38
125. Zimmer LE, Sparr C, Gilmour R (2011) Fluorine conformational effects in organocatalysis: an emerging strategy for molecular design. Angew Chem Int Ed 50:11860–11871
126. Buissonneaud DY, van Mourik T, O'Hagan D (2010) A DFT study on the origin of the fluorine *gauche* effect in substituted fluoroethanes. Tetrahedron 66:2196–2202
127. O'Hagan D (2012) Organofluorine chemistry: synthesis and conformation of vicinal fluoromethylene motifs. J Org Chem 77:3689–3699
128. Wu D, Tian A, Sun H (1998) Conformational properties of 1,3-difluoropropane. J Chem Phys A 102:9901–9905
129. Tavasli M, O'Hagan D, Pearson C, Petty MC (2002) The fluorine *gauche* effect. Langmuir isotherms report the relative conformational stability of (±)-erythro- and (±)-threo-9,10-difluorostearic acids. Chem Commun 1226–1227
130. Hunter L, Kirsch P, Slawin AMZ, O'Hagan D (2009) Synthesis and structure of stereoisomeric multivicinal hexafluoroalkanes. Angew Chem Int Ed 48:5457–5460
131. Banks JW, Batsanov AS, Howard JAK, O'Hagan D, Rzepa H, Martin-Santamaria S (1999) The preferred conformation of α-fluoroamides. J Chem Soc Perkin 2:2409–2411
132. Briggs CRS, O'Hagan D, Howard JAK, Yulfi DS (2003) The C–F bond as a tool in the conformational control of amides. J Fluorine Chem 119:9–13
133. Dalvit D, Vulpetti A (2012) Intermolecular and intramolecular hydrogen bonds involving fluorine atoms: implications for recognition, selectivity, and chemical properties. ChemMedChem 7:262–272
134. Schüler M, O'Hagan D, Slawin AMZ (2005) The vicinal F-C-C-F moiety as a tool for influencing peptide conformation. Chem Commun 4324–4326
135. O'Hagan D, Rzepa HS, Schüler M, Slawin AMZ (2006) The vicinal difluoro motif: the synthesis and conformation of *erythreo*- and *threo*-diastereomers of 1,2-difluorodiphenylethanes, 2,3-difluorosuccinic acids and their derivatives. Beilstein J Org Chem 2. doi:10.1186/1860-5397-2-19
136. Winkler M, Moraux T, Khairy HA, Scott RH, Slawin AMZ, O'Hagan D (2009) Synthesis and vanilloid receptor (TRPV1) activity of the enantiomers of α-fluorinated capsaicin. ChemBioChem 10:823–828
137. Peddie V, Butcher RJ, Robinson WT, Wilce MCJ, Traore DAK, Abell AD (2012) Synthesis and conformation of fluorinated β-peptidic compounds. Chem Eur J 18:6655–6662

138. O'Hagan D, Bilton C, Howard JAK, Knight L, Tozer DJ (2001) The preferred conformation of *N*-β-fluoroethylamides. Observation of the fluorine amide gauche effect. J Chem Soc Perkin Trans 2:605–607
139. O'Hagan D, Rzepa HS (1997) Some influences of fluorine in bioorganic chemistry. Chem Commun 645–652
140. Mascitti V, Stevens BD, Choi C, McClure KF, Guimarães CRW, Farley KA, Munchhof MJ, Robinson RP, Futatsugi K, Lavergen SY, Lefker BA, Cornelius P, Bonin PD, Kalgutkar AS, Sharma R, Chen Y (2011) Design and evaluation of a 2(2,3,6-trifluorophenyl)acetamide derivative as an agonist of the GPR119 receptor. Bioorg Med Chem Lett 21:1306–1309
141. Holmgren SK, Taylor KM, Bretscher LE, Raines RT (1998) Code for collagen's stability deciphered. Nature 392:666–667
142. Bretscher LE, Jenkins CL, Taylor KM, DeRider ML, Raines RT (2001) Conformational stability of collagen relies on a stereoelectronic effect. J Am Chem Soc 123:777–778
143. Hodges JA, Raines RT (2003) Stereoelectronic effects on collagen stability: the dichotomy of 4-fluoroproline diastereomers. J Am Chem Soc 125:9262–9263
144. Doi M, Nishi Y, Uchiyama S, Nisiuchi Y, Nakazawa T, Ohkubo T, Kobayasji Y (2003) Characterization of collagen model peptides containing 4-fluoroproline: (4(*S*)-fluoroproline-Pro-Gly)$_{10}$ forms a triple helix, but (4(*R*)-fluoroproline-Pro-Gly)$_{10}$ does not. J Am Chem Soc 125:9922–9923
145. Hodges JA, Raines RT (2005) Stereoelectronic and steric effects in the collagen triple helix: toward a code for strand association. J Am Chem Soc 127:15923–15932
146. Shoulders MD, Kamer KJ, Raines RT (2009) Origin of the stability conferred upon collagen by fluorination. Bioorg Med Chem Lett 19:3859–3862
147. DeRider ML, Wilkins SJ, Waddell MJ, Bretscher LE, Weinhold F, Raines RT, Markley JL (2002) Collagen stability: insights from NMR spectroscopic and hybrid density functional computational investigations of the effect of electronegative substituents on prolyl ring conformations. J Am Chem Soc 124:2497–2505
148. Doi M, Nishi Y, Kiritoshi N, Iwata T, Nago M, Nakano H, Uchiyama S, Nakazawa T, Wakamiya T, Kbayashi Y (2002) Simple and efficient syntheses of Boc- and Fmoc-protected 4(*R*)- and 4(*S*)-fluoroproline solely from 4(*R*)-hydroxyproline. Tetrahedron 58:8453–8459
149. Park S, Radmer RJ, Klein TE, Pande VS (2005) A new set of molecular mechanics parameters for hydroxyproline and its use in molecular dynamics simulations of collagen-like peptides. J Comput Chem 26:1612–1616
150. Kim W, Hardcastle KL, Conticello VP (2006) Fluoroproline flip-flop: regiochemcial reversal of a stereoelectronic effect on peptide and protein structures. Angew Chem Int Ed 45:8141–8814
151. Kitamoto T, Ozawa T, Abe M, Marubayashi S, Yamazaki T (2008) Incorporation of fluoroprolines to proctolin: study on the effect of a fluorine atom towards peptidic conformation. J Fluorine Chem 129:286–293
152. Briggs CRS, Allen MJ, O'Hagan D, Tozer DJ, Slawin AMZ, Goeta AE, Howard JAK (2004) The observation of a large gauche preference when 2-fluoroethylamine and 2-fluoroethanol become protonated. Org Biomol Chem 2:732–740
153. Lankin DC, Chandrakumar NS, Rao SN, Spangler DP, Snyder JP (1993) Protonated 3-fluoropiperidines: an unusual fluoro directing effect and a test for quantitative theories of solvation. J Am Chem Soc 115:3356–3357
154. Snyder JP, Chandrakumar NS, Sato H, Lankin DC (2000) The unexpected diaxial orientation of *cis*-3,5-difluoropiperidine in water: a potent CF–NH charge-dipole effect. J Am Chem Soc 122:544–545
155. Sun A, Lankin DC, Harcastle K, Snyder JP (2005) 3-Fluoropiperidines and *N*-methyl-3-fluoropiperidinium salts: the persistence of axial fluorine. Chem Eur J 11:1579–1591
156. Deniau G, Slawin AMZ, Lebl T, Chorki F, Issberner JP, van Mourik T, Heygate JM, Lambert JJ, Etherington L-A, Sillar KT, O'Hagan D (2007) Synthesis, conformation and biological

evaluation of the enantiomers of 3-fluoro-γ-aminobutyric acid ((*R*)- and (*S*)-3F-GABA): an analogue of the neurotransmitter GABA. ChemBioChem 8:2265–2274
157. Clift MD, Ji H, Deniau GP, O'Hagan D, Silverman RB (2007) Enantiomers of 4-amino-3-fluorobutanoic acid as substrates for γ-aminobutyric acid aminotransferase. Conformational probes for GABA binding. Biochemistry 46:13819–13828
158. Yamamoto I, Deniau GP, Gavande N, Chebib M, Johnston GAR, O'Hagan D (2011) Agonist responses of (*R*)- and (*S*)-3-fluoro-γ-aminobutyric acids suggest an enantiomeric fold for GABA binding to $GABA_C$ receptors. Chem Commun 47:7956–7958
159. Chia PW, Livesey MR, Slawin AMZ, van Mourik T, Wyllie DJA, O'Hagan D (2012) 3-Fluoro-*N*-methyl-D-asaprtic acid (3F-NMDA) stereoisomers as conformational probes for exploring agonist binding at NMDA receptors. Chem Eur J 18:8813–8819
160. Abraham RJ, Chambers EJ, Thomas AW (1994) Conformational analysis. Part 22. An NMR and theoretical investigation of the *gauche* effect in fluoroethanols. J Chem Soc Perkin Trans 2:949–955
161. Abraham RJ, Smith TAD, Thomas AW (1996) Conformational analysis. Part 28. OH-F hydrogen bonding and the conformation of trans-2-fluorocyclohexanol. J Chem Soc Perkin Trans 2:1949–1955
162. Myers AG, Barbay JK, Zhong B (2001) Asymmetric synthesis of chiral organofluorine compounds: use of nonracemic fluoroiodoacetic acid as a practical electrophile and its application to the synthesis of monofluoro hydroxyethylene dipeptide isosteres within a novel series of HIV protease inhibitors. J Am Chem Soc 123:7207–7219
163. Brameld KA, Kuhn B, Reuter DC, Stahl M (2008) Small molecule conformational preferences derived from crystal structure data. A medicinal chemistry focused analysis. J Chem Inf Model 48:1–24
164. Gomez R, Jolly S, Williams T, Tucker T, Tynebor R, Vacca J, McGaughey G, Lai M-T, Felock P, Munshi V, DeStefano D, Touch S, Miller M, Yan Y, Sanchez R, Liang Y, Paton B, Wan B-L, Anthony N (2011) Design and synthesis of pyridone inhibitors of non-nucleoside reverse transcriptase. Bioorg Med Chem Lett 21:7344–7350
165. Leroux F, Jeschke P, Schlosser M (2005) α-Fluorinated ethers, thioethers, and amines: anomerically biased species. Chem Rev 105:827–856
166. Massa MA, Spangler DP, Durley RC, Hickory BS, Connolly DT, Witherbee BJ, Smith ME, Sikorski JA (2001) Novel heteroaryl replacements of aromatic 3-tetrafluoroethoxy substituents in trifluoro-3-(tertiaryamino)-2-propanols as potent inhibitors of cholesterol ester transfer protein. Bioorg Med Chem Lett 11:1625–1628
167. Horne DB, Bartberger MD, Kaller MR, Monenschein H, Zhong W, Hitchcock SA (2009) Synthesis and conformational analysis of α, α-difluoroalkyl heteroaryl ethers. Tetrahedron Lett 50:5452–5455
168. Anderson GM III, Kollman PA, Domelsmith LN, Houk KN (1979) Methoxy group nonplanarity in o-dimethoxybenzenes. Simple predictive models for conformations and rotational barriers in alkoxyaromatics. J Am Chem Soc 101:2344–2352
169. Klocker J, Karpfen A, Wolschann P (2003) On the structure and torsional potential of trifluoromethoxybenzene: an ab initio and density functional study. Chem Phys Lett 367:566–575
170. Chien RJ, Corey EJ (2010) *S*trong conformational preferences of heteroaromatic ethers and electron pair repulsion. Org Lett 12:132–135
171. Phillips GB, Buckman BO, Davey DD, Eagen KA, Guilford WJ, Hinchman J, Ho E, Koovakkat S, Liang A, Light DR, Mohan R, Ng HP, Post JM, Shaw KJ, Smith D, Subramanyam B, Sullivan ME, Trinh L, Vergona R, Walters J, White K, Whitlow M, Wu S, Xu W, Morrissey MM (1998) Discovery of *N*-[2-[5-[amino(imino)methyl]-2-hydroxyphenoxy]-3, 5-difluoro-6-[3-(4, 5-dihydro-1-methyl-1*H*-imidazol-2-yl)phenoxy] pyridin-4-yl]-*N*-methylglycine (ZK-807834): a potent, selective, and orally active inhibitor of the blood coagulation enzyme factor Xa. J Med Chem 41:3557–3562

172. Phillips G, Davey DD, Eagen KA, Koovakkat SK, Liang A, Ng HP, Pinkerton M, Trinh L, Whitlow M, Beatty AM, Morrissey MM (1999) Design, synthesis, and activity of 2,6-diphenoxypyridine-derived factor Xa inhibitors. J Med Chem 42:1749–1756
173. Adler M, Davey DD, Phillips GB, Kim S-H, Jancarik J, Rumennik G, Light DR, Whitlow M (2000) Preparation, characterization, and the crystal structure of the inhibitor ZK-807834 (CI-1031) complexed with factor Xa. Biochemistry 39:12534–12542
174. Chen YL, Mansbach RS, Winter SM, Brooks E, Collins J, Michael L. Corman ML, Dunaiskis AR, Faraci WS, Gallaschun RJ, Schmidt A, Schulz DW (1997) Synthesis and oral efficacy of a 4-(butylethylamino)pyrrolo[2,3-d]pyrimidine: a centrally active corticotropin-releasing factor-1 receptor antagonist. J Med Chem 40:1749–1754
175. Semple G, Lehmann J, Wong A, Ren A, Bruce M, Shin Y-J, Sage CR, Morgan M, Chen W-C, Sebring K, Chu Z-L, Leonard JN, Al-Shamma H, Grottick AJ, Du F, Liang Y, Demarest K, Jones RM (2012) Discovery of a second generation agonist of the orphan G-protein coupled receptor GPR119 with an improved profile. Bioorg Med Chem Lett 22:1750–1755
176. Qiao JX, Cheney DL, Alexander RS, Smallwood AM, King SR, He K, Rendina AR, Luettgen JM, Knabb RM, Wexler RR, Lam PYS (2008) Achieving structural diversity using the perpendicular conformation of *alpha*-substituted phenylcyclopropanes to mimic the bioactive conformation of *ortho*-substituted biphenyl P4 moieties: discovery of novel, highly potent inhibitors of factor Xa. Bioorg Med Chem Lett 18:4118–4123
177. Leeson PD, Springthorpe B (2007) The influence of drug-like concepts on decision making in medicinal chemistry. Nat Rev Drug Discov 6:881–890
178. Tarcsay A, Nyíri K, Keserű GM (2012) Impact of lipophilic efficiency on compound quality. J Med Chem 55:1252–1260
179. Keserű GM, Makara GM (2009) The influence of lead discovery strategies on the properties of drug candidates. Nat Rev Drug Discov 8:203–212
180. Hann M, Keserű GM (2012) Finding the sweet spot: the role of nature and nurture in medicinal chemistry. Nat Rev Drug Discov 11:355–365
181. Lovering F, Bikker J, Humblet C (2009) Escape from flatland: increasing saturation as an approach to improving clinical success. J Med Chem 52:6752–6756
182. Lovering F (2013) Escape from flatland 2: complexity and promiscuity. Med Chem Commun 4:515–519
183. Pellicciari R, Raimondo M, Marinozzi M, Natalini B, Costantino G, Thomsen C (1996) (*S*)-(+)-2-(3'-Carboxybicyclo[1.1.1]pentyl)glycine, a structurally new group 1 metabotropic glutamate receptor antagonist. J Med Chem 39:2874–2876
184. Pellicciari R, Costantino G, Giovagnoni E, Mattoli L, Brabet I, Pin J-P (1998) Synthesis and preliminary evaluation of (*S*)-2-(4'-carboxycubyl)glycine, a new selective mGluR1 antagonist. Bioorg Med Chem Lett 8:1569–1574
185. Costantino G, Maltoni K, Marinozzi M, Camaioni E, Prezeau L, Pin J-P, Pellicciari R (2001) Synthesis and biological evaluation of 2-(3'-(1*H*-tetrazol-5-yl)bicyclo[1.1.1]pent-1-yl)glycine (S-TBPG), a novel mGlu1 receptor antagonist. Bioorg Med Chem 9:221–227
186. Stepan AF, Subramanyam C, Efremov IV, Dutra JK, O'Sullivan TJ, DiRico KJ, McDonald WS, Won A, Dorff PH, Nolan CE, Becker SL, Pustilnik LR, Riddell DR, Kauffman GW, Kormos BL, Zhang L, Lu Y, Capetta SH, Green ME, Karki K, Sibley E, Atchison KP, Hallgren AJ, Oborski CE, Robshaw AE, Sneed B, O'Donnell CJ (2012) Application of the bicyclo[1.1.1]pentane motif as a nonclassical phenyl ring bioisostere in the design of a potent and orally active γ-secretase inhibitor. J Med Chem 55:3414–3424
187. Pinto DJP, Orwat MJ, Wang S, Fevig JM, Quan ML, Amparo E, Cacciola J, Rossi KA, Alexander RS, Smallwood AM, Luettgen JM, Liang L, Aungst BJ, Wright MR, Knabb RM, Wong PC, Wexler RR, Lam PYS (2001) Discovery of 1-[3-(aminomethyl)phenyl]-*N*-[3-fluoro-2′-(methylsulfonyl)-[1,1′-biphenyl]-4-yl]-3-(trifluoromethyl)-1*H*-pyrazole-5-carboxamide (DPC423), a highly potent, selective, and orally bioavailable inhibitor of blood coagulation factor Xa. J Med Chem 44:566–578

188. Quan ML, Lam PYS, Han Q, Pinto DJP, He MY, Li R, Ellis CD, Clark CG, Teleha CA, Sun J-H, Alexander RS, Bai S, Luettgen JM, Knabb RM, Wong PC, Wexler RR (2005) Discovery of 1-(3′-aminobenzisoxazol-5′-yl)-3-trifluoromethyl-*N*-[2-fluoro-4-[(2′-dimethylaminomethyl) imidazol-1-yl]phenyl]-1*H*-pyrazole-5-carboxyamide hydrochloride (razaxaban), a highly potent, selective, and orally bioavailable factor Xa inhibitor. J Med Chem 48:1729–1744
189. Nayak SK, Reddy MK, Guru Row TN, Chopra D (2011) Role of hetero-halogen (F···X, X = Cl, Br, and I) or homo-halogen (X···X, X = F, Cl, Br, and I) interactions in substituted benzanilides. Crystal Growth Des 11:1578–1596
190. Chopra D, Row TNG (2008) Evaluation of the interchangeability of C–H and C–F groups: insights from crystal packing in a series of isomeric fluorinated benzanilides. Cryst Eng Comm 10:54–67
191. Sehon CA, Wang GZ, Viet AQ, Goodman KB, Dowdell SE, Elkins PA, Semus SF, Evans C, Jolivette LJ, Kirkpatrick RB, Dul E, Khandekar SS, Yi T, Wright LL, Smith GK, Behm DJ, Bentley R, Doe CP, Hu E, Lee D (2008) Potent, selective and orally bioavailable dihydropyrimidine inhibitors of rho kinase (ROCK1) as potential therapeutic agents for cardiovascular diseases. J Med Chem 51:6631–6634
192. Dai Y, Hartandi K, Ji Z, Ahmed AA, Albert DH, Bauch JL, Bouska JJ, Bousquet PF, Cunha GA, Glaser KB, Harris CM, Hickman D, Guo J, Li J, Marcotte PA, Marsh KC, Moskey MD, Martin RL, Olson AM, Osterling DJ, Pease LL, Soni NB, Stewart KD, Stoll VS, Tapang P, Reuter DR, Davidsen SK, Michaelides MR (2007) Discovery of *N*-(4-(3-amino-1*H*-indazol-4-yl)phenyl)-*N*′-(2-fluoro-5-methylphenyl)urea (ABT-869), a 3-aminoindazole-based orally active multitargeted receptor tyrosine kinase inhibitor. J Med Chem 50:1584–1597
193. Weiss MM, Williamson T, Babu-Khan S, Bartberger MD, Brown J, Chen K, Cheng Y, Citron M, Croghan MD, Dineen TA, Esmay J, Graceffa RF, Harried SS, Hickman D, Hitchcock SA, Horne DB, Huang H, Imbeah-Ampiah R, Judd T, Kaller MR, Kreiman CR, La DS, Li V. Lopez P, Louie S, Monenschein H, Nguyen TT, Pennington LD, Rattan C, San Miguel T, Sickmier EA, Wahl RC, Wen PH, Wood S, Xue Q, Yang BH, Patel VF, Zhong W (2012) Design and preparation of a potent series of hydroxyethylamine containing β-secretase inhibitors that demonstrate robust reduction of central β-amyloid. J Med Chem 55:9009–9024
194. Dineen TA, Weiss MM, Williamson T, Acton P, Babu-Khan S, Bartberger MD, Brown J, Chen K, Cheng Y, Citron M, Croghan MD, Dunn RT, Esmay J, Graceffa RF, Harried SS, Hickman D, Hitchcock SA, Horne DB, Huang H, Imbeah-Ampiah R, Judd T, Kaller MR, Kreiman CR, La DS, Li V, Lopez P, Louie S, Monenschein H, Nguyen TT, Pennington LD, San Miguel T, Sickmier EA, Vargas HM, Wahl RC, Wen PH, Whittington DA, Wood S, Xue Q, Yang BH, Patel VF, Zhong W (2012) Design and synthesis of potent, orally efficacious hydroxyethylamine derived β-site amyloid precursor protein cleaving enzyme (BACE1) inhibitors. J Med Chem 55:9025–9044
195. Kaller MR, Harried SS, Albrecht B, Amarante P, Babu-Khan S, Bartberger MD, Brown J, Brown R, Chen K, Cheng Y, Citron M, Croghan MD, Graceffa R, Hickman D, Judd T, Kriemen C, La D, Li V, Lopez P, Luo Y, Masse C, Monenschein H, Nguyen T, Pennington LD, Miguel TS, Sickmier EA, Wahl RC, Weiss MM, Wen PH, Williamson T, Wood S, Xue M, Yang B, Zhang J, Patel V, Zhong W, Hitchcock S (2012) A potent and orally efficacious, hydroxyethylamine-based inhibitor of β-secretase. ACS Med Chem Lett 3:886–891
196. Hitchcock SA (2012) Structural modifications that alter the P-glycoprotein efflux properties of compounds. J Med Chem 55:4877–4895
197. Desai PV, Raub TJ, Blanco M-J (2012) How hydrogen bonds impact P-glycoprotein transport and permeability. Bioorg Med Chem Lett 22:6540–6548
198. Kuduk SD, Di Marco CN, Chang RK, Wood MR, Schirripa KM, Kim JJ, Wai JMC, DiPardo RM, Murphy KL, Ransom RW, Harrell CM, Reiss DR, Holahan MA, Cook J, Hess JF, Sain N, Urban MO, Tang C, Prueksaritanont T, Pettibone DJ, Bock MG (2007) Development of orally bioavailable and CNS penetrant biphenylaminocyclopropane carboxamide bradykinin B1 receptor antagonists. J Med Chem 50:272–282

199. Ettorre E, D'Andrea P, Mauro S, Porcelloni M, Rossi C, Altamura M, Catalioto RM, Giuliani S, Maggi CA, Fattori D (2011) hNK_2 receptor antagonists. The use of intramolecular hydrogen bonding to increase solubility and membrane permeability. Bioorg Med Chem Lett 21:1807–1809
200. Tran C, Ouk S, Clegg NJ, Chen Y, Watson PA, Arora V, Wongvipat J, Smith-Jones PM, Yoo D, Kwon A, Wasielewska T, Welsbie D, Chen C, Higano CS, Beer TM, Hung DT, Scher HI, Jung ME, Sawyers CL (2009) Development of a second-generation antiandrogen for treatment of advanced prostate cancer. Science 324:787–790
201. Jung ME, Ouk S, Yoo D, Sawyers CL, Chen C, Tran C, Wongvipat J (2010) Structure–activity relationship for thiohydantoin androgen receptor antagonists for castration-resistant prostate cancer (CRPC). J Med Chem 53:2779–2796
202. Marsham PR, Wardleworth JM, Boyle FT, Hennequin LF, Kimbell R, Brown M, Jackman AL (1999) Design and synthesis of potent non-polyglutamatable quinazoline antifolate thymidylate synthase inhibitors. J Med Chem 42:3809–3820
203. Niculesco-Duvaz I (2000) ZD-9331 (Astra-Zeneca). Curr Opin Investig Drugs 1:141–149
204. Swahn B-M, Kolmodin K, Karlstroem S, von Berg S, Soederman P, Holenz J, Berg S, Lindstroem J, Sundstroem M, Turek D, Kihlstroem J, Slivo C, Andersson L, Pyring D, Rotticci D, Oehberg L, Kers A, Bogar K, Bergh M, Olsson L-L, Janson J, Eketjaell S, Georgievska B, Jeppsson F, Faelting J (2012) Design and synthesis of β-site amyloid precursor protein cleaving enzyme (BACE1) inhibitors with in vivo brain reduction of β-amyloid peptides. J Med Chem 55:9346–9361
205. Peterlin-Mašič L, Kikelj D (2001) Arginine mimetics. Tetrahedron 57:7073–7105
206. Peterlin-Mašič L (2006) Arginine mimetic structure in biologically active antagonists and inhibitors. Curr Med Chem 13:3627–3648
207. Pinto DJP, Smallheer JM, Cheney DL, Knabb RM, Wexler RR (2010) Factor Xa inhibitors: next generation antithrombotic agents. J Med Chem 53:6243–6274
208. Danalev D (2012) Inhibitors of serine proteinases from blood coagulation cascade – view on current developments. Mini Rev Med Chem 12:721–730
209. Nar H (2012) The role of structural information in the discovery of direct thrombin and factor Xa inhibitors. Trends Pharmacol Sci 33:279–288
210. Srivastave S, Goswami LN, Dikshit DK (2005) Progress in the design of low molecular weight thrombin inhibitors. Med Res Rev 25:66–92
211. Ghorai P, Kraus A, Keller M, Gotte C, Igel P, Schneider E, Schnell D, Bernhardt G, Dove S, Zabel M, Elz S, Seifert R, Buschauer A (2008) Acylguanidines as bioisosteres of guanidines: N^G-acylated Imidazolylpropylguanidines, a new class of histamine H_2 receptor agonists. J Med Chem 51:7193–7204
212. Kraus A, Ghorai P, Birnkammer T, Schnell D, Elz S, Seifert R, Dove S, Bernhardt G, Buschauer A (2009) N^G-acylated aminothiazolylpropylguanidines as potent and selective histamine H_2 receptor agonists. ChemMedChem 4:232–240
213. Pluym N, Brennauer A, Keller M, Ziemek R, Pop N, Bernhardt G, Buschauer A (2011) Application of the guanidine–acylguanidine bioisosteric approach to argininamide-type NPY Y2 receptor antagonists. ChemMedChem 6:1727–1738
214. Tomczuk B, Lu T, Soll RM, Fedde C, Wang A, Murphy L, Crysler C, Dasgupta M, Eisennagel S, Spurlino J, Bone R (2003) Oxyguanidines: application to non-peptidic phenyl-based thrombin inhibitors. Bioorg Med Chem Lett 13:1495–1498
215. Lu T, Markotan T, Coppo F, Tomczuk B, Crysler C, Eisennagel S, Spurlino J, Gremminger L, Soll RM, Giardino EC, Bone R (2004) Oxyguanidines. Part 2: discovery of a novel orally active thrombin inhibitor through structure-based drug design and parallel synthesis. Bioorg Med Chem Lett 14:3727–3731
216. Lee L, Kreutter KD, Pan W, Crysler C, Spurlino J, Player MR, Tomczuk B, Lu T (2007) 2-(2-Chloro-6-fluorophenyl)acetamides as potent thrombin inhibitors. Bioorg Med Chem Lett 17:6266–6269

217. Kreutter KD, Lu T, Lee L, Giardino EC, Patel S, Huang H, Xu G, Fitzgerald M, Haertlein BJ, Mohan V, Crysler C, Eisennagel S, Dasgupta M, McMillan M, Spurlino JC, Huebert ND, Maryanoff BE, Tomczuk BE, Damiano BP, Player MR (2008) Orally efficacious thrombin inhibitors with cyanofluorophenylacetamide as the P2 motif. Bioorg Med Chem Lett 18:2865–2870
218. Lu T, Markotan T, Ballentine SK, Giardino EC, Spurlino J, Brown K, Maryanoff BE, Tomczuk BE, Damiano BP, Shukla U, End D, Andrade-Gordon P, Bone RF, Player MR (2010) Discovery and clinical evaluation of 1-{N-[2-(amidinoaminooxy)ethyl]amino} carbonylmethyl-6-methyl-3-[2,2-difluoro-2-phenylethylamino]pyrazinone (RWJ-671818), a thrombin inhibitor with an oxyguanidine P1 motif. J Med Chem 53:1843–1856
219. Lam PYS, Clark CG, Li R, Pinto DJP, Orwat MJ, Galemmo RA, Fevig JM, Teleha CA, Alexander RS, Smallwood AM, Rossi KA, Wright MR, Bai SA, He K, Luettgen JM, Wong PC, Knabb RM, Wexler RR (2003) Structure-based design of novel guanidine/benzamidine mimics: potent and orally bioavailable factor Xa inhibitors as novel anticoagulants. J Med Chem 46:4405–4418
220. Pinto DJP, Orwat MJ, Koch S, Rossi KA, Alexander RS, Smallwood A, Wong PC, Rendina AR, Luettgen JM, Knabb RM, He K, Xin B, Wexler RR, Lam PYS (2007) Discovery of 1-(4-methoxyphenyl)-7-oxo-6-[4-(2-oxo-1-piperidinyl]phenyl)-4,5,6,7-tetrahydro-1*H*-pyrazolo [3,4-c]pyridine-3-carboxamide (apixaban, BMS-562247), a highly potent, selective, efficacious, and orally bioavailable inhibitor of blood coagulation factor Xa. J Med Chem 50:5339–5356
221. Rye CS, Baell JB (2005) Phosphate isosteres in medicinal chemistry. Curr Med Chem 12:3127–3141
222. Romanenko VD, Kukhar VP (2006) Fluorinated phosphonates: synthesis and biomedical application. Chem Rev 106:3868–3935
223. Elliott TS, Slowey A, Yeb Y (2012) Conway SJ (2012) The use of phosphate bioisosteres in medicinal chemistry and chemical biology. Med Chem Commun 3:735–751
224. Blackburn GM, Kent DE (1981) A novel synthesis of α- and γ-fluoroalkylphosphonates. JCS Chem Comm 511–513
225. Blackburn GM, England DA, Kolkmann F (1981) Monofluoro- and difluoro-methylenebisphosphonic acids : isopolar analogues of pyrophosphoric acid. JCS Chem Comm 930–932
226. Smyth MS, Ford H Jr, Burke TR Jr (1992) A general method for the preparation of benzylic α, α-difluorophosphonic acids; non-hydrolyzable mimetics of phosphotyrosine. Tet Lett 33:4137–4140
227. Hecker SJ, Erion MD (2008) Prodrugs of phosphates and phosphonates. J Med Chem 51:2328–2345
228. Hostetler KY (2009) Alkoxyalkyl prodrugs of acyclic nucleoside phosphonates enhance oral antiviral activity and reduce toxicity: current state of the art. Antiviral Res 82:A84–A98
229. Pertusati F, Serpi M, McGuigan C (2012) Medicinal chemistry of nucleoside phosphonate prodrugs for antiviral therapy. Antiviral Chem Chemother 22:181–203
230. Combs AP (2007) Structure-based drug design of new leads for phosphatase research. IDrugs 10:112–115
231. Combs AP (2010) Recent advances in the discovery of competitive protein tyrosine phosphatase 1B inhibitors for the treatment of diabetes, obesity, and cancer. J Med Chem 53:2333–2344
232. Savarino A (2006) A historical sketch of the discovery and development of HIV-1 integrase inhibitors. Exp Opin Investig Drugs 15:1507–1522
233. Johns BA, Svolto AC (2008) Advances in two-metal chelation inhibitors of HIV integrase. Exp Opin Ther Patents 18:1225–1237
234. Ramkumar K, Serrao E, Odde S, Neamati N (2010) HIV-1 integrase inhibitors: 2007–2008 update. Med Res Rev 30:890–954

235. Pendri A, Meanwell NA, Peese KM, Walker MA (2011) New first and second generation inhibitors of human immunodeficiency virus-1 integrase. Exp Opin Ther Patents 21:1173–1189
236. Ingale KB, Bhatia MS (2011) HIV-1 integrase inhibitors: a review of their chemical development. Antiviral Chem Chemother 22:95–105
237. Beare KD, Coster MJ, Rutledge PJ (2012) Diketoacid inhibitors of HIV-1 integrase: from L-708,906 to raltegravir and beyond. Curr Med Chem 19:1177–1192
238. Leeson PD, St-Gallay SA, Wenlock MC (2011) Impact of ion class and time on oral drug molecular properties. Med Chem Commun 2:91–105
239. Manallack DT, Prankerd RJ, Yuriev E, Oprea TI, Chalmers DK (2013) The significance of acid/base properties in drug discovery. Chem Soc Rev 42:485–496
240. Azzaoui K, Hamon J, Faller B, Whitebread S, Jacoby E, Bender A, Jenkins JL, Urban L (2007) Modeling promiscuity based on in vitro safety pharmacology profiling data. ChemMedChem 2:874–880
241. Peters J-E, Schnider P, Mattei P, Kansy M (2009) Pharmacological promiscuity: dependence on compound properties and target specificity in a set of recent Roche compounds. ChemMedChem 4:680–686
242. Waring MJ, Johnstone C (2007) A quantitative assessment of hERG liability as a function of lipophilicity. Bioorg Med Chem Lett 17:1759–1764
243. Jamieson C, Moir EM, Rankovic Z, Wishart G (2006) Medicinal chemistry of hERG optimizations: highlights and hang-ups. J Med Chem 49:5029–5046
244. Hanumegowda UM, Wenke G, Regueiro-Ren A, Yordanova R, Corradi JP, Adams SP (2010) Phospholipidosis as a function of basicity, lipophilicity, and volume of distribution of compounds. Chem Res Toxicol 23:749–755
245. Ratcliffe AJ (2009) Medicinal chemistry strategies to minimize phospholipidosis. Curr Med Chem 16:2816–2823
246. Bernstein PR, Ciaccio P, Morelli J (2011) Drug-induced phospholipidosis. Ann Rep Med Chem 46:419–430
247. Morgenthaler M, Schweizer E, Hoffman-Röder A, Benini F, Martin RE, Jaeschke G, Wagner B, Fischer H, Bendels S, Zimmeli D, Scheider J, Diedeich F, Kansy M, Müller K (2007) Predicting and tuning physicochemical properties in led optimization: amine-basicities. ChemMedChem 2:1100–1115
248. Cox CD, Coleman PJ, Breslin MJ, Whitman DB, Garbaccio RM, Fraley ME, Buser CA, Walsh ES, Hamilton K, Schaber MD, Lobell RB, Tao W, Davide JP, Diehl RE, Abrams MT, South VJ, Huber HE, Torrent M, Prueksaritanont T, Li C, Slaughter DE, Mahan E, Fernandez-Metzler C, Yan Y, Kuo LC, Kohl NE, Hartman GD (2008) Kinesin spindle protein (KSP) inhibitors. 9. Discovery of (2*S*)-4-(2,5-difluorophenyl)-*N*-[(3*R*,4*S*)-3-fluoro-1-methylpiperidin-4-yl]-2-(hydroxymethyl)-*N*-methyl-2-phenyl-2,5-dihydro-1*H*-pyrrole-1-carboxamide (MK-0731) for the treatment of taxane-refractory cancer. J Med Chem 51:4239–4252
249. Kalgutkar AS, Obach RS, Maurer TS (2007) Mechanism-based inactivation of cytochrome P450 enzymes: chemical mechanisms, structure–activity relationships and relationship to clinical drug–drug interactions and idiosyncratic adverse drug reactions. Curr Drug Metab 8:407–447
250. Goncharov NV, Jenkins RO, Radilov AS (2006) Toxicology of fluoroacetate: a review, with possible directions for therapy research. J Appl Toxicol 26:148–161
251. Sani M, Volonterio A, Zanda M (2007) The trifluoroethylamine function as peptide bond replacement. ChemMedChem 2:1693–1700
252. Zanda M (2004) Trifluoromethyl group: an effective xenobiotic function for peptide backbone modification. New J Chem 28:1401–1411
253. Molteni M, Pesenti C, Sani M, Volonterio A, Zanda M (2004) Fluorinated peptidomimetics: synthesis, conformational and biological features. J Fluorine Chem 125:1735–1743
254. Molteni M, Bellucci MC, Bigotti S, Mazzini S, Volonterio A, Zanda M (2009) Ψ[CH(CF_3)NH]Gly-peptides: synthesis and conformation analysis. Org Biomol Chem 7:2286–2296

255. Black WC, Bayly C, Davis DE, Desmarais S, Falgueyret J-P, Leger S, Li CS, Masse F, McKay DJ, Palmer JT, Percival MD, Robichaud J, Tsou N, Zamboni R (2005) Trifluoroethylamines as amide isosteres in inhibitors of cathepsin K. Bioorg Med Chem Lett 15:4741–4744
256. Gauthier JY, Chauret N, Cromlish W, Desmarais S, Duong LT, Falgueyret J-P, Kimmel DB, Lamontagne S, Leger S, LeRiche T, Li CS, Masse F, McKay DJ, Nicoll-Griffith DA, Oballa RM, Palmer JT, Percival MD, Riendeau D, Robichaud J, Rodan GA, Rodan SB, Seto C, Therien M, Truong V-L, Venuti MC, Wesolowski G, Young RN, Zamboni R, Black WC (2008) The discovery of odanacatib (MK-0822), a selective inhibitor of cathepsin K. Bioorg Med Chem Lett 18:923–928
257. Langdahl B, Binkley N, Bone H, Gilchrist N, Resch H, Rodriguez Portales J, Denker A, Lombardi A, Le Bailly De Tilleghem C, Da Silva C, Rosenberg E, Leung A (2012) Odanacatib in the treatment of postmenopausal women with low bone mineral density: five years of continued therapy in a phase 2 study. J Bone Mineral Res 27:2251–2258
258. Brixen K, Chapurlat R, Cheung AM, Keaveny TM, Fuers T, Engelke K, Recker R, Dardzinski B, Verbruggen N, Ather S, Rosenberg E, de Papp AE (2013) Bone density, turnover, and estimated strength in postmenopausal women treated with odanacatib: a randomized trial. J Clin Endocrinol Metab 98:571–580
259. Ng KW (2012) Potential role of odanacatib in the treatment of osteoporosis. Clin Intervent Aging 7:235–247
260. Isabel E, Mellon C, Boyd MJ, Chauret N, Deschênes D, Desmarais S, Falgueyret J-P, Gauthier JY, Khougaz K, Lau CK, Léger S, Levorse DA, Li CS, Massé F, Percival MD, Roy B, Scheigetz J, Thérien M, Truong VL, Wesolowski G, Young RN, Zamboni R, Black WC (2011) Difluoroethylamines as an amide isostere in inhibitors of cathepsin K. Bioorg Med Chem Lett 21:920–923
261. Grunewald GL, Seim MR, Lu J, Makboul M, Criscione KR (2006) Application of the Goldilocks effect to the design of potent and selective inhibitors of phenylethanolamine *N*-methyltransferase: balancing pK_a and steric effects in the optimization of 3-methyl-1,2,3,4-tetrahydroisoquinoline inhibitors by α-fluorination. J Med Chem 49:2939–2952
262. Wuitschik G, Rogers-Evans M, Müller K, Fischer H, Wagner B, Schuler F, Polonchuk L, Carreira EM (2006) Oxetanes as promising modules in drug discovery. Angew Chem Int Ed 45:7736–7739
263. Wuitschik G, Rogers-Evans M, Buckl A, Bernasconi M, Marki M, Godel T, Fischer H, Wagner B, Parrilla I, Schuler F, Schneider J, Alker A, Schweizer WB, Müller K, Carreira EM (2008) Spirocyclic oxetanes: synthesis and properties. Angew Chem Int Ed 47:4512–4515
264. Wuitschik G, Carreira EM, Wagner B, Fischer H, Parrilla I, Schuler F, Rogers-Evans M, Müller K (2010) Oxetanes in drug discovery: structural and synthetic insights. J Med Chem 53:3227–3246
265. Burkhard JA, Wuitschik G, Rogers-Evans M, Müller K, Carreira EM (2010) Oxetanes as versatile elements in drug discovery and synthesis. Angew Chem Int Ed 49:9052–9067
266. Jung ME, Piizzi G (2005) gem-Disubstituent effect: theoretical basis and synthetic applications. Chem Rev 105:1735–1766
267. Freire E (2008) Do enthalpy and entropy distinguish first in class from best in class? Drug Discov Today 13:869–874
268. Ladbury JE, Klebe G, Freire E (2010) Adding calorimetric data to decision making in lead discovery: a hot tip. Nat Rev Drug Discov 9:23–27
269. Lafont V, Armstrong AA, Ohtaka H, Kiso Y, Amzel LM, Freire E (2007) Compensating enthalpic and entropic changes hinder binding affinity optimization. Chem Biol Drug Des 69:413–422
270. Freire E (2009) A thermodynamic approach to the affinity optimization of drug candidates. Chem Biol Drug Des 74:468–472
271. Hann MM (2011) Molecular obesity, potency and other addictions in drug discovery. Med Chem Commun 2:349–355

272. Tarcsay A, Keserű GM (2013) Contributions of molecular properties to drug promiscuity. J Med Chem 56:1789–1795
273. Ritchie TR, Macdonald SJF (2009) The impact of aromatic ring count on compound developability – are too many aromatic rings a liability in drug design? Drug Discov Today 14:1011–1020
274. Ritchie TR, Macdonald SJF, Young RJ, Pickett SD (2011) The impact of aromatic ring count on compound developability: further insights by examining carbo- and hetero-aromatic and -aliphatic ring types. Drug Discov Today 16:164–171
275. Ritchie TJ, Macdonald SJF, Peace S, Pickett SD, Luscombe CN (2012) The developability of heteroaromatic and heteroaliphatic rings – do some have a better pedigree as potential drug molecules than others? Med Chem Commun 3:1062–1069
276. Brown A, Brown TB, Calabrese A, Ellis D, Puhalo N, Ralph M, Watson L (2010) Triazole oxytocin antagonists: identification of an aryloxyazetidine replacement for a biaryl substituent. Bioorg Med Chem Lett 20:516–520
277. Honma T, Hayashi K, Aoyama T, Hashimoto N, Machida T, Fukasawa K, Iwama T, Ikeura C, Ikuta M, Suzuki-Takahashi I, Iwasawa Y, Hayama T, Nishimura S, Morishima H (2001) Structure-based generation of a new class of potent Cdk4 inhibitors: new de novo design strategy and library design. J Med Chem 44:4615–4627
278. Furet P, Caravatti G, Guagnano V, Lang M. Meyer T, Schoepfer J (2008) Entry into a new class of protein kinase inhibitors by pseudo ring design. Bioorg Med Chem Lett 18:897–900
279. Guagnano V, Furet P, Spanka C, Bordas V, Le Douget M, Stamm C, Brueggen J, Jensen MR, Schnell C, Schmid H, Wartmann M, Berghausen J, Drueckes P, Zimmerlin A, Bussiere D, Murray J, Graus Porta D (2012) Discovery of 3-(2,6-dichloro-3,5-dimethoxy-phenyl)-1-{6-[4-(4-ethyl-piperazin-1-yl)-phenylamino]-pyrimidin-4-yl}-1-methyl-urea (NVP-BGJ398), a potent and selective inhibitor of the fibroblast growth factor receptor family of receptor tyrosine kinase. J Med Chem 54:7066–7083
280. Furet P, Bold G, Hofmann F, Manley P, Meyer T, Altmann K-H (2003) Identification of a new chemical class of potent angiogenesis inhibitors based on conformational considerations and database searching. Bioorg Med Chem Lett 13:2967–2971
281. Liu KKC, Huang X, Bagrodia S, Chen JH, Greasley S, Cheng H, Sun S, Knighton D, Rodgers C, Kristina Rafidi K, Zou A, Xiao J, Yan S (2011) Quinazolines with intra-molecular hydrogen bonding scaffold (iMHBS) as PI3K/mTOR dual inhibitors. Bioorg Med Chem Lett 21:1270–1274
282. Zhang G, Ren P, Gray NS, Sim T, Liu Y, Wang X, Che J, TianS-S SML, Spalding TA, Romeo R, Iskandar M, Chow D, Seidel HM, Karanewsky DS, He Y (2008) Discovery of pyrimidine benzimidazoles as Lck inhibitors: Part I. Bioorg Med Chem Lett 18:5618–5621
283. Wan Z, Boehm JC, Bower MJ, Kassis S, Lee JC, Zhao B, Adams JL (2003) *N*-Phenyl-*N*-purin-6-yl ureas: the design and synthesis of P38α MAP kinase inhibitors. Bioorg Med Chem Lett 13:1191–1194
284. Jansma A, Zhang Q, Li B, Ding Q, Uno T, Bursulaya B, Liu Y, Furet P, Gray NS, Geierstanger BH (2007) Verification of a designed intramolecular hydrogen bond in a drug scaffold by nuclear magnetic resonance spectroscopy. J Med Chem 50:5875–5877
285. Kuhn B, Mohr P, Stahl M (2010) Intramolecular hydrogen bonding in medicinal chemistry. J Med Chem 53:2601–2611
286. Mathieu S, Gradl SN, Ren L, Wen Z, Aliagas I, Gunzner-Toste J, Lee W, Pulk R, Zhao G, Alicke B, Boggs JW, Buckmelter AJ, Choo EF, Dinkel V, Gloor SL, Gould SE, Hansen JD, Hastings G, Hatzivassiliou G, Laird ER, Moreno D, Ran Y, Voegtli WC, Wenglowsky S, Grina J, Rudolph J (2012) Potent and selective aminopyrimidine-based B-Raf inhibitors with favorable physicochemical and pharmacokinetic properties. J Med Chem 55:2869–2881
287. Larsen AA, Lish PM (1964) A new bioisostere: alkylsulphonamidophenethanolamines. Nature 203:1283–1284
288. Hitchcock SA, Pennington LD (2006) Structure–brain exposure relationships. J Med Chem 49:7559–7583

289. Nirogi RVS, Daulatabad AV, Parandhama G, Mohammad S, Sastri KR, Shinde AK, Dubey PK (2010) Synthesis and pharmacological evaluation of aryl aminosulfonamide derivatives as potent 5-HT_6 receptor antagonists. Bioorg Med Chem Lett 20:4440–4443
290. Ahmed M, Briggs MA, Bromidge SM, Buck T, Campbell L, Deeks NJ, Garner A, Gordon L, Hamprecht DW, Holland V, Johnson CN, Medhurst AD, Mitchell DJ, Moss SF, Powles J, Seal JT, Stean TO, Stemp G, Thompson M, Trail B, Upton N, Winborn K, Witty DR (2005) Bicyclic heteroarylpiperazines as selective brain penetrant 5-HT_6 receptor antagonists. Bioorg Med Chem Lett 15:4867–4871
291. Zhao S-H, Berger J, Clark RD, Sethofer SG, Krauss NE, Brothers JM, Martin RS, Misner DL, Schwab AL (2007) 3,4-Dihydro-2*H*-benzo[1,4]oxazine derivatives as 5-HT_6 receptor antagonists. Bioorg Med Chem Lett 17:3504–3507
292. Nirogi R, Shinde A, Daulatabad A, Kambhampati R, Gudla P, Shaik M, Gampa M, Balasubramaniam S, Gangadasari P, Reballi V, Badange R, Bojja K, Subramanian R, Bhyrapuneni G, Muddana N, Jayarajan P (2012) Design, synthesis, and pharmacological evaluation of piperidin-4-yl amino aryl sulfonamides: novel, potent, selective, orally active, and brain penetrant 5-HT_6 receptor antagonists. J Med Chem 55:9255–9269
293. Odan M, Ishizuka N, Hiramatsu Y, Inagaki M, Hashizume H, Fujii Y, Mitsumori S, Morioka Y, Soga M, Deguchi M, Yasui K, Arimura A (2012) CB 1/2 dual agonists with 3-carbamoyl 2-pyridone derivatives as antipruritics: reduction of CNS side effects by introducing polar functional groups. Bioorg Med Chem Lett 22:2894–2897
294. Fulp A, Bortoff K, Zhang Y, Seltzman H, Snyder R, Maitra R (2011) Towards rational design of cannabinoid receptor 1 (CB1) antagonists for peripheral selectivity. Bioorg Med Chem Lett 21:5711–5714
295. Burgey CS, Robinson KA, Lyle TA, Sanderson PEJ, Lewis SD, Lucas BJ, Krueger JA, Singh R, Miller-Stein C, White RB, Wong B, Lyle EA, Williams PD, Coburn CA, Dorsey BD, Barrow JC, Stranieri MT, Holahan MA, Sitko GR, Cook JJ, McMasters DR, McDonough CM, Sanders WM, Wallace AA, Clayton FC, Bohn D, Leonard YM, Detwiler TJ Jr, Lynch JJ Jr, Yan Y, Chen Z, Kuo L, Gardell SJ, Shafer JA, Vacca JP (2003) Metabolism-directed optimization of 3-aminopyrazinone acetamide thrombin inhibitors. development of an orally bioavailable series containing P1 and P3 pyridines. J Med Chem 46:461–473
296. Reiner JE, Siev DV, Araldi G-L, Cui JJ, Ho JZ, Reddy KM, Mamedova L, Vu PH, Lee K-SS, Minami NK, Gibson TS, Anderson SM, Bradbury AE, Nolan TG, Semple JE (2002) Non-covalent thrombin inhibitors featuring P3-heterocycles with P1-monocyclic arginine surrogates. Bioorg Med Chem Lett 12:1203–1208
297. Cui JJ, Araldi G-L, Reiner JE, Reddy KM, Kemp SJ, Ho JZ, Siev DV, Mamedova L, Gibson TS, Gaudette JA, Minami NK, Anderson SM, Bradbury AE, Nolan TG, Semple JE (2002) Non-covalent thrombin inhibitors featuring P3-heterocycles with P1-bicyclic arginine surrogates. Bioorg Med Chem Lett 12:2925–2930
298. Zhou Q, Ruffoni A, Gianatassio R, Fujiwara Y, Sella E, Shabat D, Baran PS (2013) Direct synthesis of fluorinated heteroarylether bioisosteres. Angew Chem Int Ed 52:3949–3952
299. Austin RP, Barton P, Bonnert RV, Brown RC, Cage PA, Cheshire DR, Davis AM, Dougall IG, Ince F, Pairaudeau G, Young A (2003) QSAR and the rational design of long-acting dual D2-receptor/β2-adrenoceptor agonists. J Med Chem 46:3210–3220
300. Blake MI, Crespi HL, Katz JJ (1975) Studies with deuterated drugs. J Pharm Sci 64:367–391
301. Yarnell AT (2009) Heavy-hydrogen drugs turn heads, again. Firms seek to improve drug candidates by selective deuterium substitution. Chem Eng News 87:36–39
302. Shao L, Hewitt MC (2010) The kinetic isotope effect in the search for deuterated drugs. Drug News Perspect 23:398–404
303. Harbeson SL, Tung RD (2011) Deuterium in drug discovery and development. Ann Rep Med Chem 46:403–417
304. Katsnelson A (2013) Heavy drugs draw heavy interest from pharma backers. Nature Med 19:656

305. El Tayar N, van de Waterbeemd H, Gryllaki M, Testa B, Trager WF (1984) The lipophilicity of deuterium atoms. A comparison of shake-flask and HPLC methods. Int J Pharmaceutics 19:271–281
306. Turowski M, Yamakawa N, Meller J, Kimata K, Ikegami T, Hosoya K, Tanaka N, Thornton ER (2003) Deuterium isotope effects on hydrophobic interactions: the importance of dispersion interactions in the hydrophobic phase. J Am Chem Soc 125:13836–13849
307. Kimata K, Hosoya K, Araki T, Tanaka N (1997) Direct chromatographic separation of racemates on the basis of isotopic chirality. Anal Chem 69:2610–2612
308. Perrin CL, Ohta BK, Kuperman J (2003) β-Deuterium isotope effects on amine basicity, "inductive" and stereochemical. J Am Chem Soc 125:15008–15009
309. Perrin CL, Ohta BK, Kuperman J, Liberman J, Erdélyi M (2005) Stereochemistry of β-deuterium isotope effects on amine basicity. J Am Chem Soc 127:9641–9647
310. Perrin CL, Dong Y (2008) Nonadditivity of secondary deuterium isotope effects on basicity of triethylamine. J Am Chem Soc 130:11143–11148
311. Perrin CL, Dong Y (2007) Secondary deuterium isotope effects on the acidity of carboxylic acids and phenols. J Am Chem Soc 129:4490–4497
312. Foster AB (1984) Deuterium isotope effects in studies of drug metabolism. Trends Pharmacol Sci 5:524–527
313. Nelson SD, Trager WF (2003) The use of deuterium isotope effects to probe the active site properties, mechanism of cytochrome P450-catalyzed reactions, and mechanisms of metabolically dependent toxicity. Drug Metab Disp 31:1481–1498
314. Mutlib AE (2008) Application of stable isotope-labeled compounds in metabolism and in metabolism-mediated toxicity studies. Chem Res Toxicol 21:1672–1689
315. Belleau B, Burba J, Pindell M, Reiffenstein J (1961) Effect of deuterium substitution in sympathomimetic amine on adrenergic responses. Science 133:102–104
316. Westheimer FH (1961) The magnitude of the primary kinetic isotope effect for compounds of hydrogen and deuterium. Chem Rev 61:265–273
317. Peng S, van der Donk WA (2003) An unusual isotope effect on substrate inhibition in the oxidation of arachidonic acid by lipoxygenase. J Am Chem Soc 125:8988–8989
318. Gant TG, Sarshar S (2008) Substituted phenethylamines with serotonergic and/or norepinephrinergic activity. US Patent 7,456, 317, November 25, 2008
319. Tung R (2007) Novel benzo-[D] [1,3]-dioxol derivatives. World Patent Application WO 2007/016,431, February 8th, 2007
320. Murray M (2000) Mechanisms of inhibitory and regulatory effects of methylenedioxyphenyl compounds on cytochrome P450-dependent drug oxidation. Curr Drug Metab 1:67–84
321. Bertelsen KM, Venkatakrishnan K, von Moltke LL, Obach RS, Greenblatt DJ (2003) Apparent mechanism-based inhibition of human CYP 2D6 in vitro by paroxetine: comparison with fluoxetine and quinidine. Drug Metab Disp 31:289–293
322. Venkatakrishnan K, Obach RS (2005) In vitro-in vivo extrapolation of CYP2D6 inactivation by paroxetine: prediction of nonstationary pharmacokinetics and drug interaction magnitude. Drug Metab Disp 33:845–852
323. Manley PW, Blasco F, Mestan J, Aichholz R (2013) The kinetic deuterium isotope effect as applied to metabolic deactivation of imatinib to the des-methyl metabolite, CGP74588. Bioorg Med Chem 21:3231–3239
324. Shao L, Abolin C, Hewitt MC, Koch P, Varney M (2006) Derivatives of tramadol for increased duration of effect. Bioorg Med Chem Lett 16:691–694
325. Velthuisen EJ, Baughman TM, Johns BA, Temelkoff DP, Weatherhead JG (2013) Synthesis and pharmacokinetic profile of highly deuterated brecanavir analogs. Eur J Med Chem 63:202–212
326. Maltais F, Jung YC, Chen M, Tanoury J, Perni RB, Mani N, Laitinen L, Huang H, Liao S, Gao H, Tsao H, Block E, Ma C, Shawgo RS, Town C, Brummel CL, Howe D, Pazhanisamy S, Raybuck S, Namchuk M, Bennani YL (2009) In vitro and in vivo isotope

effects with hepatitis C protease inhibitors: enhanced plasma exposure of deuterated telaprevir versus telaprevir in rats. J Med Chem 52:7993–8001
327. Mutlib AE, Gerson RJ, Meunier PC, Haley PJ, Chen H, Gan LS, Davies MH, Gemzik B, Christ DD, Krahn DF, Markwalder JA, Seitz SP, Robertson RT, Miwa GT (2000) The species-dependent metabolism of efavirenz produces a nephrotoxic glutathione conjugate in rats. Toxicol Appl Pharmacol 169:102–113
328. Zhu Y, Zhou J, Jiao B (2013) Deuterated clopidogrel analogues as a new generation of antiplatelet agents. ACS Med Chem Lett 4:349–352
329. Laizure SC, Parker RB (2010) A comparison of the metabolism of clopidogrel and prasugrel. Expert Opin Drug Metab Toxicol 6:1417–1424
330. Bains W, Tacke R (2003) Silicon chemistry as a novel source of chemical diversity in drug design. Curr Opin Drug Discov Dev 6:526–543
331. Franz AK, Wilson SO (2013) Organosilicon molecules with medicinal applications. J Med Chem 56:388–405
332. Tacke R, Popp F, Müller B, Theis B, Burschka C, Hamacher A, Kassack MU, Schepmann D, Wünsch B, Jurva U, Wellner E (2008) Sila-haloperidol, a silicon analogue of the dopamine (D_2) receptor antagonist haloperidol: synthesis, pharmacological properties, and metabolic fate. ChemMedChem 3:152–164
333. Subramanyam B, Woolf T, Castagnoli N Jr (1991) Studies on the *in-vitro* conversion of haloperidol to a potentially neurotoxic pyridinium metabolite. Chem Res Toxicol 4:123–128
334. Johansson T, Weidolf L, Popp F, Tacke R, Jurva U (2010) In vitro metabolism of haloperidol and sila-haloperidol: new metabolic pathways resulting from carbon/silicon exchange. Drug Metab Disp 38:73–83
335. Tanaka H, Shishido Y (2007) Synthesis of aromatic compounds containing a 1,1-dialkyl-2-trifluoromethyl group, a bioisostere of the tert-alkyl moiety. Bioorg Med Chem Lett 17:6079–6085
336. Barnes-Seeman D, Jain M, Bell L, Ferreira S, Cohen S, Chen X-H, Amin J, Snodgrass B, Hatsis P (2013) Metabolically stable tert-butyl replacement. ACS Med Chem Lett 4:514–516
337. Yu K-L, Sin N, Civiello RL, Wang XA, Combrink KD, Gulgeze HB, Venables BL, Wright JJK, Dalterio RA, Zadjura L, Marino A, Dando S, D'Arienzo C, Kadow KF, Cianci CW, Li Z, Clarke J, Genovesi EV, Medina I, Lamb L, Colonno RJ, Yang Z, Krystal M, Meanwell NA (2007) Respiratory syncytial virus fusion inhibitors. Part 4: optimization for oral bioavailability. Bioorg Med Chem Lett 17:895–901
338. Skuballa W, Schillinger E, C-St S, Vorbrüggen H (1986) Synthesis of a new chemically and metabolically stable prostacyclin analogue with high and long-lasting oral activity. J Med Chem 29:313–315
339. Kim J-JP, Battaile KP (2002) Burning fat: the structural basis of fatty acid β-oxidation. Curr Opin Struct Biol 12:721–728
340. Świzdor A, Panek A, Milecka-Tronina N, Kołek T (2012) Biotransformations utilizing β-oxidation cycle reactions in the synthesis of natural compounds and medicines. Int J Mol Sci 13:16514–16543
341. Li C, Benet LZ, Grillo MP (2002) Studies on the chemical reactivity of 2-phenylpropionic acid 1-*O*-acyl glucuronide and *S*-acyl-CoA thioester metabolites. Chem Res Toxicol 5:1309–1317
342. Grillo MP (2011) Drug-*S*-acyl-glutathione thioesters: synthesis, bioanalytical properties, chemical reactivity, biological formation and degradation. Curr Drug Metab 12:229–244
343. Darnell M, Weidolf L (2013) Metabolism of xenobiotic carboxylic acids: focus on coenzyme A conjugation, reactivity, and interference with lipid metabolism. Chem Res Toxicol. doi:10.1021/tx400183y
344. Ballatore C, Huryn DM, Smith AB III (2013) Carboxylic acid (bio)isosteres in drug design. ChemMedChem 8:385–395
345. Hamada Y, Kiso Y (2012) The application of bioisosteres in drug design for novel drug discovery: focusing on acid protease inhibitors. Expert Opin Drug Discov 7:903–922

346. Stachulski AV, Harding JR, Lindon JC, Maggs JL, Park BK, Wilson ID (2006) Acyl glucuronides: biological activity, chemical reactivity, and chemical synthesis. J Med Chem 49:6931–6945
347. Regan SL, Maggs JL, Hammond TG, Lambert C, Williams DP, Park BK (2010) Acyl glucuronides: the good, the bad and the ugly. Biopharm Drug Dispos 31:367–395
348. Baba A, Yoshioka T (2009) Structure–activity relationships for degradation reaction of 1-β-*O*-acyl glucuronides: kinetic description and prediction of intrinsic electrophilic reactivity under physiological conditions. Chem Res Toxicol 22:158–172
349. Baba A, Yoshioka T (2009) Structure–activity relationships for degradation reaction of 1-β-*O*-acyl glucuronides. Part 2: Electronic and steric descriptors predicting the reactivity of 1-β-*O*-acyl glucuronides derived from benzoic acids. Chem Res Toxicol 22:1559–1569
350. Baba A, Yoshioka T (2009) Structure–activity relationships for degradation reaction of 1-β-*O*-acyl glucuronides. Part 3: Electronic and steric descriptors predicting the reactivity of aralkyl carboxylic acid 1-β-*O*-acyl glucuronides. Chem Res Toxicol 22:1998–2008
351. Sawamura R, Okudaira N, Watanabe K, Murai T, Kobayashi Y, Tachibana M, Ohnuki T, Masuda K, Honma H, Kurihara A, Okazaki O (2010) Predictability of idiosyncratic drug toxicity risk for carboxylic acid-containing drugs based on the chemical stability of acyl glucuronide. Drug Metab Disp 38:1857–1864
352. Krogsgaard-Larsen P, Ebert B, Lund TM, Briiuner-Osbome H, Slok FA, Johansen TN, Brehm L, Madsen U (1996) Design of excitatory amino acid receptor agonists, partial agonists and antagonists: ibotenic acid as a key lead structure. Eur J Med Chem 31:515–537
353. Pemberton N, Graden H, Evertsson E, Bratt E, Lepistö M, Johannesson P, Svensson PH (2012) Synthesis and functionalization of cyclic sulfonimidamides: a novel chiral heterocyclic carboxylic acid bioisostere. ACS Med Chem Lett 3:574–578
354. Petrillo E Jr, Ondetti M (1982) Angiotensin-converting enzyme inhibitors: medicinal chemistry and biological actions. Med Res Rev 2:1–41
355. Ishak R, Abbas O (2013) Penicillamine revisited: historic overview and review of the clinical uses and cutaneous adverse effects. Am J Clin Dermatol 14:223–233
356. Narjes F, Koehler KF, Koch U, Gerlach B, Colarusso S, Steinkühler C, Brunetti M, Altamura S, De Francesco R, Matassa VG (2002) A designed P1 cysteine mimetic for covalent and non-covalent inhibitors of HCV NS3 protease. Bioorg Med Chem Lett 12:701–704
357. Erickson JA, McLoughlin JI (1995) Hydrogen bond donor properties of the difluoromethyl group. J Org Chem 60:1626–1631
358. Albers HMHG, Ovaa H (2012) Chemical evolution of autotaxin inhibitors. Chem Rev 112:2593–2603
359. Mutoh T, Rivera R, Chun J (2012) Insights into the pharmacological relevance of lysophospholipid receptors. Br J Pharmacol 165:829–844
360. Xu Y, Qian L, Pontsler AV, McIntyre TM, Prestwich GD (2004) Synthesis of difluoromethyl substituted lysophosphatidic acid analogues. Tetrahedron 60:43–49
361. Xu Y, Prestwich GD (2002) Concise synthesis of acyl migration-blocked 1,1-difluorinated analogues of lysophosphatidic acid. J Org Chem 67:7158–7161
362. Wang T, Yin Z, Zhang Z, Bender JA, Yang Z, Johnson G, Yang Z, Zadjura LM, D'Arienzo CJ, DiGiugno PD, Gesenberg C, Yamanaka GA, Gong Y-F, Ho H-T, Fang H, Zhou N, McAuliffe BV, Eggers BJ, Fan L, Nowicka-Sans B, Dicker IB, Gao Q, Colonno RJ, Lin P-F, Meanwell NA, Kadow JF (2009) Inhibitors of human immunodeficiency virus type 1 (HIV-1) attachment. 5. An evolution from indole to azaindoles leading to the discovery of 1-(4-benzoylpiperazin-1-yl)-2-(4,7-dimethoxy-1*H*-pyrrolo[2,3-*c*]pyridin-3-yl)ethane-1,2-dione (BMS-488043), a drug candidate that demonstrates antiviral activity in HIV-1-infected subjects. J Med Chem 52:7778–7787
363. Kalgutkar AS, Griffith DA, Ryder T, Sun H, Miao Z, Bauman JN, Didiuk MT, Frederick KS, Zhao SX, Prakash C, Soglia JR, Bagley SW, Bechle BM, Kelley RM, Dirico K, Zawistoski M, Li J, Oliver R, Guzman-Perez A, Liu KKC, Walker DP, Benbow JW, Morris J (2010)

Discovery tactics to mitigate toxicity risks due to reactive metabolite formation with 2-(2-hydroxyaryl)-5-(trifluoromethyl)pyrido[4,3-*d*]pyrimidin-4(3*H*)-one derivatives, potent calcium-sensing receptor antagonists and clinical candidate(s) for the treatment of osteoporosis. Chem Res Toxicol 23:1115–1126

364. Southers JA, Bauman JN, Price DA, Humphries PS, Balan G, Sagal JF, Maurer TS, Zhang Y, Oliver R, Herr M, Healy DR, Li M, Kapinos B, Fate GD, Riccardi KA, Paralkar VM, Brown TA, Kalgutkar AS (2010) Metabolism-guided design of short-acting calcium-sensing receptor antagonists. ACS Med Chem Lett 1:219–223
365. Hartz RA, Ahuja VT, Zhuo X, Mattson RJ, Denhart DJ, Deskus JA, Vrudhula VM, Pan S, Ditta JL, Shu Y-Z, Grace JE, Lentz KA, Lelas S, Li Y-W Molski TF, Krishnananthan S, Wong H, Qian-Cutrone J, Schartman R, Denton R, Lodge NJ, Zaczek R, Macor JE, Bronson JJ (2009) A strategy to minimize reactive metabolite formation: discovery of (*S*)-4-(1-cyclopropyl-2-methoxyethyl)-6-[6-(difluoromethoxy)-2,5-dimethylpyridin-3-ylamino]-5-oxo-4,5-dihydropyrazine-2-carbonitrile as a potent, orally bioavailable corticotropin-releasing factor-1 receptor antagonist. J Med Chem 52:7653–7658
366. Hartz RA, Ahuja VT, Schmitz WD, Molski TF, Mattson GK, Lodge NJ, Bronson JJ, Macor JE (2010) Synthesis and structure–activity relationships of N^3-pyridylpyrazinones as corticotropin-releasing factor-1 (CRF1) receptor antagonists. Bioorg Med Chem Lett 20:1890–1894
367. Zhuo X, Hartz RA, Bronson JJ, Wong H, Ahuja VT, Vrudhula VM, Leet JE, Huang S, Macor JE, Shu Y-Z (2010) Comparative biotransformation of pyrazinone-containing corticotropin-releasing factor receptor-1 antagonists: minimizing the reactive metabolite formation. Drug Metab Disp 38:5–15
368. Atwal KS, Rovnyak GC, Schwartz J, Moreland S, Hedberg A, Gougoutas JZ, Malley MM, Floyd DM (1990) Dihydropyrimidine calcium channel blockers: 2-heterosubstituted 4-aryl-1,4-dihydro-6-methyl-5-pyrimidinecarboxyaliccid esters as potent mimics of dihydropyridines. J Med Chem 33:1510–1515
369. Atwal KS, Rovnyak GC, Kimball SD, Floyd DM, Moreland S, Swanson BN, Gougoutas JZ, Schwartz J, Smillie KM, Malley MF (1990) Dihydropyrimidine calcium channel blockers. 2. 3-Substituted-4-aryl-1,4-dihydro-6-methyl-5-pyrimidinecarboxyalciicd esters as potent mimics of dihydropyridines. J Med Chem 33:2629–2635
370. Atwal KS, Swanson BN, Unger SE, Floyd DM, Moreland S, Hedberg A, O'Reilly BC (1991) Dihydropyrimidine calcium channel blockers. 3. 3-Carbamoyl-4-aryl-1,2,3,4-tetrahydro-6-methyl-5-pyrimidinecarboxylic acid esters as orally effective antihypertensive agents. J Med Chem 34:806–811
371. Rovnyak GC, Atwal KS, Hedberg A, Kimball SD, Moreland S, Gougoutas JZ, O'Reilly BC, Schwartz J, Malley MF (1992) Dihydropyrimidine calcium channel blockers. 4. Basic 3-substituted-4-aryl-1,4-dihydropyrimidine-5-carboxylic acid esters. Potent antihypertensive agents. J Med Chem 35:3254–3263
372. Wood MR, Schirripa KM. Kim JJ, Wan B-L, Murphy KL, Ransom RW, Chang RSL, Tang C, Prueksaritanont T, Detwiler TJ, Hettrick LA, Landis ER, Leonard YM, Krueger JA, Lewis SD, Pettibone DJ, Freidinger RM, Bock MG (2006) Cyclopropylamino acid amide as a pharmacophoric replacement for 2,3-diaminopyridine. Application to the design of novel bradykinin B1 receptor antagonists. J Med Chem 49:1231–1234
373. Testa B, Pedretti A, Vistoli G (2012) Reactions and enzymes in the metabolism of drugs and other xenobiotics. Drug Discov Today 17:549–560
374. Testa B, Krämer SD (2007) The biochemistry of drug metabolism – an introduction Part 3. Reactions of hydrolysis and their enzymes. Chem Biodivers 4:2031–2122
375. Testa B, Krämer SD (2007) The biochemistry of drug metabolism – an introduction Part 2. Redox reactions and their enzymes. Chem Biodivers 4:257–405
376. Guengerich FP (2001) Common and uncommon cytochrome P450 reactions related to metabolism and chemical toxicity. Chem Res Toxicol 14:611–650

377. Peng HM, Raner GM, Vaz ADN, Coon MJ (1995) Oxidative cleavage of esters and amides to carbonyl products by cytochrome P450. Arch Biochem Biophys 318:333–339
378. Watjen F, Baker R, Engelstoff M, Herbert R, MacLeod A, Knight A, Merchant K, Moseley J, Saunders J, Swain CJ, Wong E, Springer JP (1989) Novel benzodiazepine receptor partial agonists: oxadiazolylimidazobenzodiazepines. J Med Chem 32:2282–2291
379. Saunders J, Cassidy M, Freedman SB, Harley EA, Iversen LL, Kneen C, MacLeod AM, Merchant KJ, Snow RJ, Baker R (1990) Novel quinuclidine-based ligands for the muscarinic cholinergic receptor. J Med Chem 33:1128–1138
380. Krogsgaard-Larsen P, Falch E, Sauerberg P, Freedman SB, Lembøl HL, Meier E (1988) Bioisosteres of arecoline as novel CNS-active muscarinic agonists. Trends Pharmacol Sci Suppl:69–74
381. Kim J, Ok T, Park C, So W, Jo M, Kim Y, Seo M, Lee D, Jo S, Ko Y, Choi I, Park Y, Yoon J, Kyeong Ju M, Ahn JY, Kim J, Han S-J, Kim T-H, Cechetto J, Nam J, Liuzzi M, Sommer P, No Z (2012) A novel 3,4-dihydropyrimidin-2(1*H*)-one: HIV-1 replication inhibitors with improved metabolic stability. Bioorg Med Chem Lett 22:2522–2526
382. Rajapakse HA, Nantermet PG, Selnick HG, Barrow JC, McGaughey GB, Munshi S, Lindsley SR, Young MB, Ngo PL, Holloway MK, Lai M-T, Espeseth AS, Shi X-P, Colussi D, Pietrak B, Crouthamel M-C, Tugusheva K, Huang Q, Xu M, Simon AJ, Kuo L, Hazuda DJ, Graham S, Vacca JP (2010) SAR of tertiary carbinamine derived BACE1 inhibitors: role of aspartate ligand amine pK_a in enzyme inhibition. Bioorg Med Chem Lett 20:1885–1889
383. Feil SC, Hamilton S, Krippner GY, Lin B, Luttick A, McConnell DB, Nearn R, Parker MW, Ryan J, Stanislawski PC, Tucker SP, Watson KG, Morton CJ (2012) An orally available 3-ethoxybenzisoxazole capsid binder with clinical activity against human rhinovirus. ACS Med Chem Lett 3:303–307
384. Sun Z-Y, Asberom T, Bara T, Bennett C, Burnett D, Chu I, Clader J, Cohen-Williams M, Cole D, Czarniecki M, Durkin J, Gallo G, Greenlee W, Josien H, Huang X, Hyde L, Jones N, Kazakevich I, Li H, Liu X, Lee J, MacCoss M, Mandal MB, McCracken T, Nomeir A, Mazzola R, Palani A, Parker EM, Pissarnitski DA, Qin J, Song L, Terracina G, Vicarel M, Voigt J, Xu R, Zhang L, Zhang Q, Zhao Z, Zhu X, Zhu Z (2012) Cyclic hydroxyamidines as amide isosteres: discovery of oxadiazolines and oxadiazines as potent and highly efficacious γ-secretase modulators in vivo. J Med Chem 55:489–502
385. Valverde IE, Bauman A, Kluba CA, Vomstein S, Walter MA, Mindt TL (2013) 1,2,3-Triazoles as amide bond mimics: triazole scan yields protease-resistant peptidomimetics for tumor targeting. Angew Chem Int Ed 52:8957–8960
386. Xia G, You X, Liu L, Liu H, Wang J, Shi Y, Li P, Xiong B, Liu X, Shen J (2013) Design, synthesis and SAR of piperidyl-oxadiazoles as 11β-hydroxysteroid dehydrogenase 1 inhibitors. Eur J Med Chem 62:1–10
387. Staben ST, Blaquiere N, Tsui V, Kolesnikov A, Do S, Bradley EK, Dotson J, Goldsmith R, Heffron TP, Lesnick J, Lewis C, Murray J, Nonomiya J, Olivero AG, Pang J, Rouge L, Salphati L, Wei BQ, Wiesmann C, Wu P (2013) *Cis*-Amide isosteric replacement in thienobenzoxepin inhibitors of PI3-kinase. Bioorg Med Chem Lett 23:897–901
388. Taylor R, Mullaley A, Mullier GW (1990) Use of crystallographic data in searching for isosteric replacements: composite crystal-field environments of nitro and carbonyl groups. Pestic Sci 29:197–213
389. Hardcastle IR, Liu J, Valeur E, Watson A, Ahmed SU, Blackburn TJ, Bennaceur K, Clegg W, Drummond C, Endicott JA, Golding BT, Griffin RJ, Gruber J, Haggerty K, Harrington RW, Hutton C, Kemp S, Lu X, McDonnell JM, Newell DR, Noble MEM, Payne SL, Revill CH, Riedinger C, Xu Q, Lunec J (2011) Isoindolinone inhibitors of the murine double minute 2 (MDM2)-p53 protein–protein interaction: structure–activity studies leading to improved potency. J Med Chem 54:1233–1243
390. Firestine SM, Davisson VJ (1993) A tight binding inhibitor of 5-aminoimidazole ribonucleotide carboxylase. J Med Chem 36:3484–3486

391. Thorson JS, Chapman E, Schultz PG (1995) Analysis of hydrogen bonding strengths in proteins using unnatural amino acids. J Am Chem Soc 117:9361–9362
392. Alston TA, Porter DJT, Bright HJ (1983) Enzyme inhibition by nitro and nitroso compounds. Acc Chem Res 16:418–424
393. Julémont F, de Leval X, Michaux C, Damas J, Charlier C, Durant F, Pirotte B, Dogné J-M (2002) Spectral and crystallographic study of pyridinic analogues of nimesulide: determination of the active form of methanesulfonamides as COX-2 selective inhibitors. J Med Chem 45:5182–5185
394. Renard J-F, Arslan D, Garbacki N, Pirotte B, de Leval X (2009) Pyridine analogues of nimesulide: design, synthesis, and in vitro and in vivo pharmacological evaluation as promising cyclooxygenase 1 and 2 inhibitors. J Med Chem 52:5864–5871
395. Gougoutas JZ, Ojala WH, Malley MF (1982) 3,4-*bis*(4-Chlorophenyl)sydnone. Cryst Struct Comm 11:1731–1736